Source Strength Impact Analysis on Insulator Flashover under Contaminated Conditions

by

Li He

A Dissertation Presented in Partial Fulfillment
of the Requirements for the Degree
Doctor of Philosophy

Approved June 2016 by the
Graduate Supervisory Committee:

Ravi Gorur, Chair
Raja Ayyanar
George Karady
Keith Holbert

ARIZONA STATE UNIVERSITY

August 2016

ABSTRACT

Transmission voltages worldwide are increasing to accommodate higher power transfer from power generators to load centers. Insulator dimensions cannot increase linearly with the voltage, as supporting structures become too tall and heavy. Therefore, it is necessary to optimize the insulator design considering all operating conditions including dry, wet and contaminated. In order to design insulators suitably, a better understanding of the insulator flashover is required, as it is a serious issue regarding the safe operation of power systems. However, it is not always feasible to conduct field and laboratory studies due to limited time and money.

The desire to accurately predict the performance of insulator flashovers requires mathematical models. Dynamic models are more appropriate than static models in terms of the instantaneous variation of arc parameters. In this dissertation, a dynamic model including conditions for arc dynamics, arc re-ignition and arc motion with AC supply is first developed.

For an AC power source, it is important to consider the equivalent shunt capacitance in addition to the short circuit current when evaluating pollution test results. By including the power source in dynamic models, the effects of source parameters on the leakage current waveform, the voltage drop and the flashover voltage were systematically investigated. It has been observed that for the same insulator under the same pollution level, there is a large difference among these flashover performances in high voltage laboratories and real power systems. Source strength is believed to be responsible for this discrepancy. Investigations of test source strength were conducted in this work in order to study its impact on different types of insulators with a variety of geometries.

Traditional deterministic models which have been developed so far can only predict whether an insulator would flashover or withstand. In practice, insulator flashover is a statistical process, given that both pollution severity and flashover voltage are probabilistic variables. A probability approach to predict the insulator flashover likelihood is presented based on the newly developed dynamic model.

ACKNOWLEDGMENTS

I would like to express my deep gratitude to my supervisor, Dr. Ravi S. Gorur for giving me this opportunity to chase my dream and work in an interesting and challenge field of research. His guidance, support, and encouragement throughout this course of work are gratefully appreciated. I would like to thank my supervisory committee, Dr. Raja Ayyanar, Dr. Keith E. Holbert, and Dr. George K. Karady for their time, comments, and suggestions.

I am also grateful for all faculties in power systems group at Arizona State University. Their commitments to students and dedications to research really inspired me. I wish to thank my colleagues Longfei Cui and Jiahong He, for their help and encouragements as well. I also wish to thank my fellow friends at Arizona State University, North China Electric Power University, and High School Attached to Hunan Normal University for their support over the years.

Lastly, I would like to thank my parents for their unconditional love and tremendous support. Words cannot express how grateful I am for having parents like them.

TABLE OF CONTENTS

Page

CHAPTER Page

CHAPTER Page

CHAPTER Page

CHAPTER Page

LIST OF TABLES

Table Page

Table Page

LIST OF FIGURES

Figure Page

Figure Page

Figure Page

Figure Page

Chapter 1

INTRODUCTION

1.1 Introduction

Electric power is transmitted from generation sites to customers in economic and reliable manners through transmission lines. Since these lines can span over several hundreds of miles, overhead high voltage transmission lines are widely used around the world to minimize losses during transmission. These lines are supported and separated by insulators both mechanically and electrically [1].

The increasing demand of electrical energy worldwide has driven the development of higher system voltages for electric power transmission. Such experimental lines of various scales can be found in many countries. For example, Ultra-High-Voltage (UHV) electricity transmission is being introduced in China and four UHV circuits are completed or under construction. This brought up a more challenge problem since higher voltage levels require insulators to withstand a large amount of electrical stresses. Along with that, the performance of outdoor insulators is largely affected by surrounding environment as well.

Environmental conditions such as pollution and moisture can have large influences on the performance of insulators. Outdoor insulators are largely subject to pollution by dirt and chemicals in industrial areas and by salt deposits near the coast [2]. When an insulator is dry, there is no problem. However, when it is wet, insulator surface resistance drops considerably. The reduction of surface resistance will result in the leakage current flows on the insulator surface and generate discharge. Under certain conditions, surface discharge can grow to complete flashover and cause successive power supply interruptions. The

conditions that lead to flashover are hard to predict given the uncertainty and unknown factors related to the physics of the arc.

With the rise in transmission line voltage levels, research work on polluted insulator flashover has increased substantially. In order to have a better understanding of the flashover process under contaminated conditions, many researchers have been studying the insulator flashover mechanisms since the last century. Despite extensive worldwide field and laboratory studies, the basic mechanism of these flashovers has not yet been fully understood. This is mainly due to the large number of parameters associated with the flashover phenomena.

For instance, there are a number of experimental records showing that source parameters are contributing factors in the dispersion of test results from different laboratories [3]. Although several international standards have been proposed on the source capacity for pollution tests, there is no general agreement on source requirements. Therefore, it is important to study the effect of source parameters in order to obtain a more reasonable and accurate prediction of insulator performance. Besides source parameters, DC or AC supply, types of pollutants, pollution degrees, surface wettings, insulator materials, and insulator geometries along with many other factors are believed to have influences on the insulator flashover performance.

The interaction between insulators and the polluting environments is so complex that it is necessary to develop mathematical models to help better understand the contamination flashover process.

1.2 Research Objectives

The objective of this work is to develop dynamic models that can account for insulator flashover process, from arc initiation to arc propagation and eventually the complete flashover.

The flashover mechanism of polymer insulators is fundamentally different from porcelain insulators due to the hydrophobicity property of polymeric material. By proposing a new dynamic flashover model for polymer insulators, flashover performance of porcelain and polymer insulators can be investigated and compared systematically.

By studying the interaction between test source and insulator at the critical arcing stage where partial arcing leads to complete flashover, this model will be used to interpret the large dispersion of insulator pollution tests results among different laboratories, as well as the different flashover outcomes between laboratories and real power systems. Therefore, this model can provide a general standard on power source requirements.

Investigating the condition that leads to arc jumping is another goal of this research as well. It has been observed that arcs do not always propagates along the insulator surface in practice, modifying the flashover model by considering arc jumping will provide more accurate and realistic results of insulator flashover performance.

The probability study of insulator flashover is another interest of current work since the actual insulator flashover is a statistical problem rather than a deterministic one. The effects of source strength, insulator materials and geometries, hydrophobicity classification levels for polymer insulators, and multiple insulator strings connected in parallel will be studied.

With a better understanding of the physical mechanisms involved in this fast and complex process, the ultimate purpose of this research is to use developed models as design tools to aid the insulators selections and applications in power systems.

Chapter 2

LITERATURE REVIEW

2.1 Types of Insulators

High voltage insulators are utilized to serve two important roles: to provide the mechanical support of the system by withstanding mechanical stress associated with conductor weight; and to maintain the electrical isolation between conductors and other structures [4]. Different insulators are selected for different purposes, and there are various aspects to classify high voltage insulators.

As far as insulator material is concerned, three main types of dielectrics that have been used for high voltage insulators are glass, porcelain and polymer. Porcelain insulators are also known as ceramic insulators, while polymer insulators are sometimes referred to as non-ceramic insulators or composite insulators. Porcelain insulators and polymer insulators are the main interests of this research and will be discussed further below.

2.1.1 Porcelain Insulators

Porcelain insulators have served for over a century and are the most widely used type of outdoor insulators. Electrical porcelain is made of a mixture of clay, quartz or alumina, and spar [4]. Porcelain insulators usually are coated with glaze to reduce localized discharges at sharp edges by ensuring the smooth surface of the insulator. Some properties of porcelain are summarized in the following [4]:

- Density = 2.5 g/cm^3
- Volume resistivity = $10^{11}\Omega \cdot m$
- Relative permittivity = 6-7

- Dielectric strength = 200 kV/cm

The above properties lead to some advantages and limitations of porcelain insulators. On the one hand, porcelain insulators are resistant to degradation due to environmental factors, as well as surface damage due to leakage current. On the other hand, however, porcelain insulators are very heavy, vulnerable to breakage, and easily wettable by water.

2.1.2 Polymer Insulators

Polymer insulator comprise a resin-embedded fiberglass core to provide mechanical strength and a polymeric cover for protection from extreme weather conditions. There are two housing materials commonly in use: Ethylene Propylene Diene Monomer (EPDM) and silicone rubber. Some properties of silicone rubber material are given in the following [4]:

- Density = 1.15 g/cm^3
- Volume resistivity = $10^{12}\Omega \cdot m$
- Relative permittivity = 4
- Dielectric strength = 160-200 kV/cm

Polymer insulators are much lighter than equivalent porcelain insulators. Moreover, the materials are non-brittle. Therefore, polymer insulators are much easier to transport and install. Another important property of polymer insulator is called hydrophobicity. Hydrophobicity refers to the ability of the material to prevent forming continuous water film. Water can only exist in a form of discrete drops on a hydrophobic surface. This property is desirable for outdoor insulators in terms of high withstand voltages. However,

the original hydrophobicity level of a polymer insulator can be reduced or completely lost in service due to several factors. Firstly, the presence of contamination and moisture can damage the polymeric material and reduce the hydrophobicity, which is also known as aging. Secondly, the corona and surface discharge can lead to hydrophobicity level drops as well. Moreover, it has been observed in service that for polymer insulators, the hydrophobicity can be completely lost due to continuous dry band arcing activities [5].

2.2 Flashover Mechanism

Insulator flashover under contaminated conditions is characterized by different stages, and the main phases are pollution layer build-up, dry band formation, partial arcing and complete flashover.

2.2.1 Pollution Layer Build-up

Outdoor insulators are exposed to a variety of contamination sources, which is mainly affected by gravity, wind and electrostatic forces [6]. Wind is the most dominant factor due to the fact that it can drive airborne contaminant particles onto insulator surfaces. After a long period of time, stabilized deposits on insulator surface will form solid layers to cover some part of or even the entire insulator surface. It is always noticeable in service that the top part of an insulator is usually less contaminated when compared to the bottom part. This is mainly attributed to the natural cleaning effect of wind and water. As a result, the pollution layer on an insulator surface is usually not uniformly distributed.

Pollution severity is expressed in terms of Equivalent Salt Deposit Density (ESDD) in mg/cm^2, which is obtained by measuring the conductivity of a mixture of the

contaminant removed from insulator surface and a known amount of distilled water [7]. Table 1 is the qualitative classification of contamination severity in terms of ESDD provided by IEC 60815 [8].

Table 1 IEC Contamination Severity Classification

ESDD (mg/cm^2)	Contamination Severity
0 – 0.03	Very light
0.03 – 0.06	Light
0.06 – 0.1	Moderate
> 0.1	Heavy

2.2.2 Dry Band Formation

When the pollution layer of an insulator becomes wet due to rain or fog, its resistance decreases significantly. The reduction of surface resistance initiates leakage current flows on the insulator surface. The ohmic heating results from leakage current flows will evaporate the moisture on the insulator surface. Areas that have the highest leakage current density, usually around narrow parts of insulator, dry more quickly than others. The uneven distribution of voltage stress will lead to the development of dry bands at these areas.

2.2.3 Partial Arcing

Because of the high resistance of dry bands, the voltage applied to the insulator is almost dropped entirely on dry bands. If a dry band cannot withstand the voltage, localized arcing will be initiated. After the formation of a partial arc, the propagate condition of the arc is determined by arc gradient [9]. Most times the arc will extinguish because its gradient is greater than the pollution layer gradient. However, when the arc gradient is less than the

pollution layer gradient, the arc will continue to propagate and develop. It is possible the arc will elongate to a critical length so that the complete flashover is inevitable.

Pollution layer build-up and dry band formation are early phases and neither constitutes a real risk of flashover [10]. It is the partial arcing phase that is actually responsible for undesirable flashovers. So far, intensive studies have been devoted to this aspect in the form of mathematical models.

2.3 DC Flashover Models

Obenaus was the first researcher to propose a mathematical model for insulator contamination flashover [11]. The insulator flashover model consists of an arc discharge connects in series with a resistance which represents the unbridged portion of an insulator. The simplified model is shown in Figure 1.

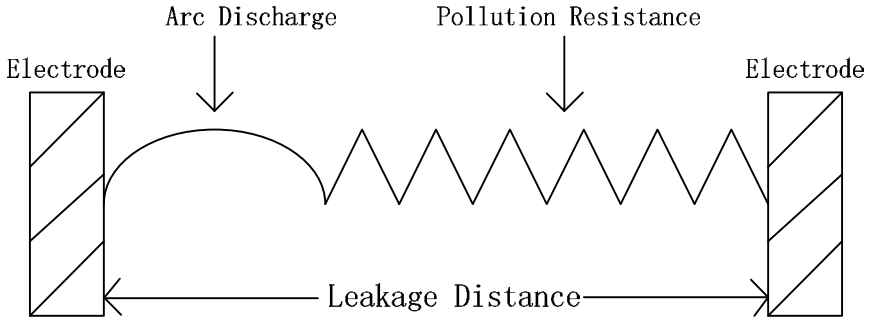

Figure 1 Arc Model

The partial arc is represented by a voltage-current characteristic with following expression:

$$V_{arc} = \frac{xN}{i^n} \tag{1}$$

where

V_{arc} is arc voltage

x is arc length

N, n are static arc constants

The voltage equation for the complete circuit is therefore:

$$V_{supply} = V_{arc} + R_p(x) \cdot I \tag{2}$$

where

$R_p(x)$ is unbridged pollution resistance

I is leakage current

Neumarker developed those equations further and by assuming a uniform pollution layer, the unbridged pollution resistance can be expressed as:

$$R_p(x) = r_{pu} \times (L - x) \tag{3}$$

where

r_{pu} is uniform pollution resistance per unit length

L is insulator leakage distance

The critical voltage gradient and critical current are deduced by Neumarker as:

$$E_c = N^{\frac{1}{n+1}} r_{pu}^{\frac{n}{n+1}} \tag{4}$$

$$i_c = \left(\frac{N}{r_{pu}}\right)^{\frac{1}{n+1}} \tag{5}$$

One interesting conclusion is that critical current is independent of the leakage distance. This was later confirmed by Alston and Zoledziowski [12]. They also modified Neumarker's model by adding the electrode voltage drop and stated that flashover is impossible below the critical current i_c.

Through water column experiments, Hampton proposed the necessary condition for flashover is that the voltage gradient in the water column should greater than that in the arc column [9]. Thus the arc propagation criterion can be expressed as:

$$E_{arc} < E_p \tag{6}$$

where

E_{arc} is arc voltage gradient

E_p is pollution layer voltage gradient

It was shown that for a uniform pollution resistance per unit length, Hampton's criterion yields critical voltage gradient and critical current results which are identical to Neumarker's model.

2.4 AC Flashover Models

Although above models are derived under DC supply, they also have been applied for AC situations. It is argued that sinusoidal AC voltage wave is almost flat near the peak, and with the peak value is selected, the above equations also apply [13]. However, the prediction results show large differences when applying DC model in AC flashovers.

Rizk used dimensional analysis method to study the similarities and differences between DC and AC flashovers [14]. Later, he proposed a dielectric re-ignition model for flashover under AC supply [15]. Because an AC arc will extinguish as the current passes through zero, there is a fundamental difference between AC and DC flashover. Arc re-ignition after the current zero is essentially a process of dielectric breakdown, which takes place when the instantaneous value of the recovery voltage exceeds the dielectric strength of the air gap.

2.5 Dynamic Flashover Models

Models that have been discussed so far are static in terms of that once an arc is initiated it cannot be stopped until flashover occurs. However, arc propagation is a rapid time varying phenomenon and it can only happen when required conditions are met. The variations of arc current, arc resistance, pollution resistance, and form factor with respect to time are not accounted for in static models. These limitations of static models lead to the development of dynamic models.

The first dynamic model that takes into consideration instantaneous arc parameter changes was developed by Jolly, Cheng and Otten [16]. By using Mayr's equation to calculate arc resistance, their model can predict the time to flashover for strips of electrolytes. Cheng also derived a multi-arc model, but discovered that parallel arcs could actually cancel one another and eventually only one single arc dominates.

Based on the idea of Mayr's equation, Rizk proposed a new arc equation [15]:

$$\frac{dr_a}{dt} = \frac{r_a}{\tau} - \frac{{r_a}^2 {i_a}^{n+1}}{N\tau} \tag{7}$$

where

r_a is arc resistance

i_a is dynamic arc current

τ is time constant

N, n are dynamic arc constants, similar to that in equation (1)

Although Rizk considered the dynamic changes of arc resistance, his model did not consider the actual insulator geometry. Later on, an improvement was accomplished by Sundararajan who successfully modeled arc propagation with time, the effect of non-

uniform pollution distribution and the role of geometry [17]. However, her model does not take into account arc re-ignition criteria. Therefore, it only valid for DC insulator flashover.

Chapter 3

SIMULATION DETAILS

3.1 Model Concept

This research aims to study arc propagation under various conditions and provide a better understanding of the pollution flashover process. The quantitative model in this work is based on Obenaus' theory, which considered a polluted insulator as an arc discharge connects in series with the pollution resistance. The AC power source parameters will also be accounted for in the proposed model. For a given supply voltage and pollution severity, the arc re-ignition criterion and arc propagation criterion both are checked. Then the instantaneous changes of arc length, arc resistance, arc propagation velocity and other parameters are calculated. If the arc length is less than 2/3 of the total insulator leakage distance, the above steps will be repeated. When arc length reaches this critical value, it is believed that complete flashover happens. If either arc re-ignition criterion or propagation criterion is not satisfied, the supply voltage will be increased and repeat above steps.

3.2 Model Development

3.2.1 Test Circuit

Figure 2 shows the basic circuit used in laboratory for insulator pollution tests. The test insulator is energized from a test transformer which is fed from an AC power source. Because both the power source and the high voltage transformer have internal parameters, the test voltage refers to the no load voltage of the power source and not the actual dynamic voltage to which the insulator is exposed during pollution test.

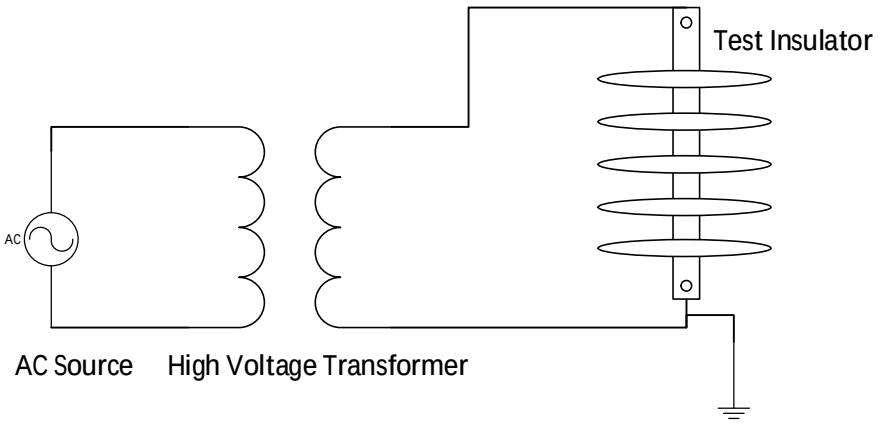

Figure 2 Insulator Pollution Tests Circuit

The simplified equivalent circuit is shown in Figure 3. The source is represented by its short circuit resistance R, inductance L, and equivalent shunt capacitance C. The insulator model is derived from Obenaus's model, which consists of a partial arc connected in series with unbridged pollution layer with the resistance R_x.

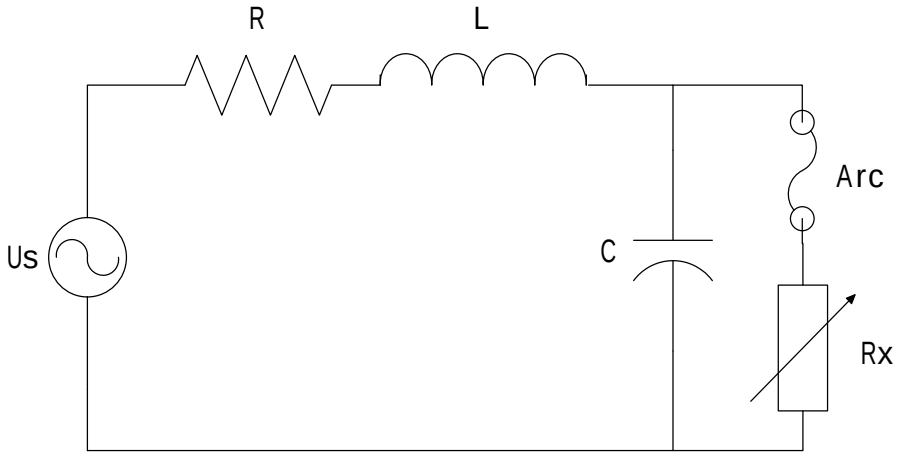

Figure 3 Simplified Equivalent Circuit

where

U_s is AC source voltage

R is short circuit resistance

L is short circuit inductance

C is equivalent shunt capacitance

R_x is unbridged pollution layer resistance

3.2.2 Dynamic Arc Equation

In order to account for dynamic arc properties, a generalization of Mayr's equation is used in this work [15]:

$$\frac{dG}{dt} = \frac{G_s - G}{\tau} \tag{8}$$

where

G is arc conductance per unit length

G_s is conductance at the point of static arc characteristic

τ is time constant

A general form of the static arc characteristic equation is:

$$E{i_a}^n = N \tag{9}$$

Substituting G_s and expressing arc resistance per unit length r_a in equation (9), the dynamic arc equation will then become,

$$\frac{dr_a}{dt} = \frac{r_a}{\tau}\left(1 - \frac{r_a {i_a}^{n+1}}{N}\right) \tag{10}$$

where

r_a is arc resistance per unit length

i_a is arc current

τ is time constant

N, n are dynamic arc constants

The values of time constants, N and n used in this research are selected as 100 μS, 60 and 0.8, respectively.

3.2.3 Arc Propagation Speed

Although many mechanisms have been proposed to account for the arc motion over contaminated insulator surfaces. Theories have been developed based on drying effect, electrostatic forces, thermal forces, magnetic force and partial breakdown ahead of the arc root. However, the subject is far from being fully understood [18]. From experimental study of arc propagations over a contaminated surface, Al-Baghdadi successfully demonstrated that for arc current exceeding the critical current i_c, the arc velocity is a function of dynamic current and pollution resistance per unit length [19]. This empirical formula was later confirmed by Rizk with dimensional analysis of the phenomenon [14].

Arc propagation speed is proportional to the fourth power of the current and affected by unbridged pollution resistance per unit length as well:

$$v = 1.5 \times 10^{-4} {r_p}^{2.5} \left(i^4 - {i_c}^4 \right) \tag{11}$$

where

v is arc propagation velocity

r_p is unbridged pollution resistance per unit length

i is arc current

i_c is critical current

3.2.4 Dielectric Recovery

Dielectric recovery is a fundamental process of arcing in AC energized insulator flashover. It was first proposed by Rizk after realizing the current will cross zero every half cycle [18]. The dielectric strength of an air gap following arc extinction can be expressed as a function of the dielectric strength of the air gap at ambient temperature, time, and current amplitude. After some manipulations, the following expression can be obtained:

$$U_d = xE_o\left[1 + \frac{51.9}{1+\frac{157.5t}{{i_{max}}^{1.26}}}\right]^{-0.636} \tag{12}$$

where

x is gap length

E_o is dielectric gradient of a non-uniform field air gap at ambient temperature amounting to 5-6 kV/cm

t is time measured from current zero

i_{max} is arc current amplitude in the previous half cycle

3.2.5 Arc Restriking

Following the dielectric recovery, arc restriking will happen when the instantaneous value of the recovery voltage exceeds the dielectric strength of the air gap. When the gap restrikes, the spark phase, which precedes arcing, can be described by Toepler's equation:

$$\frac{dr_a}{dt} = -\frac{{r_a}^2 i_a}{k} \tag{13}$$

where

$k = 0.5 \times 10^{-4}\ V \cdot s/cm$ for air at atmospheric pressure.

The transition from arc striking to arcing phase takes place as the spark voltage gradient approaches the gradient of the corresponding arc.

3.2.6 Pollution Layer Resistance

Contamination severity of the insulator surface can be quantified in terms of either layer conductivity or equivalent salt deposit density (ESDD). In this work, it is assumed that layer conductance K (μS) of an insulator is known. The pollution resistance can be calculated by:

$$R_p = \frac{1}{K} \tag{14}$$

The layer conductivity σ $(\mu S/cm)$ can be calculated by multiplying the layer conductance by form factor f:

$$\sigma = K \cdot f \tag{15}$$

The form factor of an insulator is determined from the insulator dimensions and can be obtained by integrating each time step depending on the arc distance x. Mathematically, the form factor is usually expressed as:

$$f = \int_x^L \frac{1}{2\pi r} dl \tag{16}$$

The ESDD is often used as an indication of pollution degree in practice. The determination of ESDD is standardized in both IEC and IEEE documents [7, 20]. After knowing the layer conductivity σ, the ESDD can be obtained by:

$$ESDD = (5.7\sigma)^{1.03} \times \frac{V}{A} \tag{17}$$

where

V is the volume of dissolved water

A is the area of cleaned surface

3.3 Mathematical Formulation of Insulator Model

The voltage and current of an arc are subjected to the Kirchhoff's voltage and current laws in the circuit. The mathematical model should be treated as a dynamic system which includes differential equations that govern the dynamic properties of circuit components.

3.3.1 State Variable Approach

This dynamic system can be described by four differential equations and can be solved by state variable approach, which has the following general forms,

$$\frac{dx(t)}{dt} = Ax(t) + Bu(t) \tag{19}$$

$$y(t) = Cx(t) + Du(t) \tag{20}$$

The first equation describes the next state of the system with respect to current state and input. The second equation describes the output with respect to current state and input. The state variables are a set of variables that used to describe the system response. Once the inputs are known, the system response can be determined at any time step.

3.3.2 Dynamic System Differential Equations

The inductor current I, capacitor voltage U, arc length x and arc resistance r_a are selected as state variables in this study. Based on the simplified equivalent circuit shown

in Figure 3, system differential equations can be expressed as following and after simple manipulations:

$$\frac{dI}{dt} = \frac{U_s - I \times R_s - U}{L_s} \tag{21}$$

$$\frac{dU}{dt} = \frac{I - \frac{U}{r_p \times (L-x) + r_a \cdot x}}{C_s} \tag{22}$$

$$\frac{dr_a}{dt} = \frac{ra}{\tau} - \frac{r_a^2 \times \left| \frac{U}{r_p \times (L-x) + r_a \cdot x} \right|^{n+1}}{N \times \tau} \tag{23}$$

$$\frac{dx}{dt} = v \tag{24}$$

where

U_s is supply voltage

R_s is equivalent source resistance

L_s is equivalent source inductance

C_s is equivalent source capacitance

r_p is pollution resistance per unit length

L is leakage distance

x is arc distance

v is arc velocity

τ is time constant

N, n are dynamic arc constants

The first two equations for inductor current and capacitor voltage are obtained by Kirchhoff's Law. The third equation is dynamic arc resistance derived from equation (11).

The fourth equation is arc length function with respect to arc velocity, which can be further substituted according to equation (12).

3.3.3 Runge-Kutta Method

The equations used to describe the system are coupled differential equations. Their solutions can be found by numerical methods for ordinary differential equations. Runge-Kutta method is the best approach to solve this system because it can achieve high order accuracy without requiring the calculation of higher derivatives.

The most widely used Runge-Kutta method is the fourth order, or the classic Runge-Kutta method. It has the form [21]:

$$y_{i+1} = y_i + \frac{1}{6}(k_1 + 2k_2 + 2k_3 + k_4)h \tag{25}$$

where

$$k_1 = f(t_i, y_i)$$

$$k_2 = f\left(t_i + \frac{1}{2}h, y_i + \frac{1}{2}k_1 h\right)$$

$$k_3 = f(t_i + \frac{1}{2}h, y_i + \frac{1}{2}k_2 h)$$

$$k_4 = f(t_i + h, y_i + k_3 h)$$

The local truncation error is on the order of $O(h^5)$, while the total accumulated error is on the order of $O(h^4)$. By discretizing time into small time intervals, and performing the Runge-Kutta method, the differential equations can be solved.

3.4 Program Description

3.4.1 Program Structure

This simulation program is written in Matlab (version 2015b). Program inputs are insulator profiles and AC source parameters. It can be used as a two-way approach to calculate either the critical voltage or critical pollution severity as long as the other factor is specified. If a pollution severity is specified, the program can determine the minimum flashover voltage. If a supply voltage is given, the maximum pollution severity which it will not result in flashover can be predicted. The program is applicable for predicting insulator flashover in terms of different properties, including insulating materials, insulator geometries, voltage levels, and contamination degrees.

Since this program takes into account the effects of test source parameters, it can also help researchers to have a more accurate prediction of insulator flashover performance both in service and in laboratories. In following chapters it will also show that this program can be extended to study the arc jumping phenomenon and predict the probability of insulator flashover.

3.4.2 Program Flowchart

The flowchart of this program is shown in Figure 4.

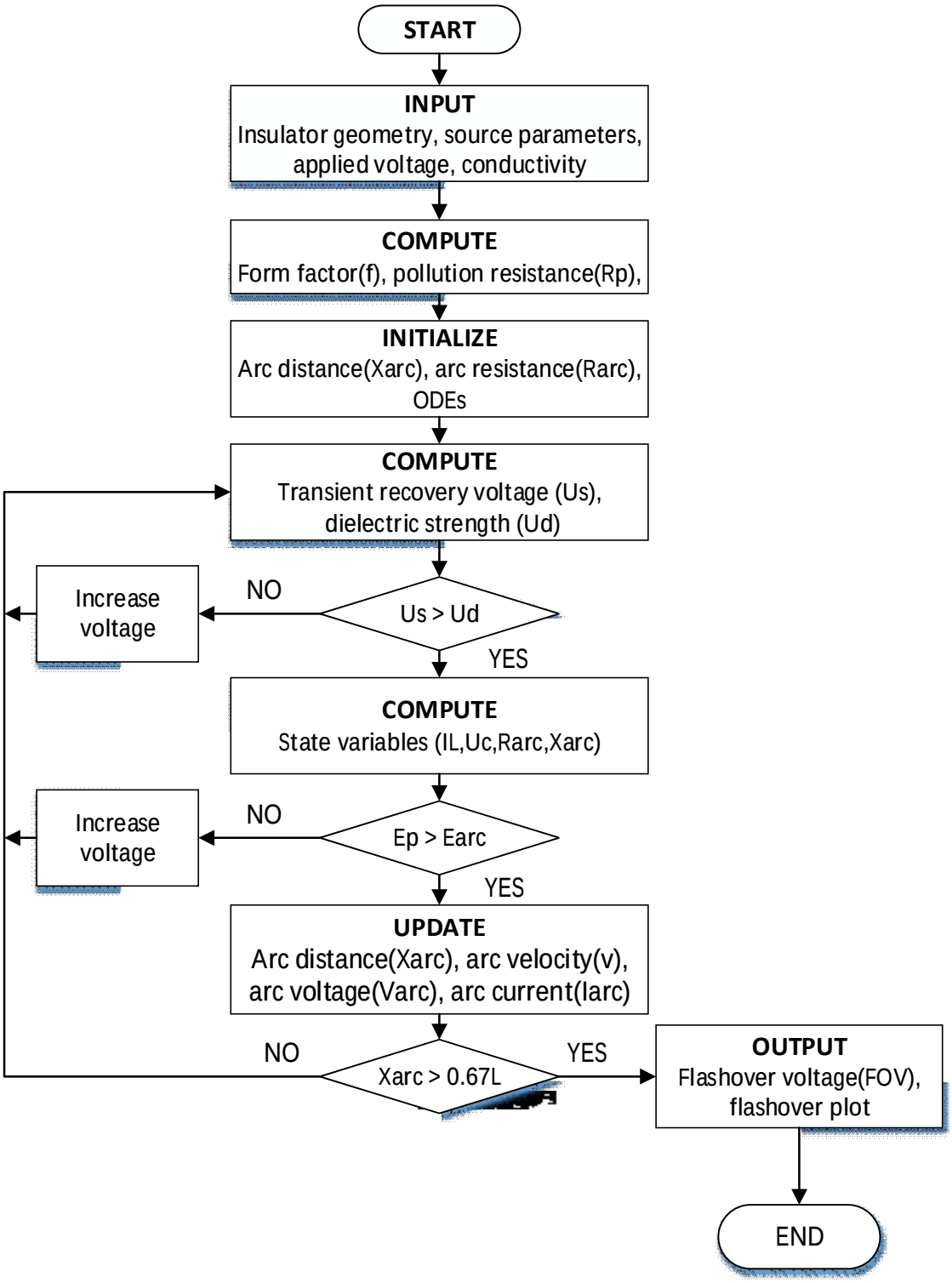

Figure 4 Program Flowchart

3.5 Validation of the Model

The model is validated by comparing the results with published literatures. By using the dynamic model introduced in this study, flashover voltage characteristics of this insulator was computed and compared. Figure 5 shows the configurations of insulator used by previous researcher [22].

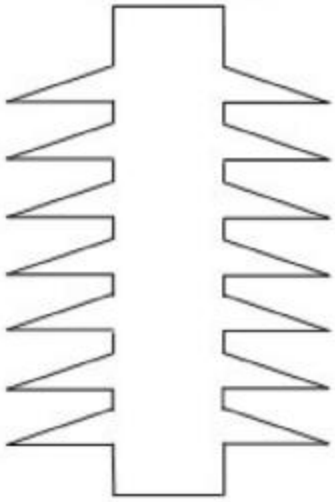

Figure 5 Reference Model

Table 2 shows the dimensions of the sample insulator.

Table 2 Model Profiles

Insulator type	Long rod
Leakage distance (cm)	77
Shank diameter cm)	4.5
Shed diameter (cm)	12
Shed spacing (cm)	1.4

Figure 6 shows the comparison of critical pollution levels in terms of ESDD between proposed model and published literature [22]. It can be seen from simulation results that present model gives the results that agree well with the reference. The largest

difference between two models is 7%. Similar results have also been obtained for other published literatures but are not shown here.

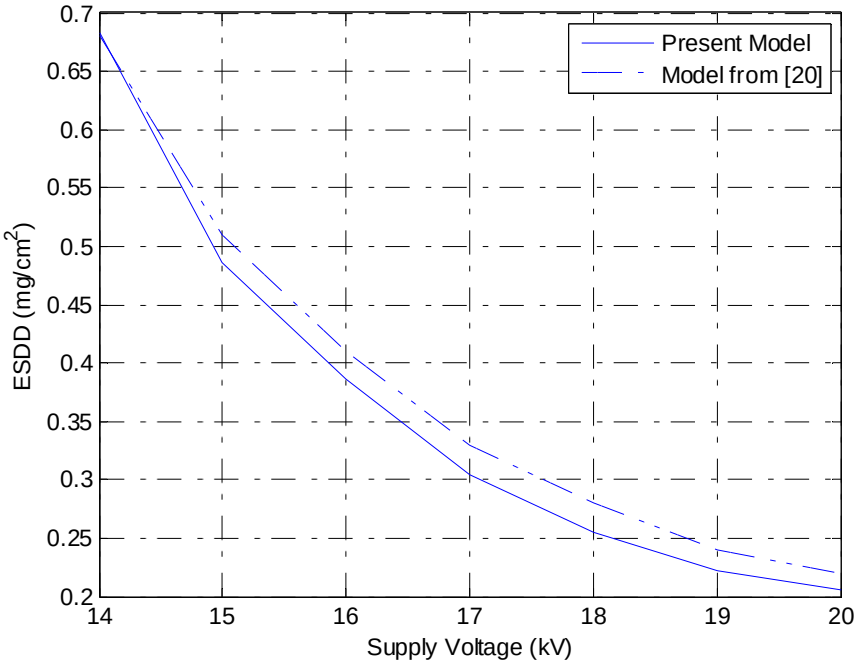

Figure 6 Comparison between Different Models

3.6 Simulation Results

3.6.1 Insulator Geometry

The insulator geometry used in this research is shown in Figure 7.

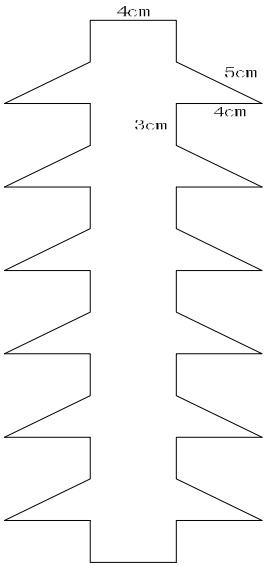

Figure 7 Insulator Geometry

The insulator profiles are shown in Table 3.

Table 3 Insulator Profiles

Insulator type	Long rod
Leakage distance (cm)	72
Shank diameter (cm)	4
Shed diameter (cm)	12
Shed spacing (cm)	3

3.6.2 Output Waveforms

The waveforms of insulator voltage, arc voltage, leakage current, arc distance, and arc velocity with respect to time are shown as results. It is recognized that the test voltage is sufficient to cause arc restrikes up to the critical length beyond which the arc elongates the insulator rapidly to reach complete flashover. In this case, the insulator flashover voltage at the pollution severity of $200\ \mu S/cm$ is 33 kV. The simulation results of outputs waveforms are shown in Figure 8.

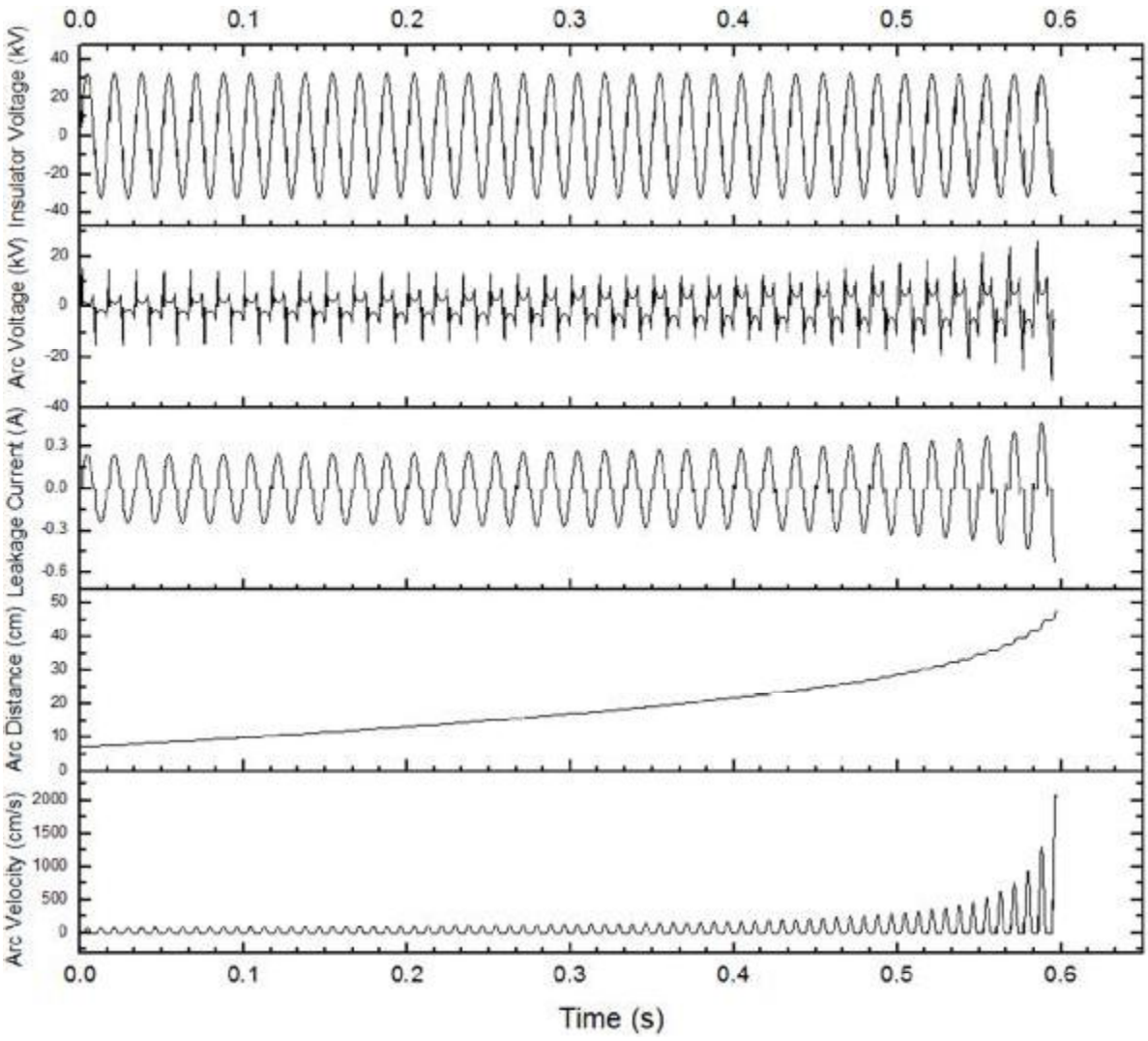

Figure 8 Simulation Results

3.6.3 Comparison of DC and AC Flashovers

For the same long rod insulator shown in Figure 7, a study of DC and AC energized flashover was performed as well. The DC flashover voltage was obtained from the DC dynamic model developed by Sundararajan [17]. The comparison of flashover voltages with AC and DC application with respect to different pollution severity is shown in Figure 9, and the DC/AC rms flashover voltage ratio is shown in Figure 10.

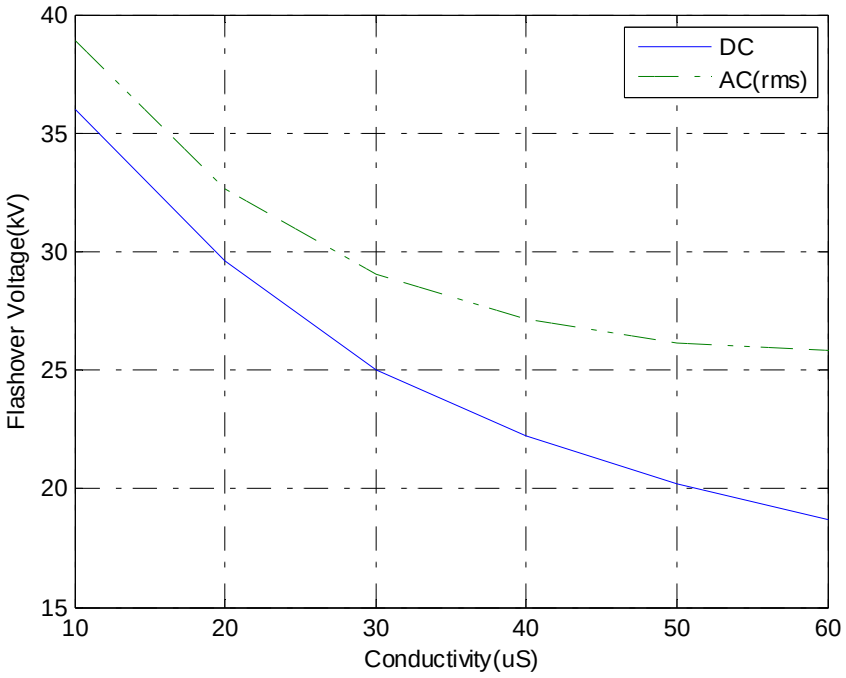

Figure 9 Comparison between DC and AC Flashover Voltage

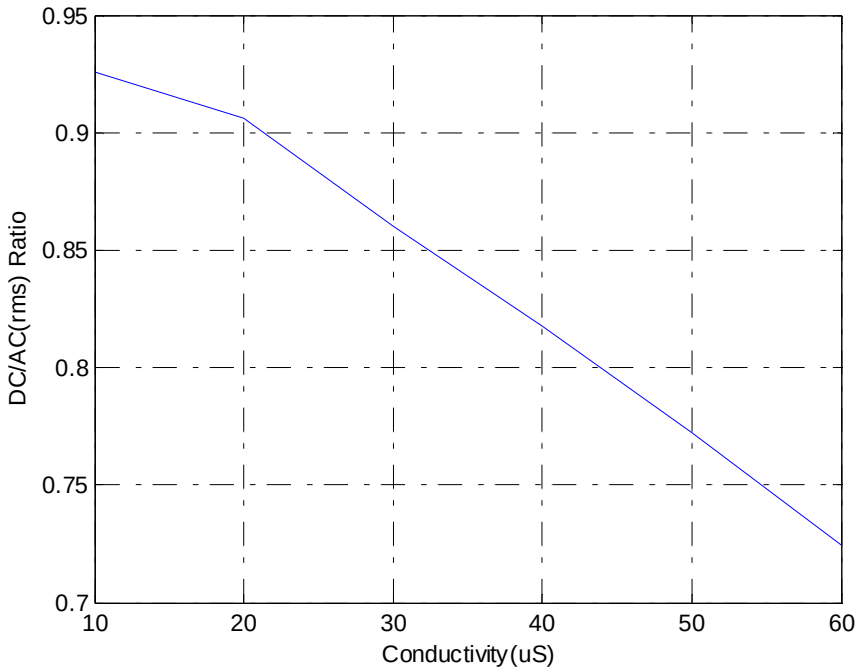

Figure 10 DC/AC Flashover Voltage Ratio

From comparison results, it can be seen that DC flashover voltage is lower than AC flashover voltage under the same contamination condition. There is a tendency that a higher pollution degree will have a lower ratio of DC/AC flashover voltage. The simulation results agree well with other researchers' conclusions [23-25]. Moreover, DC flashover voltage is less than AC flashover voltage due to the following reasons:

1. There is no alternation of voltage with time in the case of DC flashover, arc tends to continue a longer time and propagate to a greater extent.

2. Heavier contamination density is observed in the case of DC because of the dust collection effect, which will result in a lower flashover voltage. Thus the DC/AC flashover voltage ratio obtained above could be even lower in practice given that the DC voltage has a greater attraction of pollutants on the insulator.

Chapter 4

STUDY OF SOURCE PARAMETERS

4.1 Problem Statement

The flashover performance of polluted insulators is usually evaluated by artificial pollution tests in laboratories to simulate the situations in service. However, there is a large dispersion of pollution test results among different high voltage laboratories [3]. The effects of source parameters on the insulator flashover voltage is believed to be the contributing factor.

Although there are several international standards on the source parameters for pollution tests available, there is no general agreement on the source requirements [7, 20]. Many researchers have been studied in this area, however, the interaction between the test source and the insulator is far from fully understood [15, 26-30].

4.2 Effects of Inductance on Flashover

Most studies of source parameters influence on flashover tests only focus on X/R ratio, no work on source inductance has been reported yet. Since there is a counter effect between inductance and capacitance, source inductance is expected to be an important factor as well.

The value of equivalent inductance varies among different high voltage laboratories. The reported typical range of this value is from 10 H to 80 H [31-32]. For a source of R = 3000 Ω, C = 1 nF, the effect of source inductance on flashover voltage is shown in Figure 11.

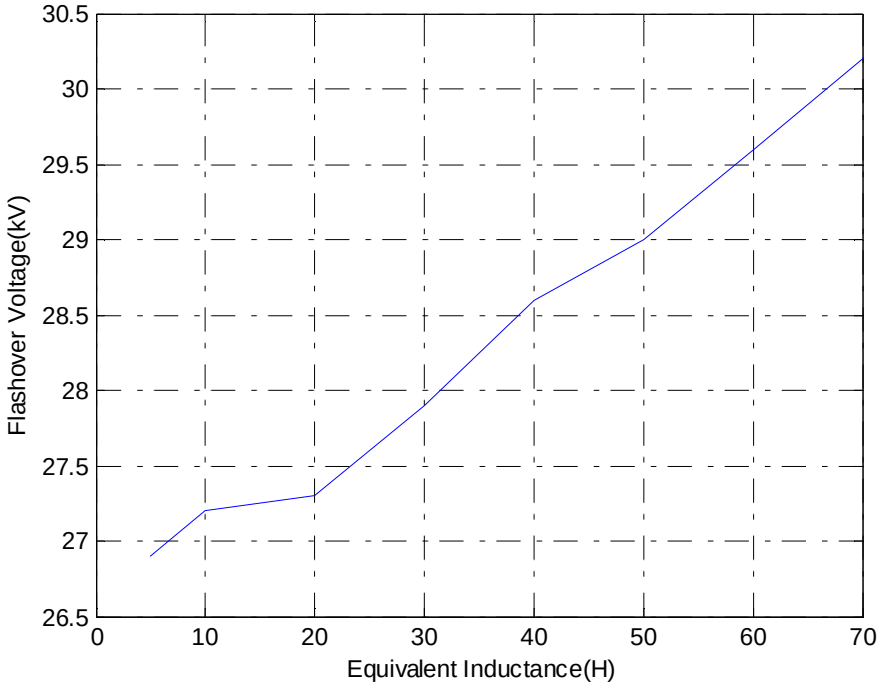

Figure 11 Equivalent Inductance Effect on Flashover Voltage

It can be seen from Figure 11 that larger inductance will lead to a higher flashover voltage. Moreover, it can be also noticed that there is an obvious difference between leakage current waveforms for different source inductance. It can be seen from Figure 12 that following current zero, the transient recovery voltage will result in an early arc restrike as it exceeds the dielectric strength of air gap. Following restrike and a rapid discharge of capacitor, large inductance will lead to a slow current build up which delays the instant of the current maximum value. As a result, partial arc is more likely to extinguish because insufficient current could be fed through the inductance to sustain the arc. For a small inductance case as shown in Figure 13, however, shows a different waveform with sharp arc current rise and no sign of current delay.

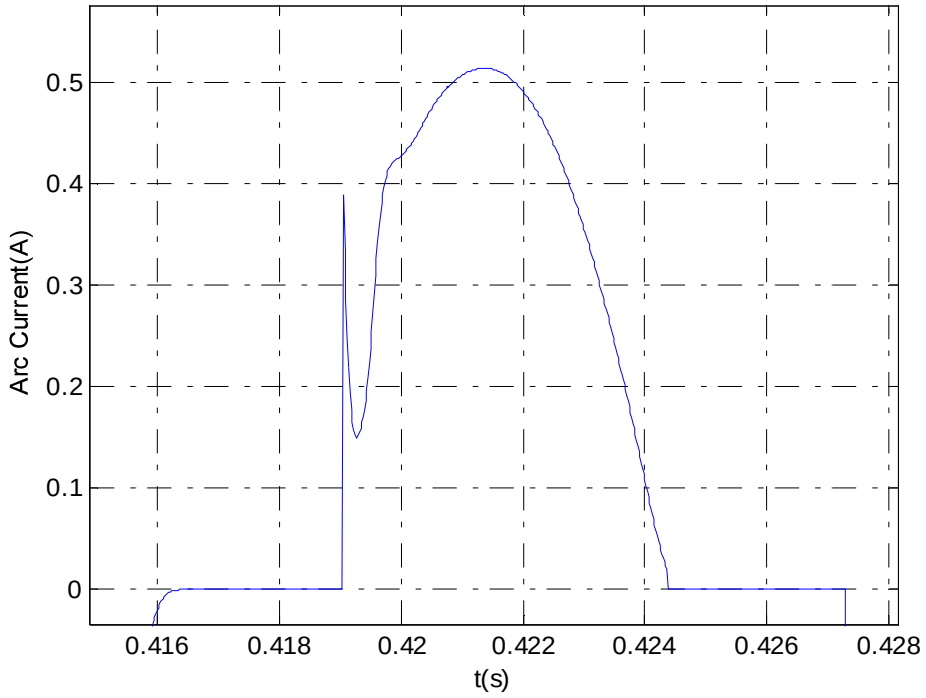

Figure 12 Arc Current Waveform under High Inductance

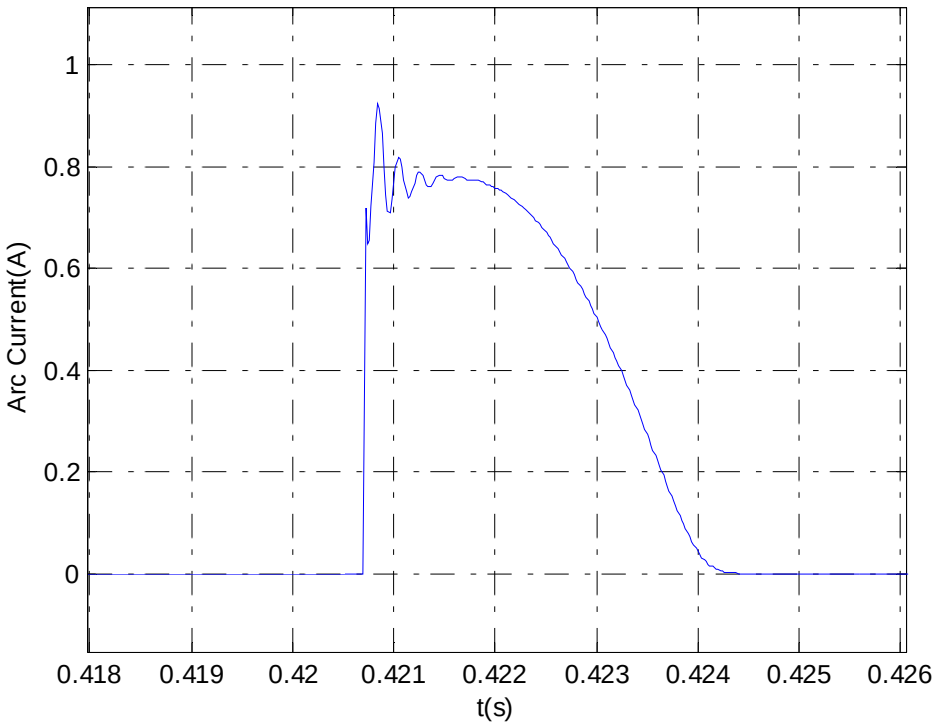

Figure 13 Arc Current Waveform under Low Inductance

4.3 Effects of Capacitance on Flashover

Special attention was paid to the effect of the equivalent source capacitance because there has been reported that it has a large influence on the flashover voltage. It is important to first study and compare the typical source capacitance values used in laboratories.

For AC and DC insulation tests, the requirements of source capacitances are different. The DC application requires an additional smoothing capacitance in order to convert AC output to DC supply. The reported capacitance values for AC application are shown in Table 4. The detailed information regarding source parameters of laboratories 1 to 4 can be found in reference [15], [26], [30] and [31], respectively. Laboratory 5 is the high voltage insulation laboratory in Arizona State University.

Table 4 Shunt Capacitance Values in Different Laboratories

Laboratories	Capacitor Value (nF)
1	0.3~3
2	1.1
3	1~20
4	3.2
5	0.5

The long-rod type insulator was studied to investigate the influence of capacitance on the flashover voltage. The simulation result is shown in Figure 14. From Figure 14, it can be seen that extra shunt capacitance in power source can lower the flashover voltage. This is due to the fact that after a restrike, insufficient capacitance will discharge so quickly that the current from the inductive source is unable to reach a high enough value to maintain the conduction in the spark channel. As a result, the arc will die out and increase the flashover voltage.

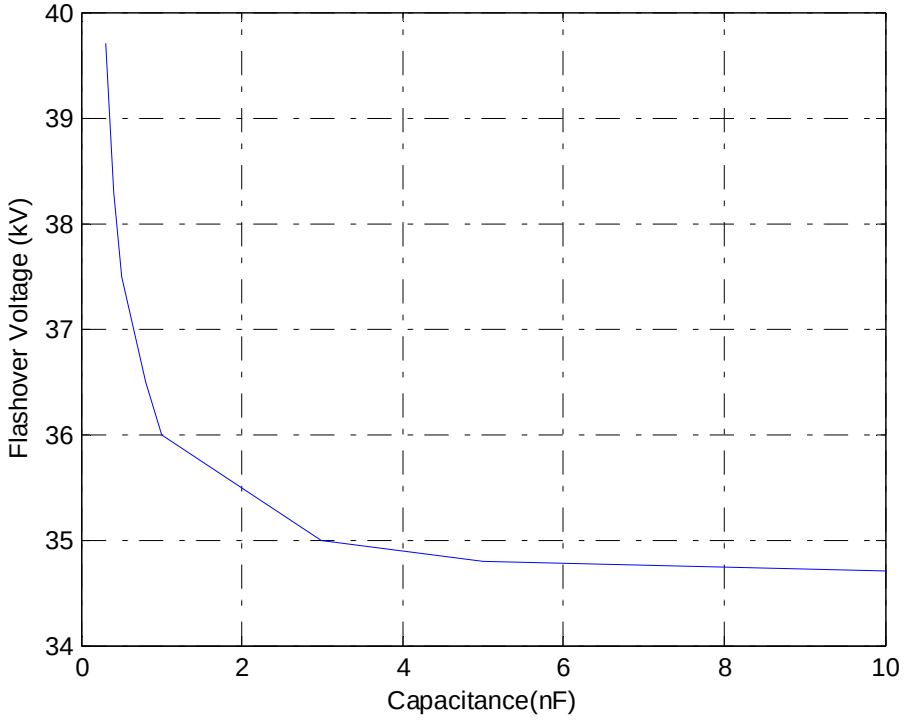

Figure 14 Shunt Capacitance Effect on Flashover Voltage

4.4 Effects of Short Circuit Current

The short circuit capacity is usually used to represent the power source strength. The short circuit current is defined by the following equation:

$$I_{sc} = \frac{I_{full\ load}}{Z\%} = \frac{S/V}{Z\%} \tag{26}$$

Test source with high short circuit current is considered as powerful source and weak source is the one has very limited short circuit current. IEC 60506 and IEEE Standard 4 both list a minimum requirements of short circuit current [7, 20]. Although the short circuit current has been reported in many published papers, detailed information of source impedances are not clear. For the purpose of providing a full information of power sources that are used in high voltage laboratories, calculation of test source impedance is performed with data obtained from published literatures.

From following tables, it can be seen that even for powerful sources in the laboratory, the maximum short circuit current is no greater than 50 A. On the other hand, the short circuit current in real power system is infinite ideally speaking or at least a few thousand amperes. Thus, it is reasonable to assume that the equivalent impedance in the field is much smaller than that measured in laboratory.

Table 5 shows the information of AC power sources which used in insulator pollution tests obtained from [31].

Table 5 AC Power Sources Characteristics

Laboratory Source	Weak Source	Powerful Source
Rated Power	25 kVA	200 kVA
Rated Voltage	150 kV	200 kV
Short Circuit Impedance	3.07%	4.0%
R/X Ratio	0.36	0.1

From above parameters, the short circuit current and source equivalent resistance and inductance can be calculated, which is shown in Table 6.

Table 6 Calculated Source Parameters

Laboratory Source	Weak Source	Powerful Source
Short Circuit Current	5.43 A	25 A
Equivalent Impedance	27630 Ω	8000 Ω
Equivalent Resistance	9358.82 Ω	796.03 Ω
Equivalent Inductance	68.96 H	21.11 H

Table 7 shows the information of AC power source which used in insulator pollution tests obtained from [33].

Table 7 AC Power Sources Characteristics

Laboratory Source	Weak Source	Powerful Source
Rated Power	300 kVA	200 kVA
Rated Voltage	300 kV	200 kV
Short Circuit Impedance	7.0%	2.03%

From above parameters, the short circuit current and source equivalent impedance can be calculated, which is shown in Table 8.

Table 8 Calculated Source Parameters

Laboratory Source	Weak Source	Powerful Source
Short Circuit Current	14.29 A	50 A
Equivalent Impedance	21000 Ω	4060 Ω

Based on the developed long rod type insulator model, simulations were performed to study the flashover performance when it is energized by powerful and weak sources. The parameters for both sources are shown in Table 9.

Table 9 Source Parameters

Source Type	Weak Source	Powerful Source
Short Circuit Current	2 A	200 A
Shunt Capacitance	1 nF	1 nF
X/R Ratio	8	1

The research is focus on different waveforms of insulator voltage and current. For the powerful source, it can be seen that restrike takes place at very late stage with almost no sign of capacitor discharge. In the weak source case, however, it is clearly shows the existence of capacitive discharge with the restrike happening at an early stage.

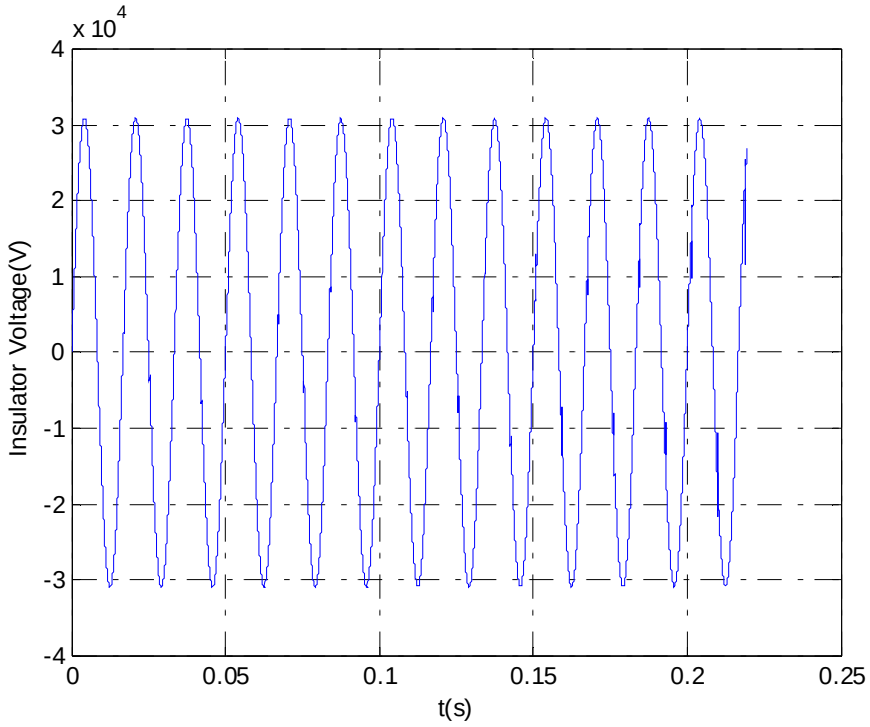

Figure 15 Insulator Voltage under Powerful Source

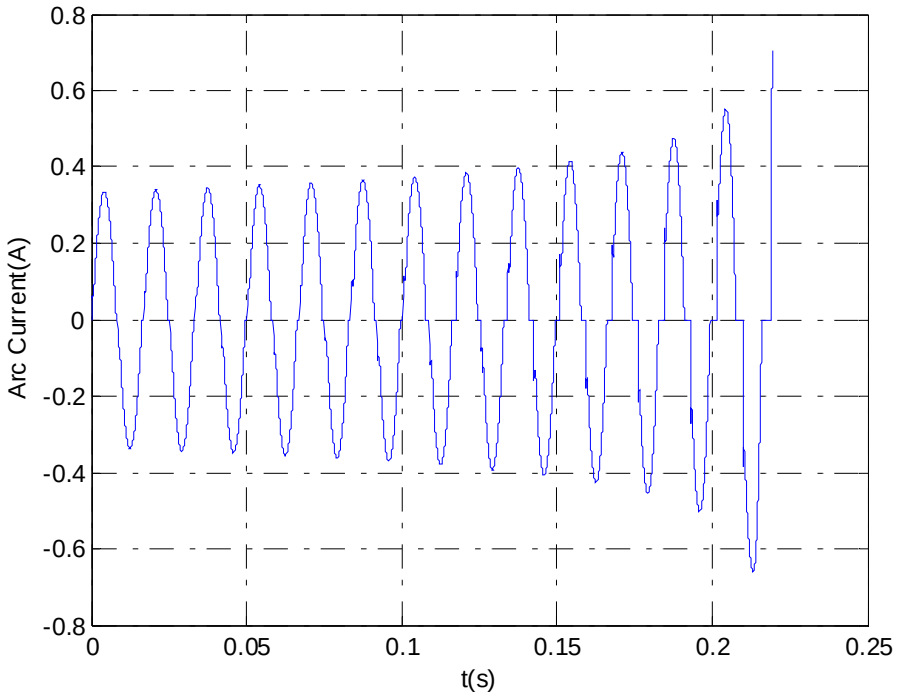

Figure 16 Arc Current under Powerful Source

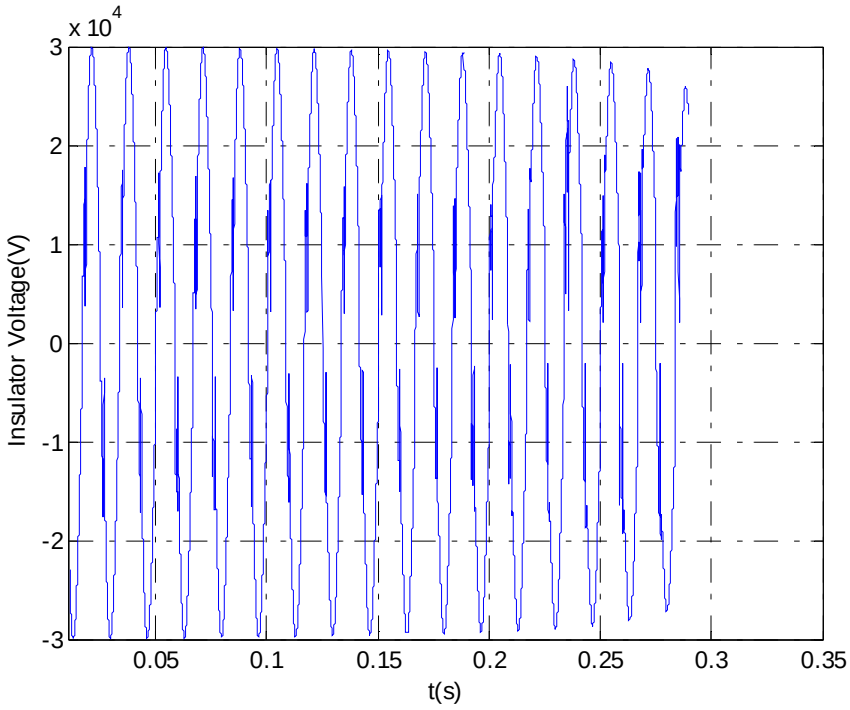

Figure 17 Insulator Voltage under Weak Source

After zoom in,

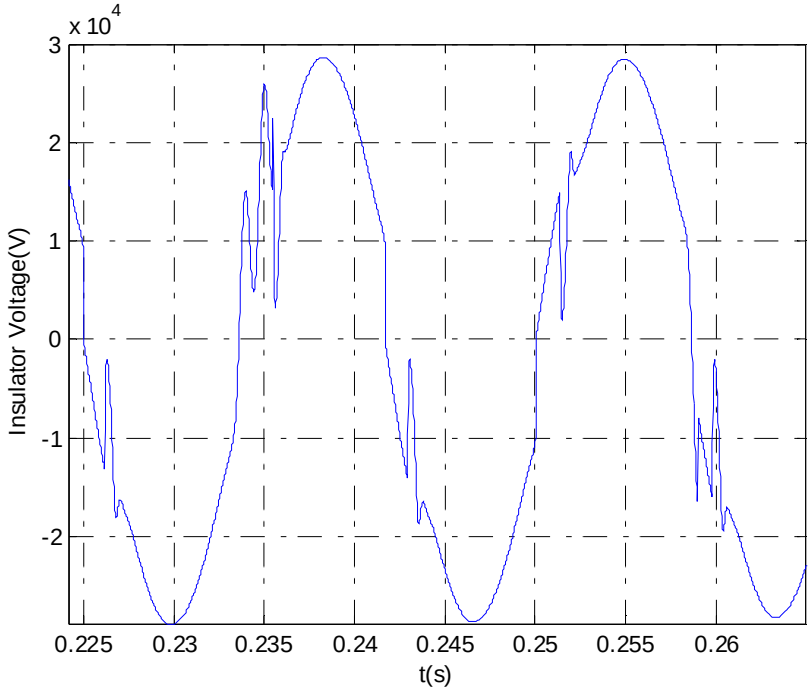

Figure 18 Insulator Voltage under Weak Source after Zoomed in

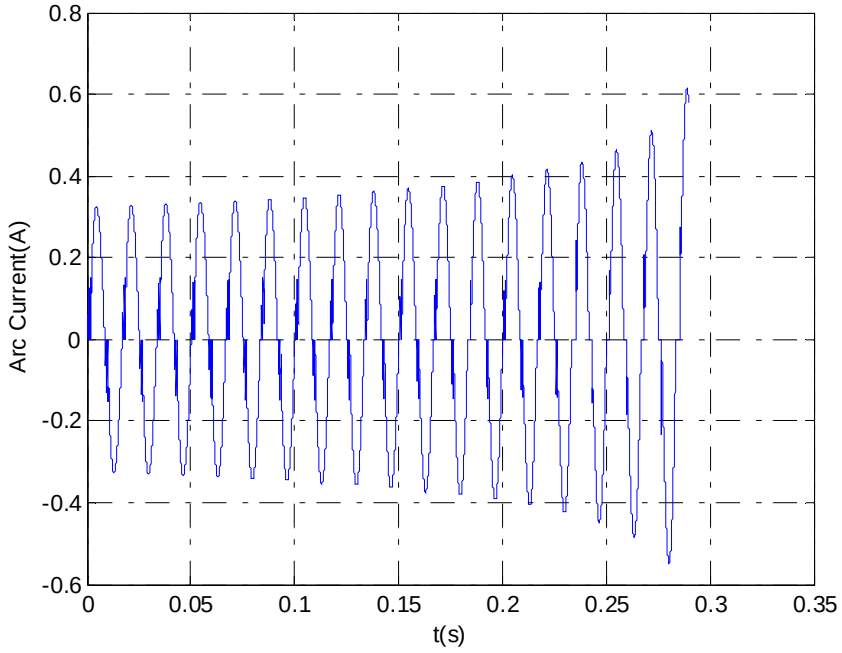

Figure 19 Arc Current under Weak Source

After zoom in,

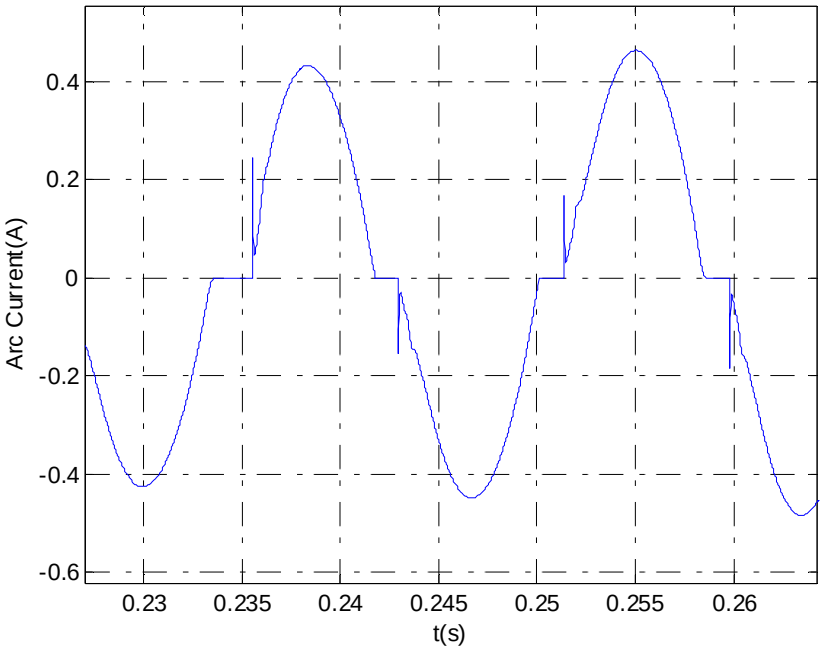

Figure 20 Arc Current under Weak Source after Zoomed in

The comparison between powerful source and weak source also has been done with respect to different source shunt capacitances. The source parameters used in this simulation are:

Table 10 Powerful and Weak Source Parameters

Test Source	Powerful Source	Weak Source
Short Circuit Current	1000 A	6 A
Equivalent Resistance	42.59 Ω	9358.82 Ω
Equivalent Inductance	0.24 H	68.96 H

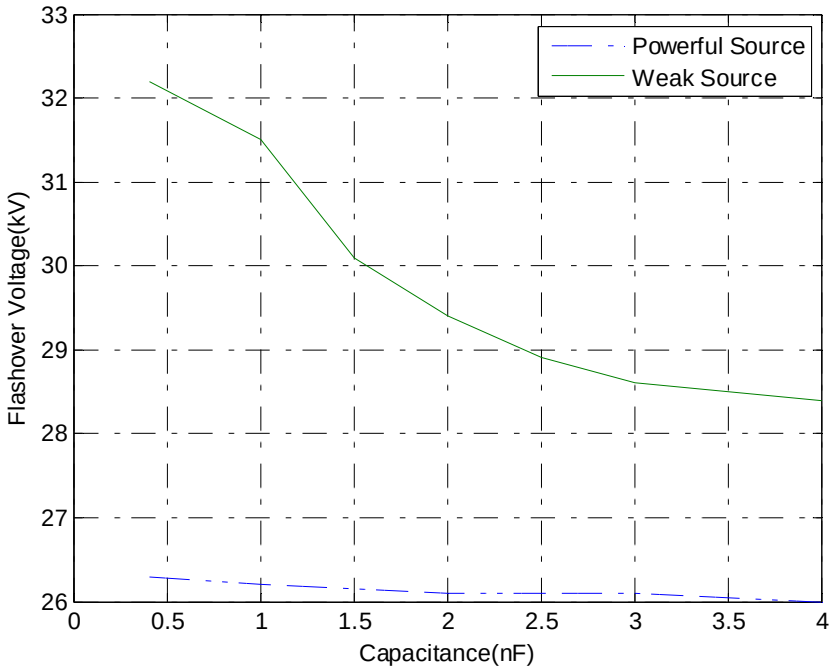

Figure 21 Source Strength Effect on Flashover Voltage

The percentage difference of powerful source and weak source flashover voltage is shown in Figure 22.

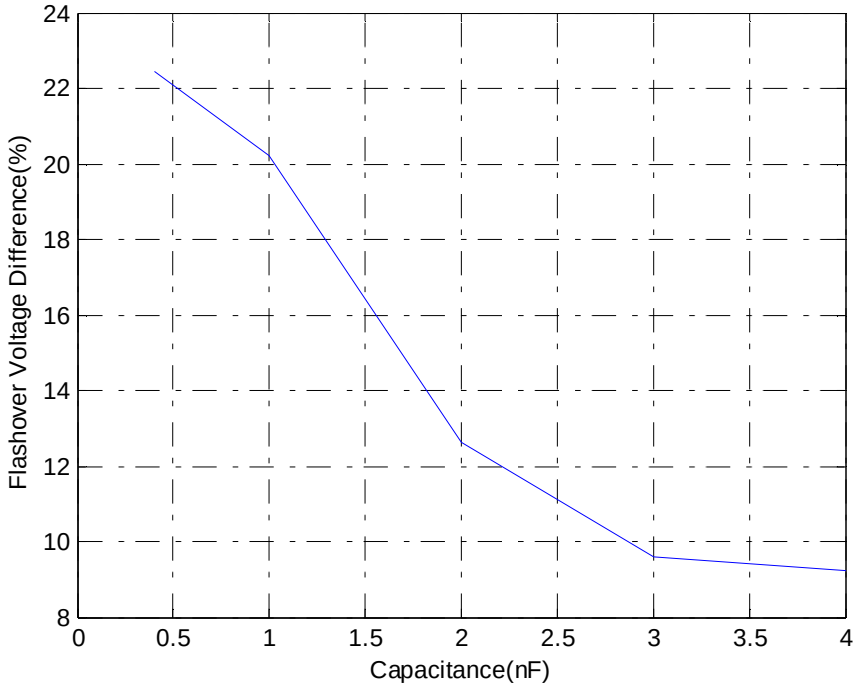

Figure 22 Percentage Flashover Voltage Difference

It can be seen from Figure 22 that the AC source with limited short circuit current will lead to a large voltage drop during the pollution tests and result in higher flashover voltage. Flashover voltage obtained by the weak source can be as high as 22% more than that energized by the powerful source. Extra shunt capacitance can partially mitigate the high flashover voltage caused by weak source, however, it has little influence on flashover voltage of a powerful source.

4.5 Conclusions

Several conclusions can be reached in this chapter:

1. A test source with high internal impedance directly interferes with the arc re-ignition process.
2. Capacitive discharge is essential for maintaining the arc until enough current can be fed through the source inductance to sustain the arc. In other words, shunt capacitance can lower the flashover voltage energized by a weak source, but has little effect on powerful source.
3. Simulation shows that power source strength has an influence on contamination flashover voltage. For a weak source, there will be a larger leakage current flows along the insulator surface than stiff source. This leakage current causes a large drop in the applied test voltage. Therefore, there is a possibility that a withstand voltage obtained from laboratory tests will be higher than that obtained in the field.
4. From another aspect, this means flashover can occur at a lower contaminant level if the source is powerful enough. Therefore, the testing power source should be as stiff as possible, and extra capacity of output capacitor is an effective method to achieve it.

Chapter 5

STUDY OF ARC JUMPING

5.1 Problem Statement

For most polluted insulator flashover models and the model developed in Chapter 3, they only consider the arc movement of propagating along the insulator surface. However, it has been observed that sometimes the local arcing will jump over sheds instead of following the insulator geometry surface [34-35]. The exact reasons and conditions to have arc jumping have not been fully known.

Arc jumping usually happens at insulator with complex closely spaced sheds, and it is more likely to be observed at high voltage stresses [34]. Because lightly polluted insulators require a high stress to initiate partial arcing, it is conceivable for some researchers that arc jumping between sheds may occur for lightly contaminated insulators [35].

Arc jumping is a phenomenon resulting from air breakdown, which happens after high electric field accelerates the free electrons around the insulator. The collision between atoms of air and the fast moving electrons cause more electrons to be freed. This will lead to electron avalanche which followed by the air around the insulator gets ionized. It is believed that arc most likely to happen at the water film-porcelain-air interface due to the non-uniform electric field distribution, and there is a threshold value of electric field exists for air breakdown [36]. Published literatures suggest that electric field value of 4.5 kV/cm is the threshold value to initiate positive streamer, and 11.5 kV/cm for negative streamer [37].

5.2 Simulation of Electric Field

In order to study the conditions to have arc jumping, electric field analysis was performed. The 3D electric field analysis software COULOMB, which is based on boundary elements method, was used to calculate the electric field distribution along the insulator [38]. The simulation process is discussed in following sections.

5.2.1 Simulation Setup

Considering the fact that insulators are rotational symmetric, only an angular section is needed to be investigated. The insulator geometry is first constructed in COULOMB, which is shown in Figure 23. The insulator profiles are shown in Table 11.

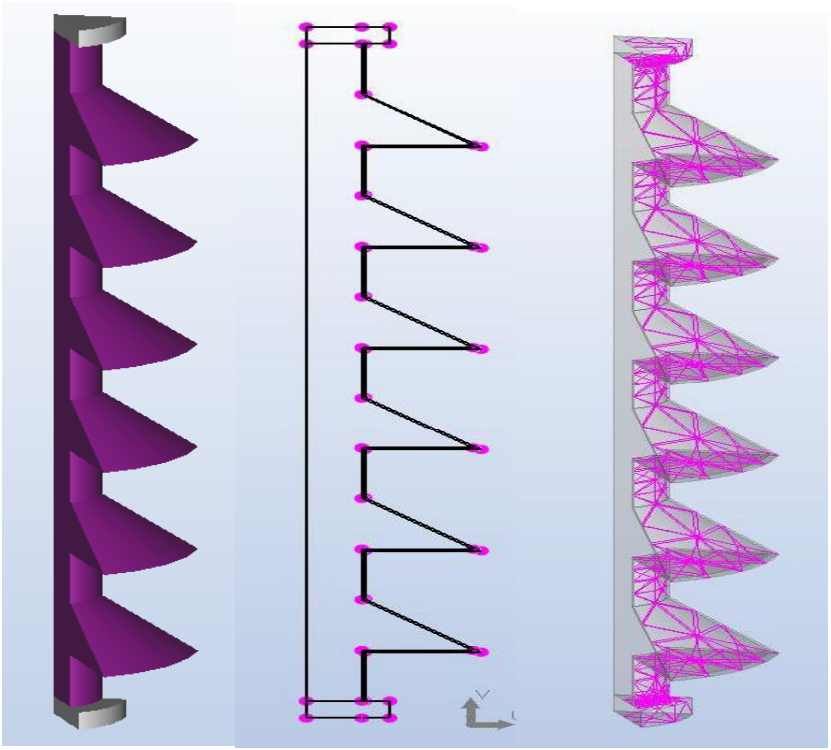

Figure 23 Insulator Model Developed in COULOMB

Table 11 Insulator Profiles Used in COULOMB

Arcing distance(cm)	39
Leakage distance(cm)	72
Shank diameter(cm)	4
Shed diameter(cm)	12
Shed spacing(cm)	3

After insulator geometry is specified, COULOMB allows the user to select or create material type of dielectric sections. The different parts of the insulator are assigned with different materials. The rated line-to-ground voltage is applied to the electrodes of the insulator and the angular periodic surfaces are defined. As stated earlier, COULOMB is based on boundary element methods to perform the electric field analysis. The number of boundary elements are assigned in next step to ensure accurate results. Triangular boundary elements are created on the insulator surface as shown in Figure 23. It is noted that more the number of boundary elements are simulated, the higher the solution accuracy is. However, when the boundary elements number is increased, the processing time to solve the electric field distribution will increase significantly. Therefore, it is desired to achieve a relatively accurate electric field solution without costing a lot of time. In this work, the maximum error is set as 5%.

5.2.2 Dry Insulator Case

The electric field distribution of an insulator under dry condition was first studied. The electric field was calculated along the line joining the tips of sheds of the insulator since the electric field is usually highest at the tips of the sheds. The variation in electric field is shown in Figure 24. It can be seen from Figure 24 that the highest electric field

value occurs at the first shed, and it decreases rapidly as the distance away from high voltage electrode.

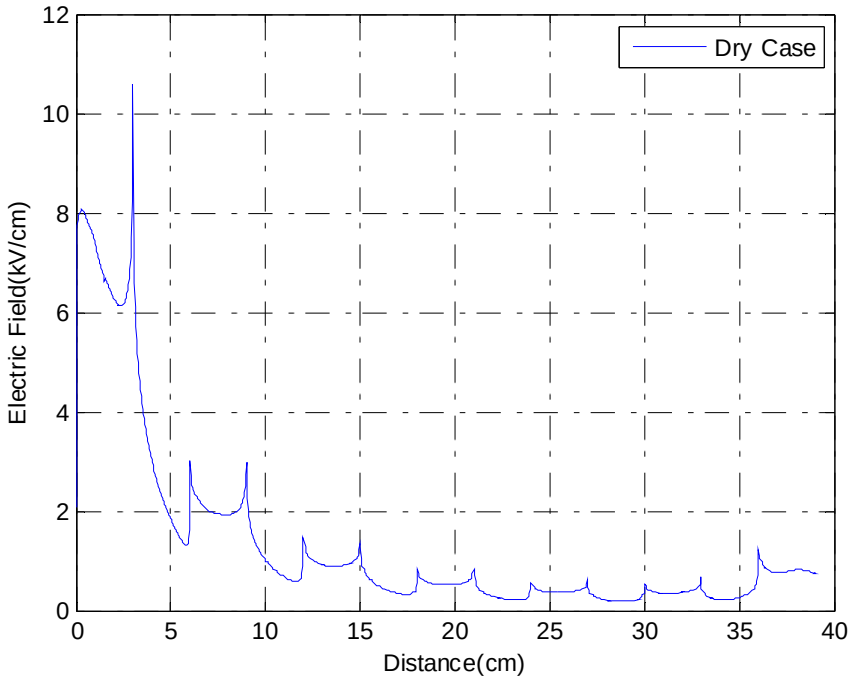

Figure 24 Electric Field Distribution under Dry Case

5.2.3 Wet Insulator Case

Because the arc jumping always happen when insulator is energized under wet condition, it is assumed that a 1 mm thickness water film exists on the insulator surface. The electric field distribution was calculated with respect to different surface conductivities. The simulation results are shown in Figure 25-27.

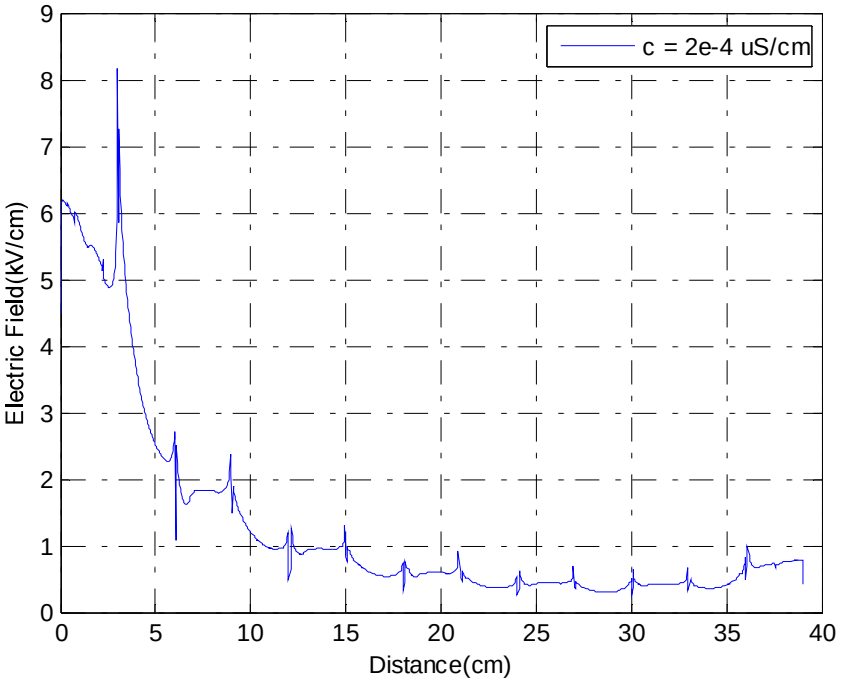

Figure 25 Electric Field Distribution under c = $2 \times 10^{-4}\ \mu S/cm$

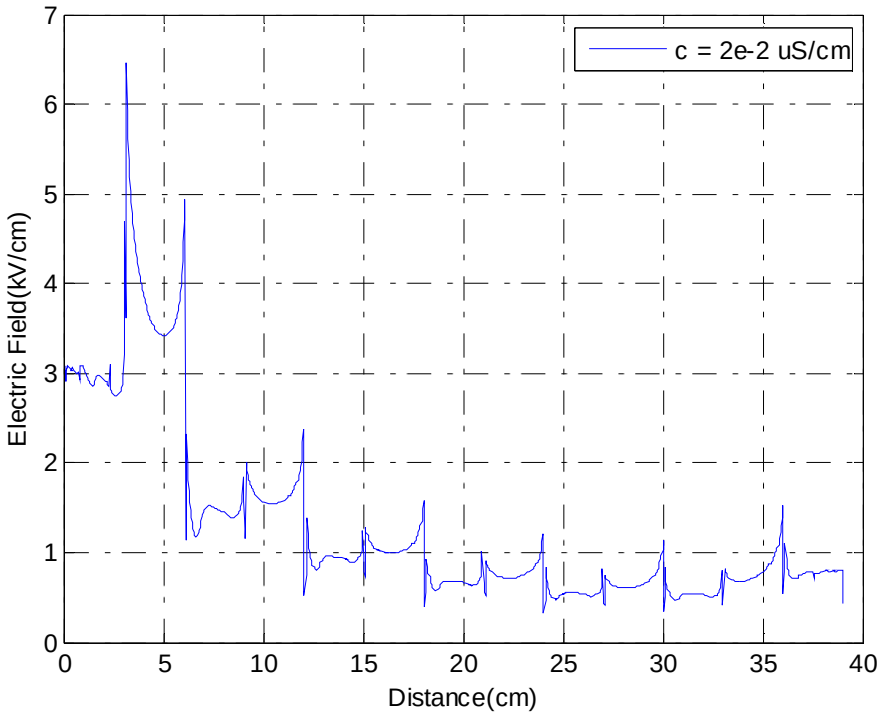

Figure 26 Electric Field Distribution under c = $2 \times 10^{-2}\ \mu S/cm$

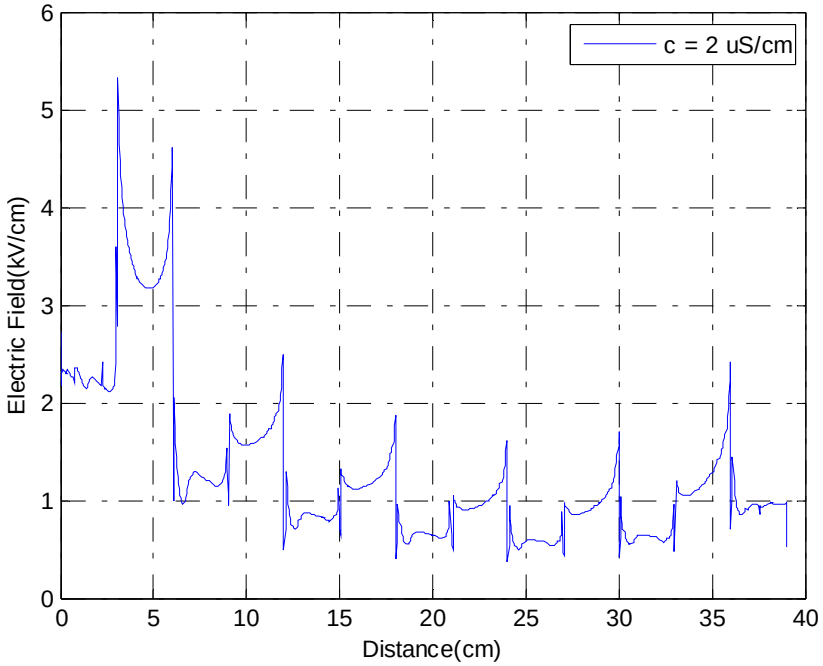

Figure 27 Electric Field Distribution under c = 2 $\mu S/cm$

5.2.4 Error Checks

The error of electric field simulation is calculated by taking the integration of electric field distribution with respect to insulator distance, and comparing it with applied voltage. The difference between the applied voltage and the calculated voltage is the electric field simulation error. The electric field calculation errors are shown in Table 12, which shows that simulation errors in all cases are under 5%. Therefore, the simulation results are believed to be reasonable and accurate.

Table 12 Simulation Errors

Conductivity ($\mu S/cm$)	Dry	2×10^{-4}	2×10^{-2}	2
Error (%)	3.07	1.98	0.96	0.89

5.2.5 Conclusions

There are some conclusions can be drawn from the electric field simulation. The electric field under dry condition is most non-uniform distributed. With the increasing of surface conductivity, the electric field distribution becomes more uniform and the maximum electric field value decreases.

5.3 Proposed Arc Jumping Mechanism

In electric field simulations, the dry insulator case has the highest voltage stress compares to all other wet cases. However, when the insulator is dry, there is no danger of either arc jumping or complete flashover. Moreover, from experimental pollution tests, it is noticed that arc jumping can happen at high conductivity condition as well. It is believed that voltage gradient is not the only requirement to have arc jumping.

In this study, it is proposed that the leakage current should also meet specific requirement in order to have arc jumping. A new arc jumping mechanism including both electric field and leakage current was proposed and explained in following.

Based on a practical method proposed by Holtzhausen, the potential gradient E next to the arc root, as a function of arc root position can be accounted for [13]. After regression analysis, the following relationship was obtained:

$$E = 0.495(1-x)^{-0.45} I R_P \tag{27}$$

where

x is normalized arc length

I is peak current in A

R_P is layer resistance in Ω

In this equation, the instantaneous voltage gradient is calculated through arc position and leakage current. This value is used to compare with the air breakdown threshold value.

5.4 Arc Jumping Simulation

5.4.1 Cylinder Insulator

A uniform polluted cylinder insulator with following profiles is studied first.

Table 13 Cylinder Insulator Profiles

Insulator Length	63.5 cm
Insulator Diameter	5.08 cm

There are two cases investigated in this study, with details shown in Table 14. The threshold value of air breakdown is selected as 8 kV/cm.

Table 14 Two Cases Studied in Cylinder Model

Case	Conductivity(μS)	Voltage(kV)
A	20	30
B	5	55

CASE A

The arc length is shown in Figure 28 and the calculated electric field near the arc root versus air breakdown threshold is shown in Figure 29. It can be seen from Figure 28 that the arc can only propagate along the insulator surface until approximately 30 cm due to the insufficient applied voltage. By comparing with threshold value, it is shown that the field strength at the end point is less than the air breakdown threshold, which means arc jumping will not happen in this case. As a result, the arc will extinguish.

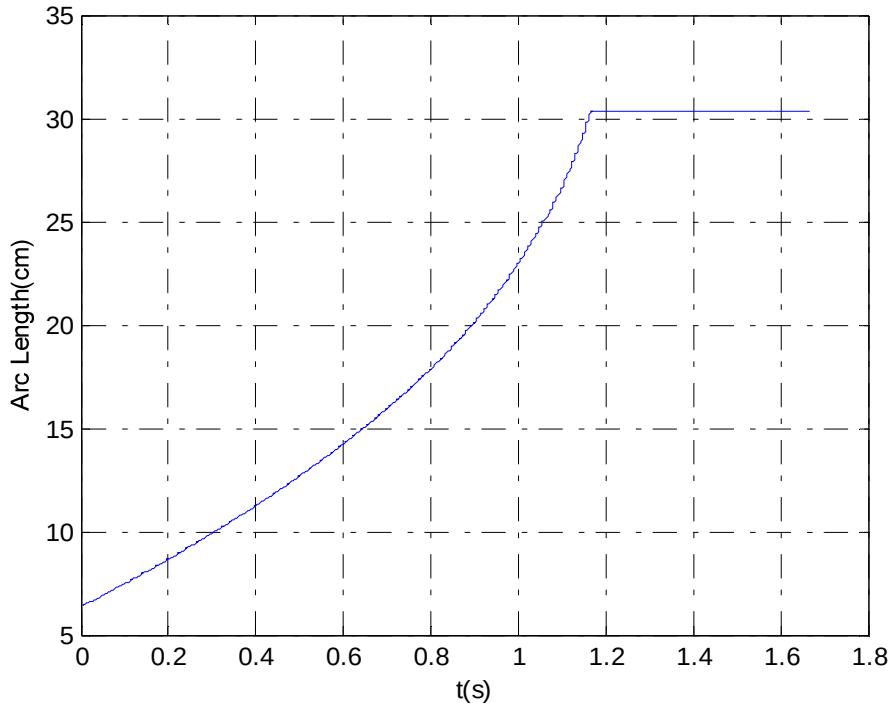

Figure 28 Arc Length for Cylinder Model Case A

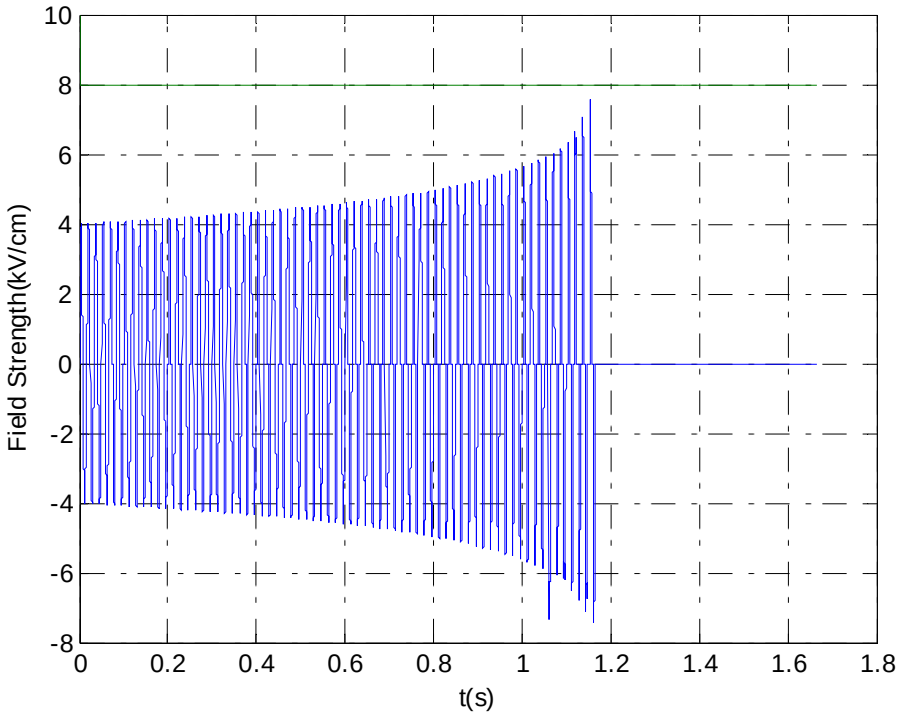

Figure 29 Field Strength for Cylinder Model Case A

CASE B

The arc length is shown in Figure 30 and the calculated electric field near the arc root versus air breakdown threshold is shown in Figure 31.

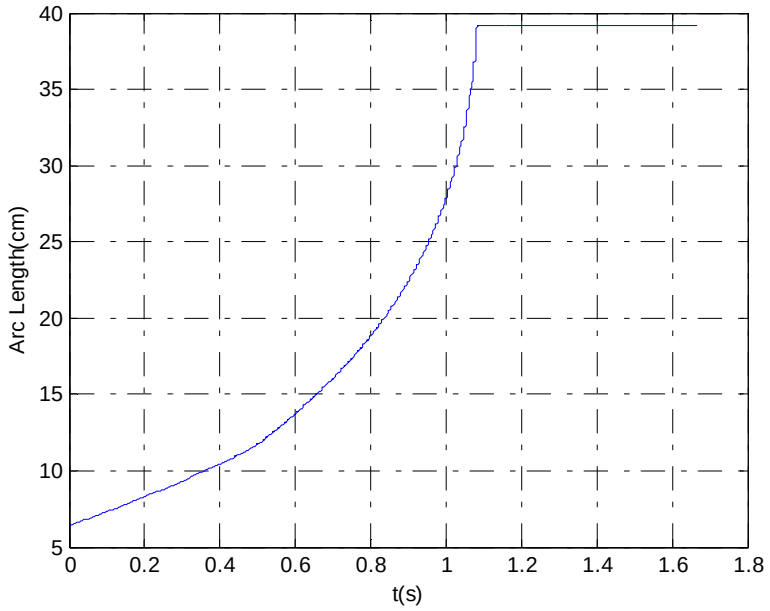

Figure 30 Arc Length for Cylinder Model Case B

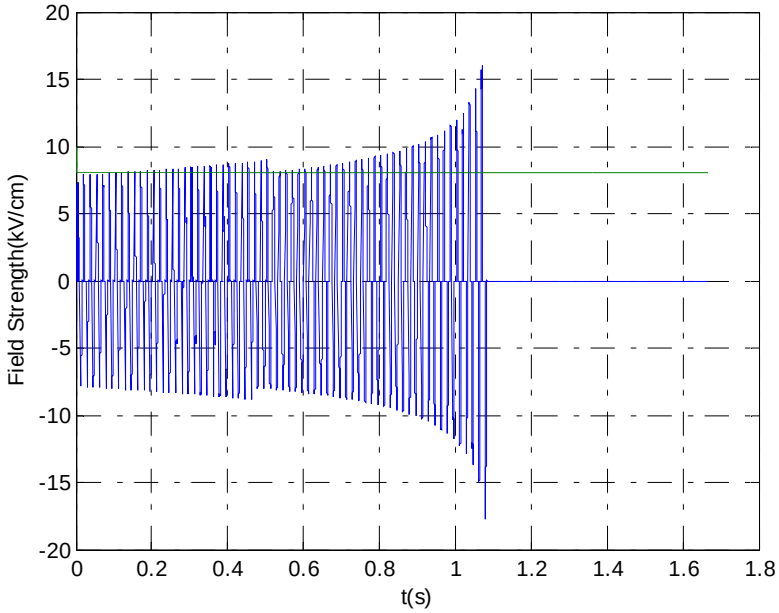

Figure 31 Field Strength for Cylinder Model Case B

It can be seen from Figure 30 that the arc can only propagate along the insulator surface until approximate 31 cm due to the insufficient applied voltage. By comparing with threshold value, it is shown that the field strength at the end point is greater than the air breakdown threshold, which means arc jumping can happen in this case. The arc will jump over the insulator and continue to extend.

From Case A, it can be seen that under high conductivity when arc cannot propagate along the insulator at one point, it is most likely that arc will extinguish. For Case B with relatively low conductivity, the arc will jump over the insulator instead if it cannot propagate along the surface.

5.4.2 Long-rod Insulator

The long rod insulator profiles are shown in Table 15.

Table 15 Long-rod Insulator Profiles

Leakage distance (cm)	72
Shank diameter (cm)	4
Shed diameter (cm)	12
Shed spacing (cm)	3

There are two cases investigated in this study, with details shown in Table 16. The threshold value of air breakdown is selected as 8 kV/cm.

Table 16 Two Cases Studied in Long-rod Insulator

Case	Conductivity (μS)	Voltage (kV)
A	20	40
B	10	50

CASE A

The arc length is shown in Figure 32 and the calculated electric field near the arc root versus air breakdown threshold is shown in Figure 33. It can be seen from Figure 32 that the arc can only propagate along the insulator surface until approximate 44 cm due to insufficient applied voltage. By comparing with threshold value, it is shown that the field strength at the end point is larger than the air breakdown threshold, which means arc jumping will happen in this case.

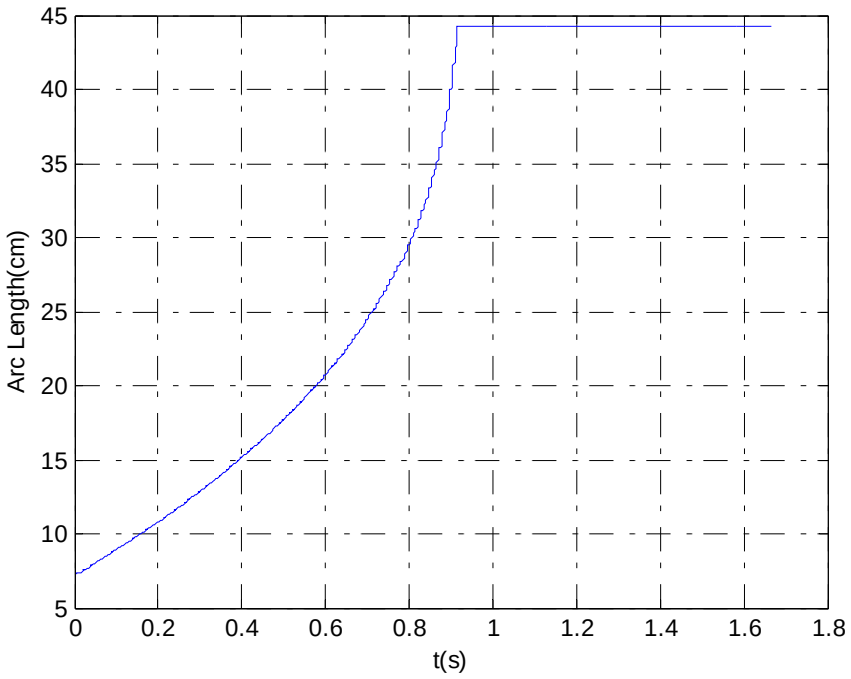

Figure 32 Arc Length for Long-rod Model Case A

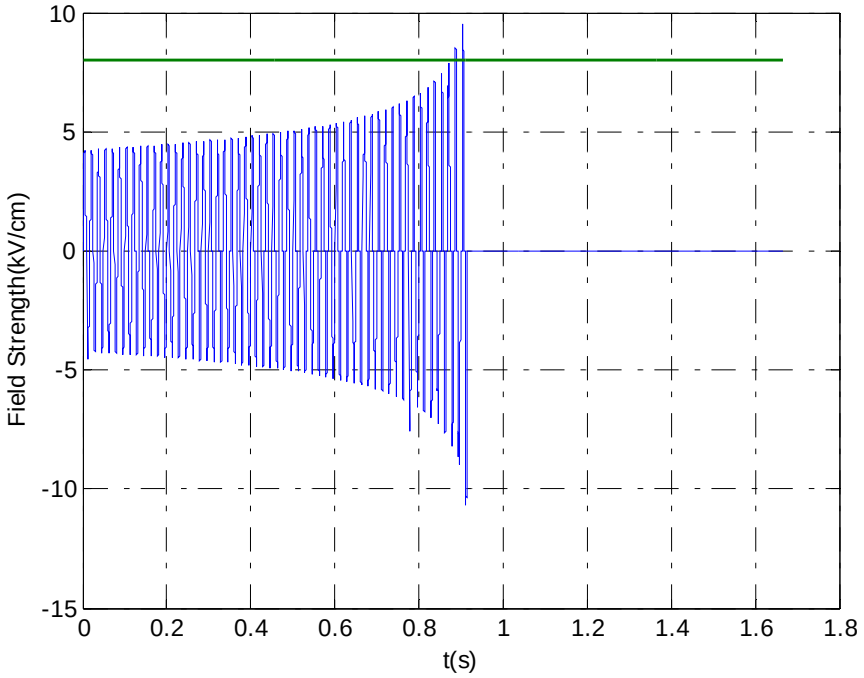

Figure 33 Field Strength for Long-rod Model Case A

CASE B

The arc length is shown in Figure 34 and the calculated electric field near the arc root versus air breakdown threshold is shown in Figure 35.

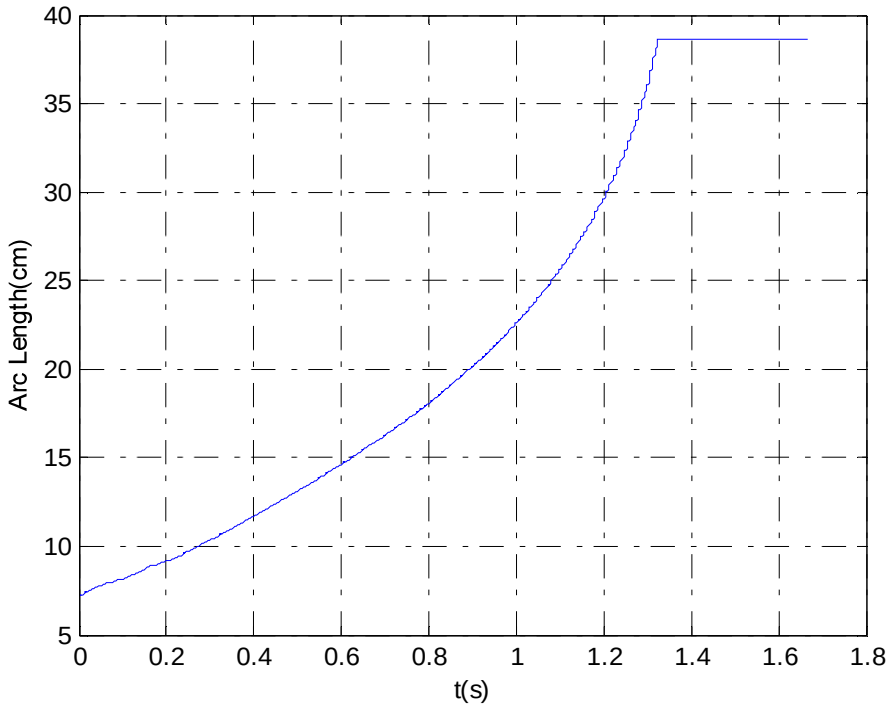

Figure 34 Arc Length for Long-rod Model Case B

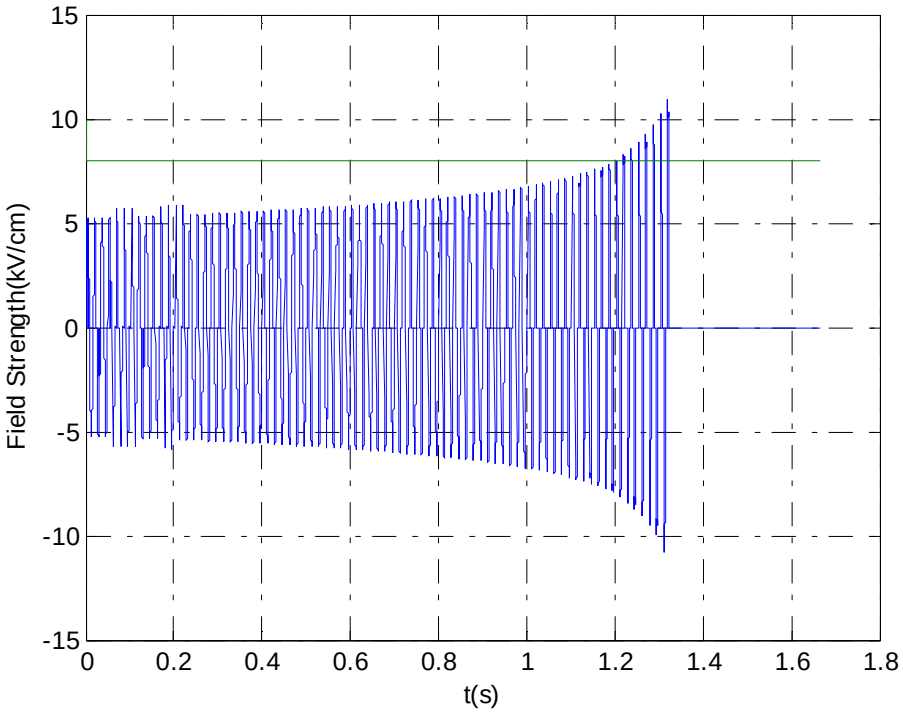

Figure 35 Field Strength for Long-rod Model Case B

It can be seen from Figure 34 that the arc can only propagate along the insulator surface until approximate 39 cm due to the insufficient applied voltage. By comparing with threshold value, it is shown that the field strength at the end point is greater than the air breakdown threshold, which means arc jumping can happen in this case. The arc will jump over the insulator and continue to extend.

5.5 Conclusions

Case A and Case B represent high and low conductivity, respectively. In the cylinder model, arc jumping can happen at low conductivity case but that is not the case with high conductivity. In the long-rod model, however, it shows that arc jumping can happen at both low and high conductivities conditions. As it already shown that electric field threshold criterion alone is insufficient to explain arc jumping phenomenon. With the new criterion accounting for both electric field strength and leakage current, it successfully shows that arc jumping can happen on heavily polluted insulator at certain conditions as well.

Chapter 6

FLASHOVER OF POLYMER INSULATORS

6.1 Polymer Insulators Flashover Mechanism

The flashover phenomenon of polymer insulators is fundamentally different than that of porcelain insulators because of the hydrophobicity property of its polymeric surface. This lead to a new flashover mechanism which can be classified into following stages:

1) Contamination build-up

There are two types of contamination: inland and sea pollution. Water droplets driven by wind first contaminate insulators near the sea. The pollutants contains salts and dirt, which are dissolved in the water droplets. When the insulator is new, its surface has perfect hydrophobicity which can only be covered by spot contaminations. However, the combined influences of dry band arcing and corona can reduce the hydrophobicity level. This will lead to the formation of continuous water films on insulator surface. For inland pollution, airborne particles generated by wind driven dust or industrial pollution are collected on the insulator surface. Later on, the contaminated surface will be wetted by dew and fog. Insulators usually covered by a uniform pollution layer in this type of pollution.

2) Diffusion of Low Molecular Weight (LMW) chains

This phenomenon is first reported by Karady [39]. Diffusion drives LMW polymer chains out of the bulk to the surface. The speed of this migration is controlled by the temperature and chain length. A lattice type layer is formed on the pollution surface by the LMW polymer chains. This phenomenon is very important since it allows the polymer insulator recover its hydrophobicity after 10 to 12 hours arc free period. Moreover,

hydrophobicity recovery can happen even the surface is still contaminated. This is due to the fact that LMW chains can penetrate the pollution layer.

3) Surface Wetting

It has been observed that there are two possible ways of wetting: migration of pollutant to the droplets or migration of water into dry pollutant. Migration of pollutant happens when diffusion drives the pollutant through the thin LMW chains of the insulator surface. Pollutants such as salt will dissolve in the water droplets making it conductive. The latter happens when diffusion drives water from the droplets through the polymer layer and into the dry pollutant. As a result, high resistive pollution layer will be formed and covered by conductive water droplets.

4) Localized discharges

After ohmic heating, the polymer insulator is covered by a high resistance layer, which is scattered with conducting water droplets. The intensification of electric field between the adjacent droplets produces surface discharges. These discharges are randomly distributed along the insulator surface at this stage.

5) Loss of hydrophobicity

The appearance of localized surface discharges can reduce hydrophobicity, which leads to irregular shape of wet regions. The reduction of hydrophobicity results in the droplets to form filaments. The filaments can be extended due to the high electric field stress. These wet regions are randomly distributed and appear as patches. The high resistance layer is surrounded and covered by water droplets.

6) Flashover

The enlargement of wet regions eventually connects the insulator with a conductive path. The arc can only extend on this path when the same arc propagation criterion ($E_{arc} < E_p$) is satisfied. The complete flashover is believed to take place when the arc distance is at least 2/3 of the insulator leakage distance, which is the same as porcelain insulator.

6.2 Flashover Mathematical Model

Due to the hydrophobicity property of polymer insulator, there is a fundamental difference of pollution flashover between polymer insulator and porcelain insulator. As a result, their mathematical flashover models should be developed differently as well.

It has been reported that silicone rubber insulator resists the formation of a continuous conductive layer, therefore limiting leakage current. Several experiments demonstrated that an initially hydrophobic polymeric surface was observed to be fully wettable after several hours of exposure to arcing [40]. The required time of this transition is determined by the dry band arcing activity. Flashover in polymer insulators usually occurred after their surfaces loses hydrophobicity and becomes wettable.

It is believed that for porcelain insulator there is usually only one long arc connecting in series with the residual pollution layer. The arc most likely to start from the high voltage electrode and end at the ground electrode. However, it is a different phenomenon for polymer insulator, as there are many discrete water droplets on polymeric surfaces. With the intensification of electric field by water droplets, many short arcs can form on a polymeric surface. These arcs will have cathode drops and anode drops, which in total about 900 V per arc [41]. Therefore, polymeric insulator will have a higher flashover voltage than porcelain insulator due to the existence of series arcs.

The applied voltage U can be written as:

$$U = V_{arc} + R_p(x) \cdot I + k(V_a + V_c) \tag{28}$$

where V_{arc} is arc voltage

$R_p(x)$ is pollution resistance

I is leakage current

k is the number of short arcs

V_a is anode drop

V_c is cathode drop

Based on this observation, the dynamic flashover model for porcelain insulator which developed in Chapter 3 was used as the basis for developing the new polymer insulator flashover model. According to Venkataraman's results [42], the arc constants for silicone rubber insulator are:

$$N = 340 \qquad n = 0.5 \tag{29}$$

The dynamic arc equation for polymer insulator becomes:

$$\frac{dr_a}{dt} = \frac{r_a}{\tau}\left(1 - \frac{r_a {i_a}^{1.5}}{340}\right) \tag{30}$$

where

r_a is arc resistance per unit length

i_a is arc current

τ is time constant

The required dielectric strength of a polymer insulator following arc extinction is:

$$U_d = xE_o\left[1 + \frac{51.9}{1 + \frac{157.5t}{{i_{max}}^{1.26}}}\right]^{-0.636} \tag{31}$$

where

x is gap length

E_o is dielectric gradient of a non-uniform field air gap at ambient temperature amounting to 5-6 kV/cm

t is time measured from current zero

i_{max} is arc current amplitude in the previous half cycle

With a lower leakage current, i_{max} for a polymer insulator will be lower than that of a porcelain insulator. Therefore, a higher U_d, or dielectric strength is required for arc reignition for polymer insulator, which results in a higher flashover voltage. Assume the same insulator test circuit in Figure 3, a similar dynamic system differential equations can be formed. Their solutions can be found by numerical methods for ordinary differential equations. Like porcelain insulator, Runge-Kutta method is used to obtain the numerical results.

6.3 Validation of Proposed Model

The model was validated by comparing the results with published literature. Using the dynamic model introduced in this work, flashover voltage characteristics of a polymer insulator can be simulated and compared.

6.3.1 Validation with a Silicone Rubber Insulator

The HTV silicone rubber insulator is selected from [42] with the geometry shown in Figure 36.

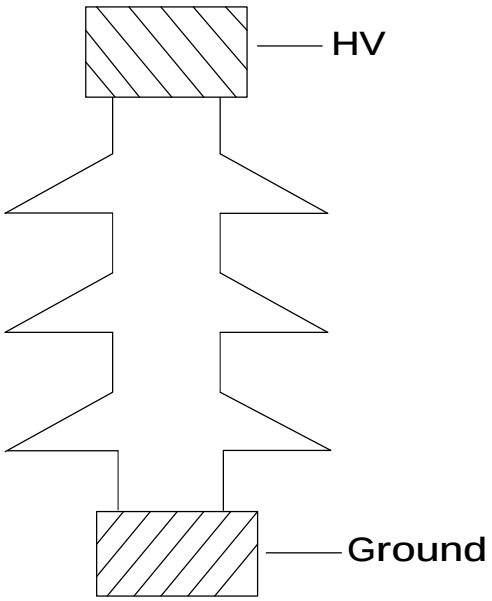

Figure 36 HTV Silicone Rubber Insulator

The dimensions are shown in Table 17.

Table 17 HTV Silicone Rubber Insulator Dimensions

Insulator Type	Silicone Rubber
Shed spacing (cm)	3
Shed diameter (cm)	9
Leakage distance (cm)	27

Based on the flashover model developed for polymer insulator, the simulation of above insulator was done. The simulation results and comparisons with published literature are shown in Figure 37.

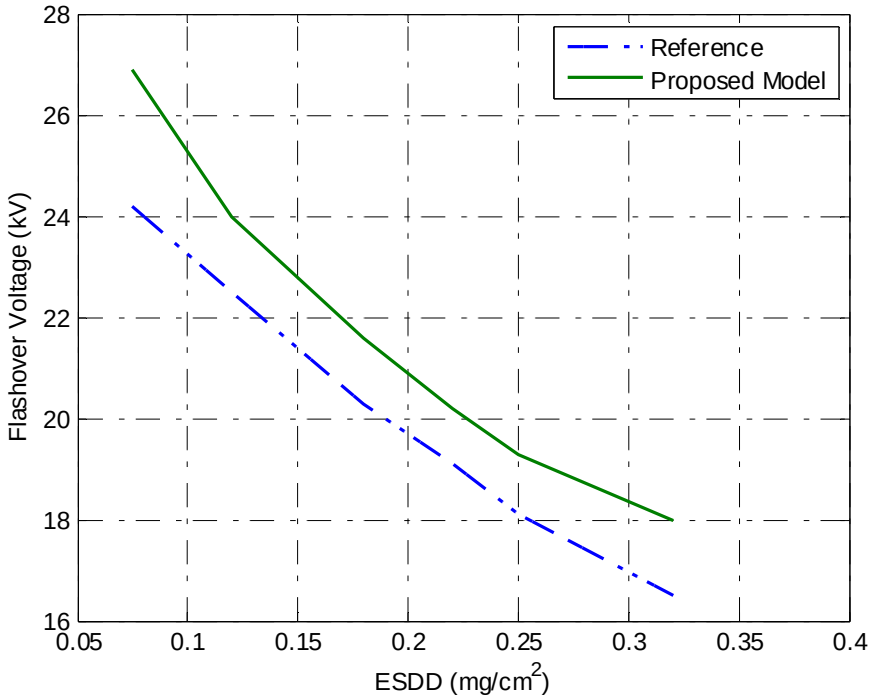

Figure 37 Comparison with Reference Model

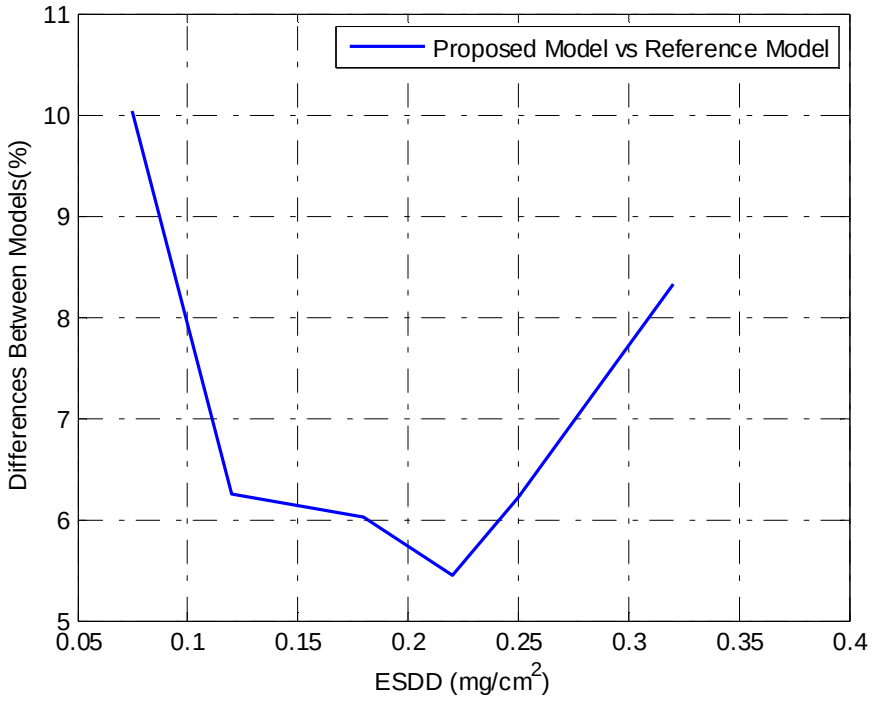

Figure 38 Percentage Difference of Silicone Rubber Insulator

From Figure 38, it can be seen that proposed model is well agree with the reference model, with the largest difference is about 10%. The reason that the smallest difference happens in the middle range of ESDD is because the flashover voltage at low and high ESDD in the reference are based on regression analysis instead of practical experiments.

6.3.2 Validation with Different Polymeric Materials

Figure 39 shows the configurations of insulator used in published literature [43]. The insulator dimensions are shown in Table 18.

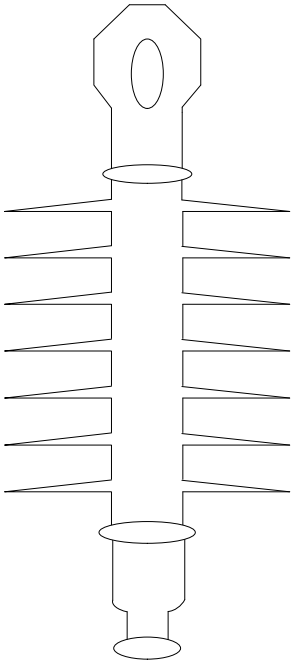

Figure 39 Polymer Insulator

Table 18 Insulator Dimensions

Insulator material	Polymer
Number of sheds	7
Shed diameter	126 mm
Trunk diameter	26 mm
Unit spacing	623 mm
Leakage distance	980 mm

Based on the flashover model developed for polymer insulator, the simulation of above insulator was done. The simulation results are compared with published literature which is shown in Figure 40.

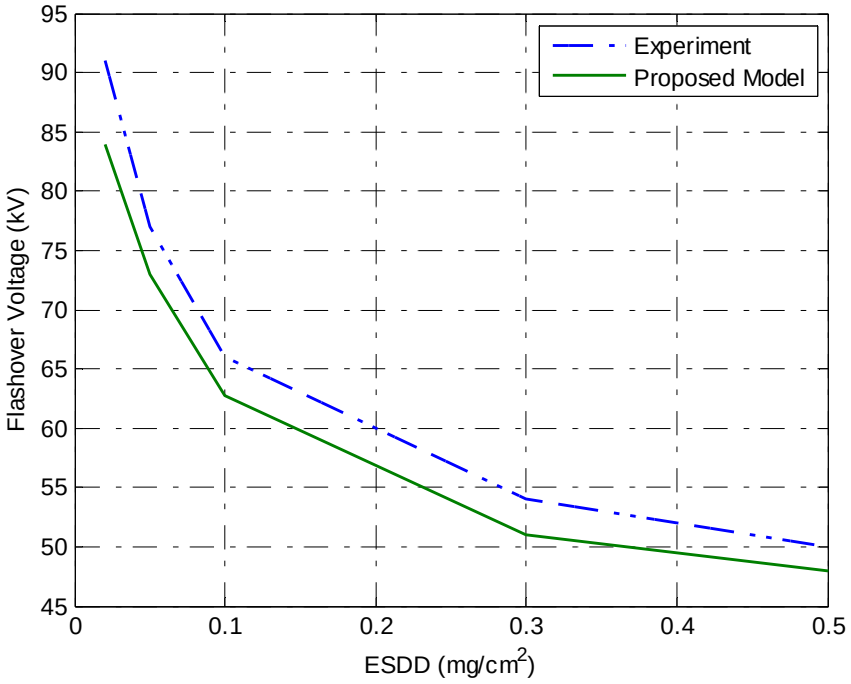

Figure 40 Silicone Rubber Insulator

The percentage difference of flashover voltage is shown in Figure 41.

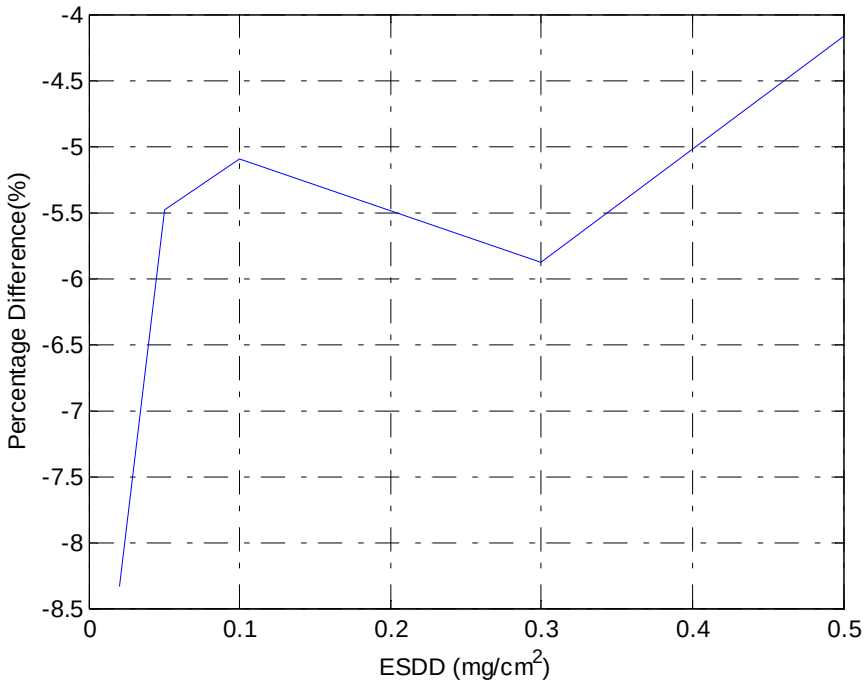

Figure 41 Percentage Difference of Polymer Insulator

For the same insulator sample, an EPDM insulator is also investigated in this research. The simulation results are shown in Figure 42-43.

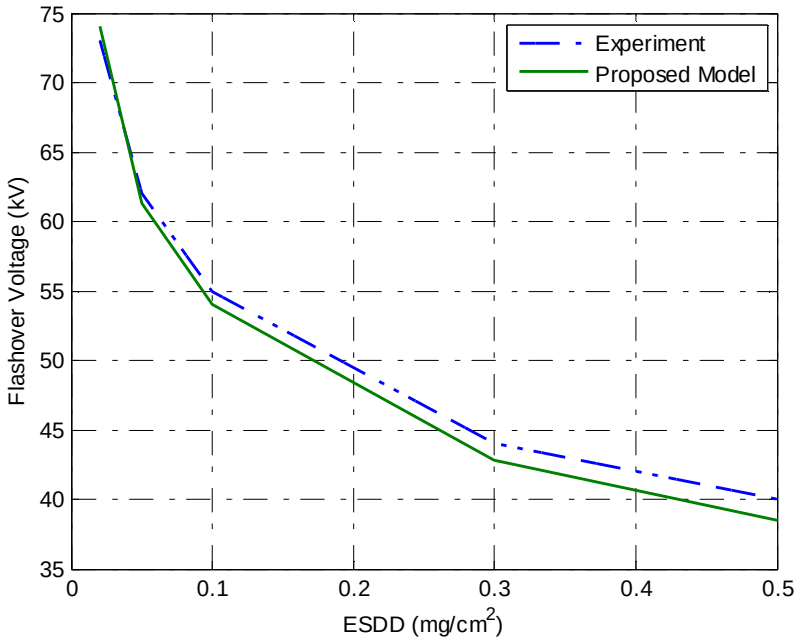

Figure 42 EPDM Insulator

The percentage difference of flashover voltage is shown in Figure 43.

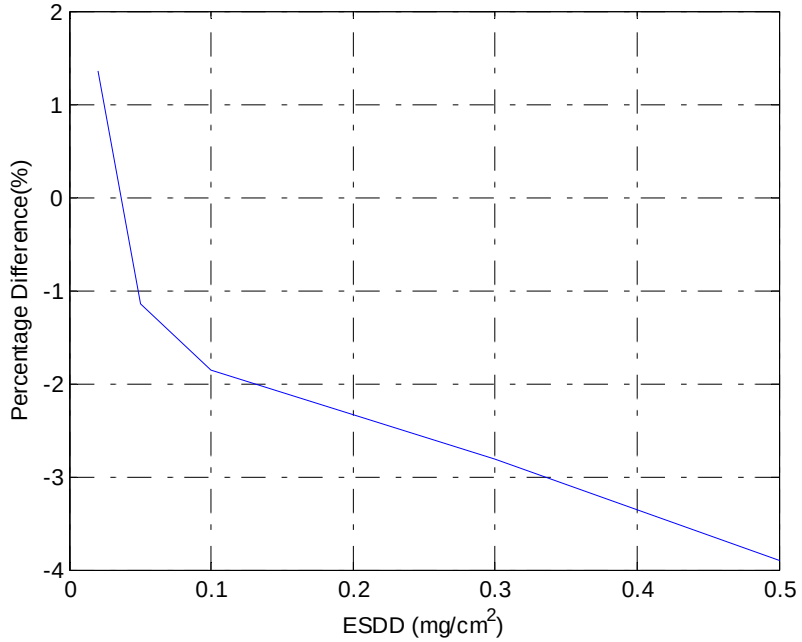

Figure 43 Percentage Difference of EPDM Insulator

From the simulation results it can be seen that for the sample silicone rubber insulator, the proposed model gives a flashover voltage about 4% to 8% lower than the published literature. For the sample EPDM insulator, the difference is less than 4%.

The comparison between silicone rubber insulator and EPDM insulator was also performed based on the proposed model. The results are shown in Figure 44.

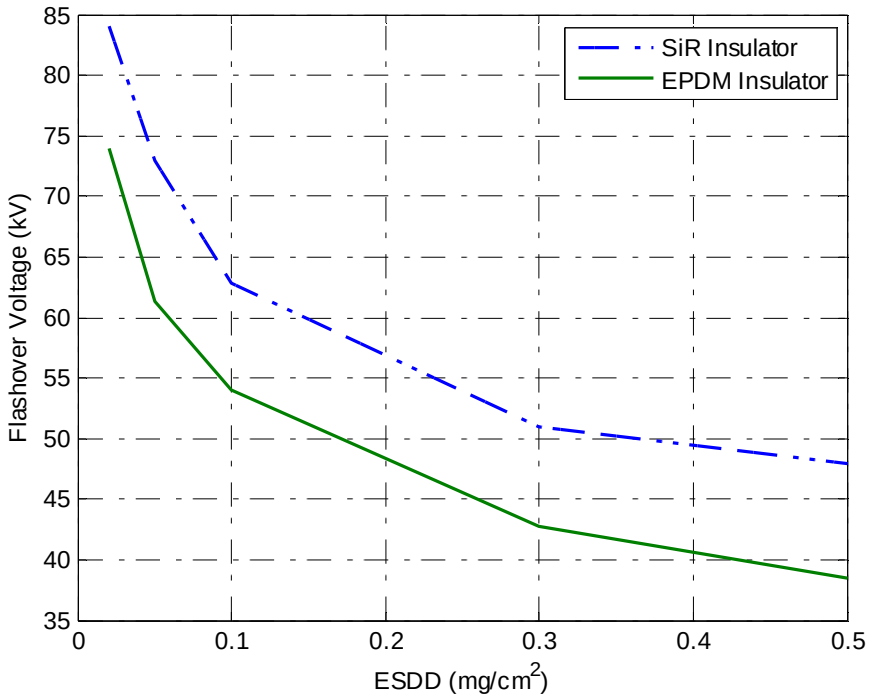

Figure 44 Comparison of SiR and EPDM Insulators

It can be seen from Figure 44 that under the same contamination level, silicon rubber insulator has a better flashover performance than EPDM insulator. For the studied ESDD range, silicone rubber insulator can withstand approximately 20% higher voltage than EPDM insulator.

6.4 Polymer Insulator Aging

6.4.1 Polymer Insulator Aging

Polymer insulators outperform traditional porcelain insulators in flashover performance due to their hydrophobicity property. However, polymeric materials are very susceptible to environment, where they interact and change over time. The degradation of polymeric material may result in polymer insulator aging.

Polymer insulator aging is a complex process which involved with a lot of factors. One hypothesis for polymer insulator aging is considered as a result of dry band arcing [44]. The aging mechanism can be categorized as following processes: dry band arcing leads to the loss of hydrophobicity; the reduction of Low Molecular Weight chains results in the increasing of leakage current on insulator surface; increased surface roughness promotes the wetting and leakage current as well; the tracking and erosion resistance is decreased due to the depolymerization of the top surface layers and changes of physical structure; in the end, there is the ultimate tracking and erosion of polymer material.

The understanding of aging is far from fully understood and there are serious concerns about the accuracy of existing aging models.

6.4.2 Hydrophobicity Classification

Service experience has shown that polymer insulators have better flashover performance than porcelain under polluted conditions [45-46]. This is due to the hydrophobicity of the polymeric material which is known to vary with time of exposure in service [47-48]. Swedish Transmission Research Institute (STRI) proposed a pictorial hydrophobicity chart which is now an IEC document [49-50]. When the polymeric material

is new, the hydrophobicity is maximum and is classified as Hydrophobicity Class 1 (HC 1). When the surface is completely wettable, it is classified as HC 7, or hydrophilic. Higher hydrophobicity class leads to a lower surface resistance, which will result in a lower flashover voltage.

In this work, polymer insulator aging process is categorized by its hydrophobicity classification (HC). When the insulator is new, its surface is completely hydrophobic with HC 1. After several years in service, it will gradually lost its hydrophobicity with a typical HC value at HC 3-4. In the end, the degradation of polymeric material will result in a HC level at HC 6-7.

Water exists as discrete droplets on polymer insulator surface. Even when the insulator loses its hydrophobicity, the arcing activity on polymer insulator is restrained compared to a wet porcelain insulator. The corresponding current is smaller than that on a porcelain surface [51].

Although the contact angle between the water drops and the surface is a good indicator of hydrophobicity class, it is not always possible to measure it in the field [52]. A correlation between hydrophobicity class and surface resistance is illustrated in this section.

The surface resistance of a cylinder can be described as:

$$R = \frac{4L}{\sigma\pi[(D+d)^2-D^2]} \tag{31}$$

where R is the surface resistance, L is leakage distance, σ is the surface conductivity, D is the mean value of shed and shank diameter, d is the pollution layer thickness.

The hydrophobicity of silicone rubber is due to a thin layer of low molecular weight (LMW) poly-dimethylsiloxane (PDMS) that diffuses from the bulk to the surface. The diffusion of LMW chains can be demonstrated as [52]:

$$d = \frac{M_t / M_o * \pi}{4 \sqrt[2]{Kt}} \tag{32}$$

where M_t is mass change at time t

M_0 is initial mass

t is time

K is diffusion coefficient.

The relationship between HC and surface resistance based on previous published experimental data can be described as [53-54]:

$$R = [(52 - 7 * HC)/45)] * R_0 \tag{33}$$

where R_0 is the surface resistance at HC 1

HC is the present hydrophobicity class.

6.4.3 Impact of Hydrophobicity on Flashover Performance

The model was validated by comparing results with published literature [43]. Figure 39 shows the insulator geometry modeled and Table 18 lists the important dimensions.

For the same insulator, the correlation between hydrophobicity class and ESDD was investigated based on equation (33). The completely hydrophobic (HC 1) was assumed to have an ESDD of 0.02 mg/cm^2 with short circuit current 50 A. The corresponding ESDD of the same insulator as a function of HC is shown in Figure 45. The hydrophobicity effect on flashover voltage is shown in Figure 46. Similar results can be found in recent published literature [55].

From Figure 45, it can be seen that with a base ESDD of $0.02\ mg/cm^2$ at HC 1, the corresponding ESDD at higher HC levels will increase gradually. Simulation results from Figure 46 shows that flashover voltage will decrease with the increase of hydrophobicity classification levels. For HC 7, the flashover voltage is about 62% of the flashover voltage at HC 1.

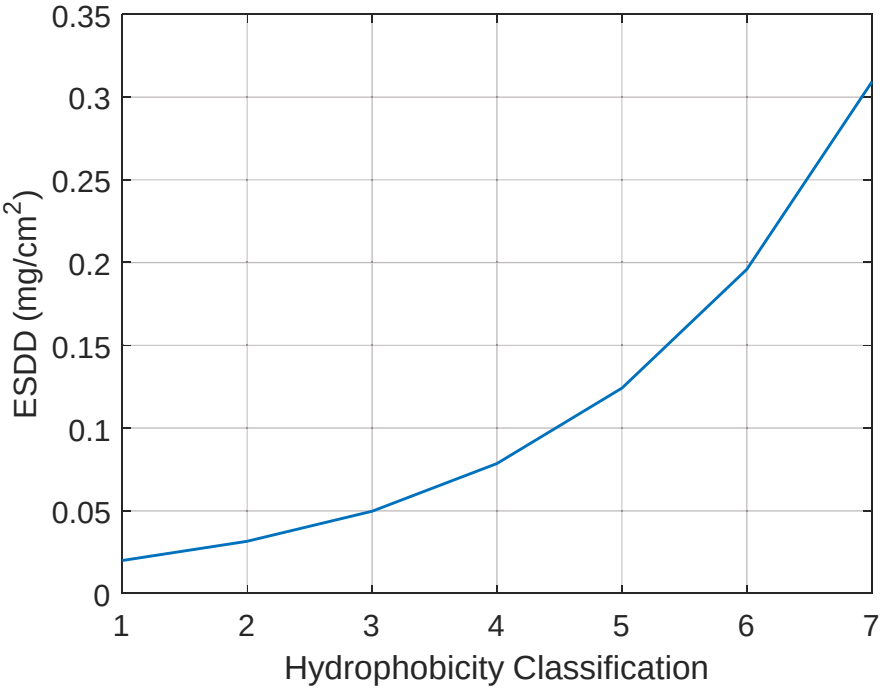

Figure 45 Relationship between Hydrophobicity Classification and ESDD

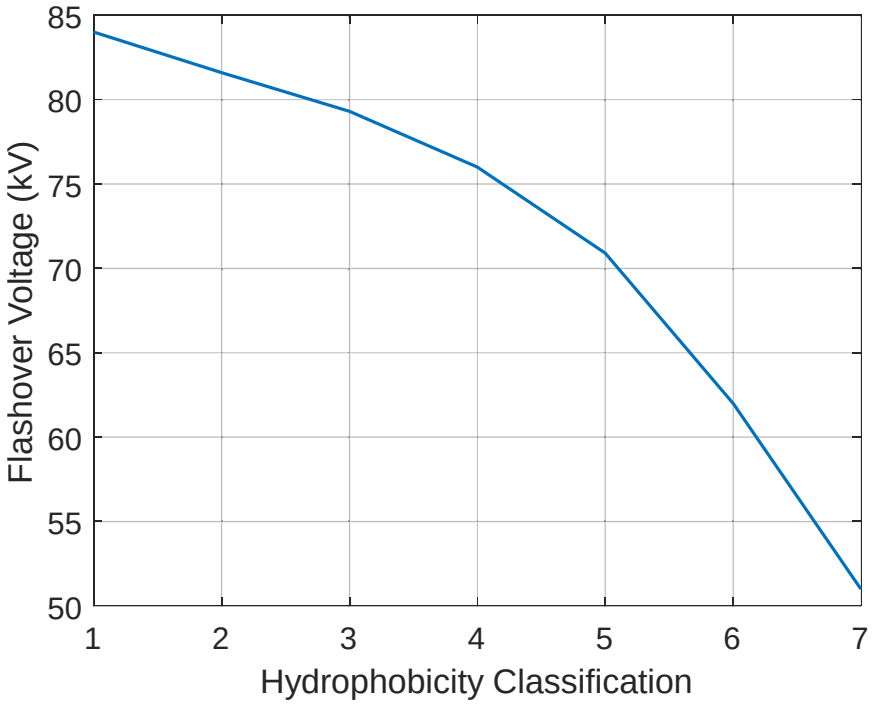

Figure 46 Hydrophobicity Classification Effect on Flashover Voltage

Chapter 7

SOURCE STRENGTH IMPACT ON FLASHOVER

7.1 Short Circuit Current Estimation

From Chapter 4, it was demonstrated that test source strength has significant influence on the insulator flashover performance. The short circuit current is a good indicator of a power source strength. A test source with high short circuit current is considered to be a powerful source and weak source is one that has limited short circuit current. IEC 60506 and IEEE Standard 4 both list recommended minimum requirements of short circuit current [5, 18].

From published data, it can be seen that even for powerful source in the laboratory, the maximum short circuit current is no greater than 50 A [3]. On the other hand, the short circuit current in real power systems is at least a few thousand amperes. To estimate the short circuit capacity of a practical power system, the IEEE 30-bus system as shown in Figure 47 was studied [56].

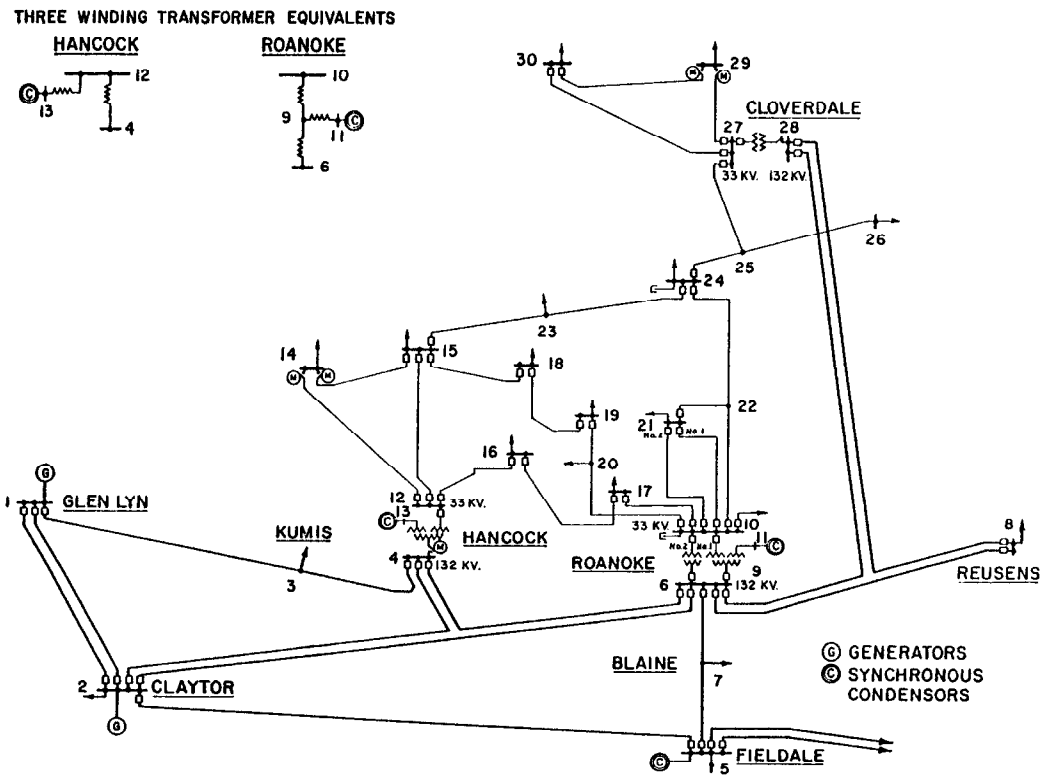

Figure 47 IEEE 30-bus System

A fault was created at different locations in the system. The short circuit was determined and used to calculated equivalent impedance parameters.

Table 19 Short Circuit Current Calculation

Fault at Bus	Short Circuit Current (p.u.)	Short Circuit Current (A)
1	5.4	2353
2	5.9	2585
3	5.1	2244
4	5.8	2531
5	4.9	2133
6	6.1	2675
7	4.9	2149
8	5.4	2383
9	4.4	254586
10	4.2	7295
11	3.3	17098
12	4.1	7237
13	3.4	17812
14	2.6	4613

15	3.4	6005
16	3.1	5441
17	3.5	6084
18	2.6	4563
19	2.6	4598
20	2.8	4816
21	3.6	6295
22	3.6	6250
23	2.6	4586
24	2.9	5113
25	2.2	3806
26	1.1	1948
27	2.3	4045
28	4.9	2136
29	1.3	2320
30	1.2	2154

Three different locations that have smallest short circuit current are shown in Table 20. The short circuit current results agree well with the published literature [57].

Table 20 IEEE 30-bus Test System Short Circuit Capacity

Fault at Bus	Short Circuit Current	Equivalent Resistance	Equivalent Inductance
26	1948 A	30 Ω	0.19 H
5	2133 A	17 Ω	0.12 H
28	2136 A	15 Ω	0.1 H

Other IEEE test cases including 14-bus and 118-bus were investigated as well. After the study of short circuit capacity of different IEEE test cases of practical power systems, the equivalent resistance was found to be in the range 12-52 Ω, and the equivalent inductance 0.1-0.7 H.

After test source short circuit current was determined, following test source parameters will be used throughout this chapter. For the power system in the field represented by a powerful source, it has a short circuit current of 1600 A, equivalent resistance 31 Ω, and equivalent inductance 0.3 H. For the laboratory power source, it is

represented by a relatively weak source with short circuit current at 16 A, equivalent resistance 7648 Ω, and equivalent inductance 51 H.

Table 21 Typical Source Parameters

Test Source	Power System	Laboratory
Short Circuit Current	1600 A	16 A
Equivalent Resistance	31 Ω	7648 Ω
Equivalent Inductance	0.3 H	51 H

7.2 Source Strength Impact with Respect to Source Capacitance

In this study, a NGK porcelain suspension insulator is used [43]. The insulator geometry is shown in Figure 48 and its dimensions are shown in Table 22.

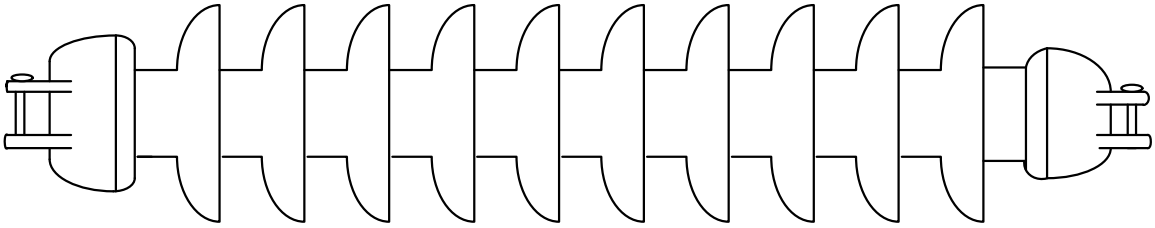

Figure 48 NGK Porcelain Suspension Insulator

Table 22 NGK Porcelain Insulator Geometry

Insulator material	Porcelain
Number of sheds	10
Shed diameter	160 mm
Trunk diameter	80 mm
Unit spacing	585 mm
Leakage distance	1020 mm

To begin with, the source strength impact on insulator flashover voltage with respect to equivalent capacitance was studied. With the contamination severity at 0.1 mg/cm^2, the simulation result is shown in Figure 49-52.

The simulation result of porcelain insulator is shown in Figure 49. The percentage difference of flashover voltage is shown in Figure 50.

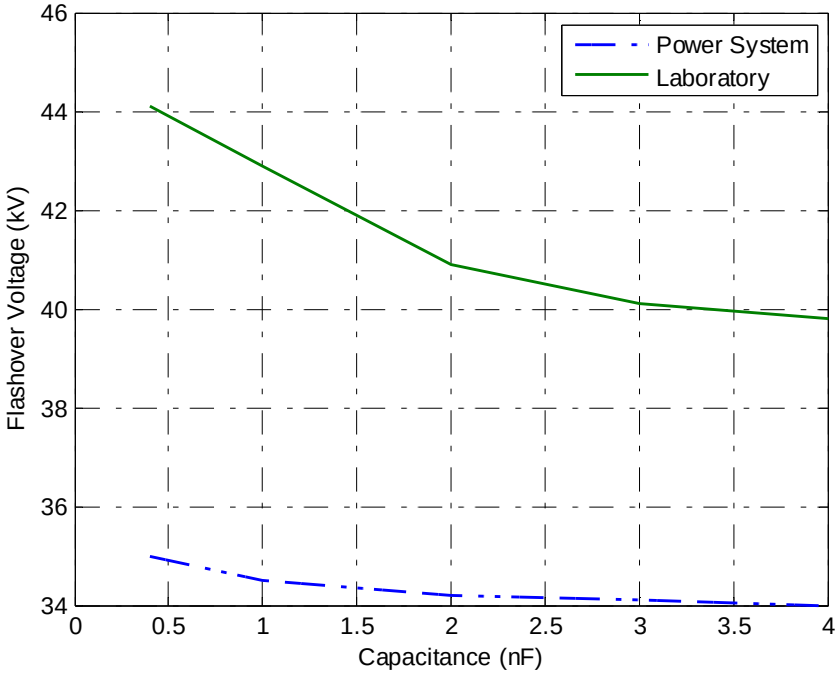

Figure 49 Source Strength Impact on Porcelain Insulator

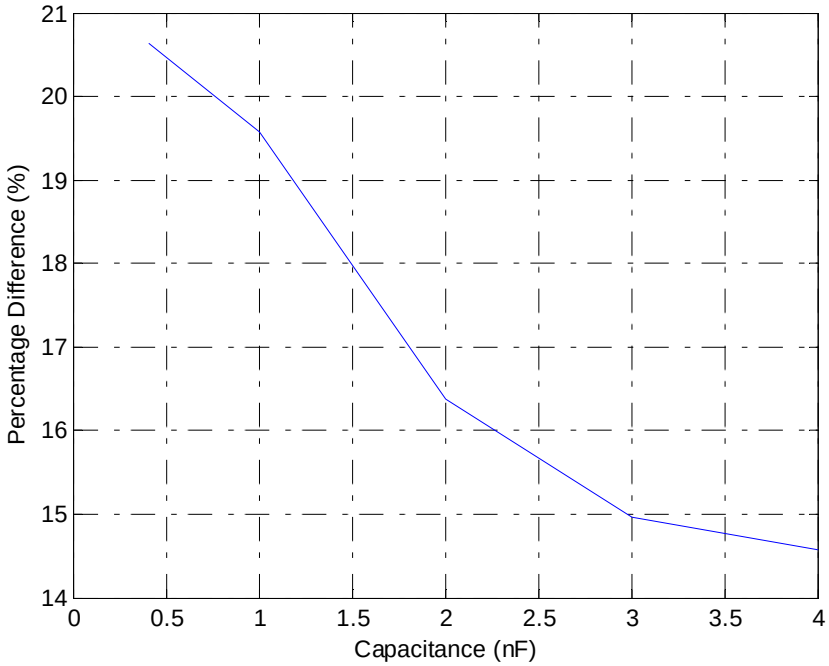

Figure 50 Percentage Difference of Source Strength on Porcelain Insulator

The simulation result of polymer insulator is shown in Figure 51. The percentage difference of flashover voltage is shown in Figure 52.

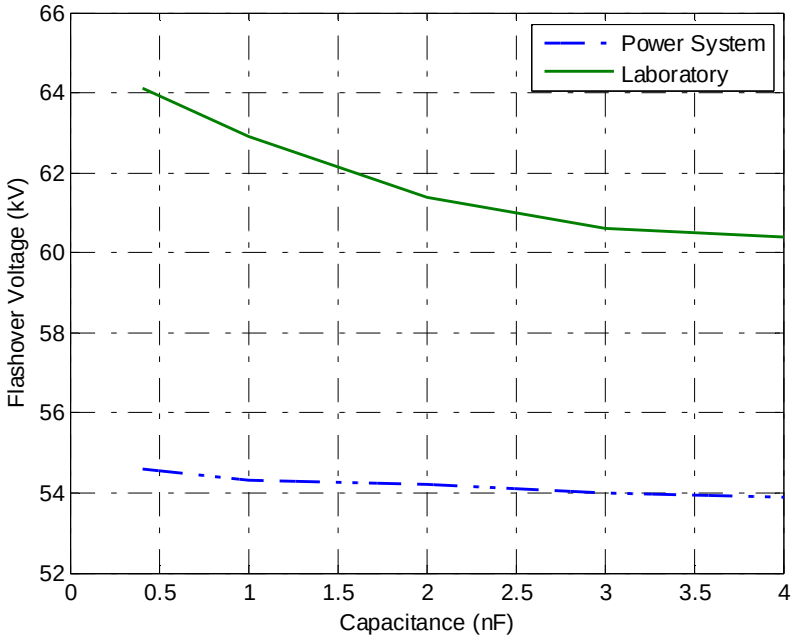

Figure 51 Source Strength Impact on Polymer Insulator

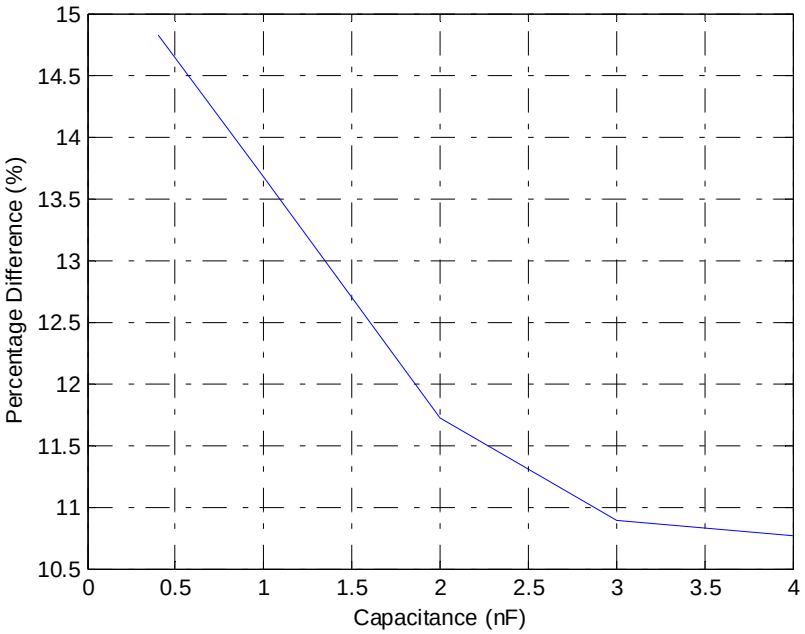

Figure 52 Percentage Difference of Source Strength on Polymer Insulator

7.3 Source Strength Impact with Respect to ESDD

Besides the influence of capacitance on source strength impact, the performance of source strength under different contamination severity is also the interest of this research. For the same sources parameters shown in Table 21, the simulation results of source strength impact on flashover voltage with respect of ESDD are shown in Figure 53-56.

The simulation result of porcelain insulator is shown in Figure 53.

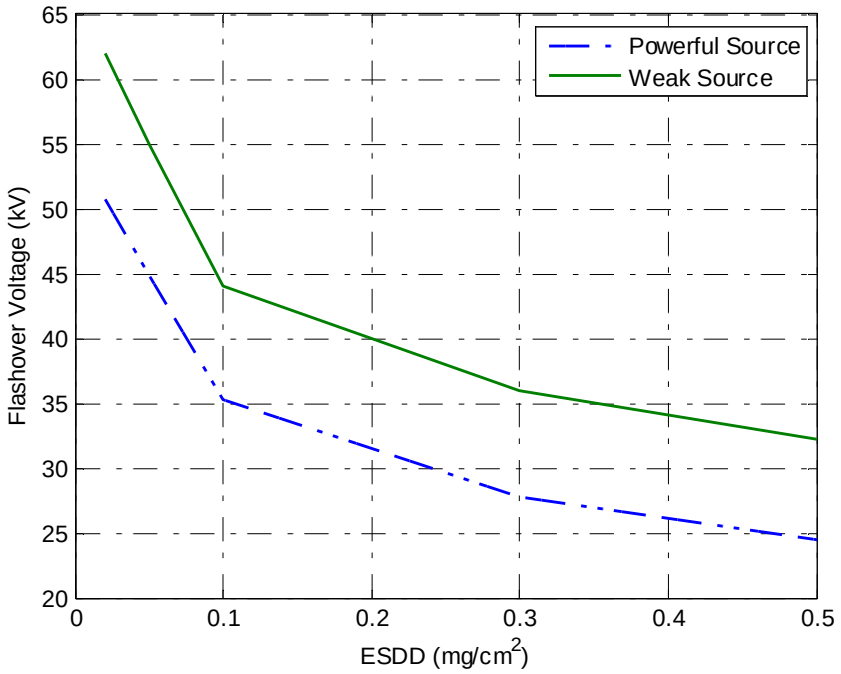

Figure 53 Source Strength Impact on Porcelain Insulator with Different ESDD

The percentage difference of flashover voltage is shown in Figure 54.

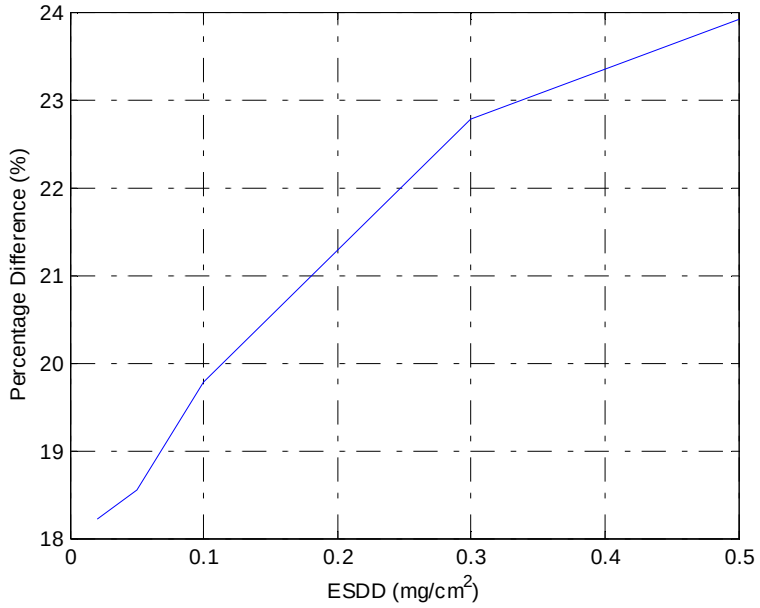

Figure 54 Percentage Difference of Porcelain Insulator with Different ESDD

The simulation result of polymer insulator is shown in Figure 55.

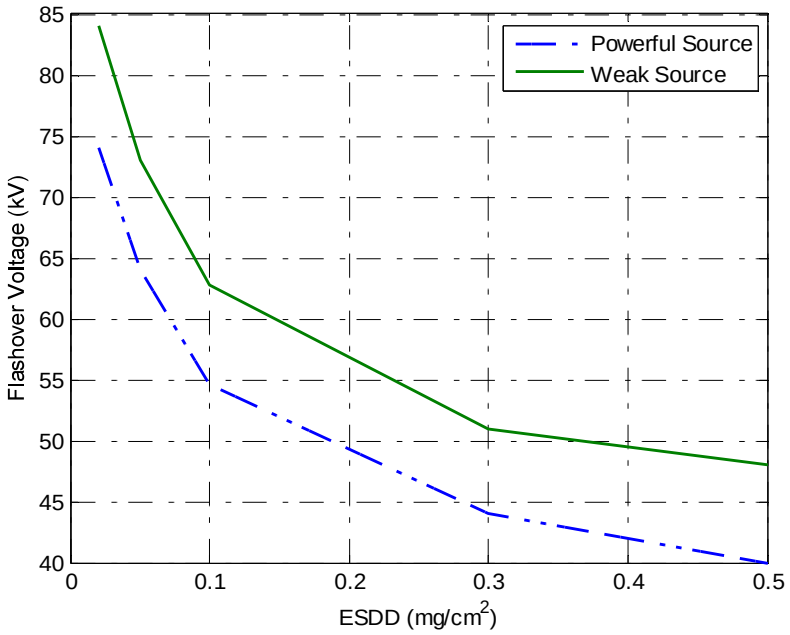

Figure 55 Source Strength Impact on Polymer Insulator with Different ESDD

The percentage difference of flashover voltage is shown in Figure 56.

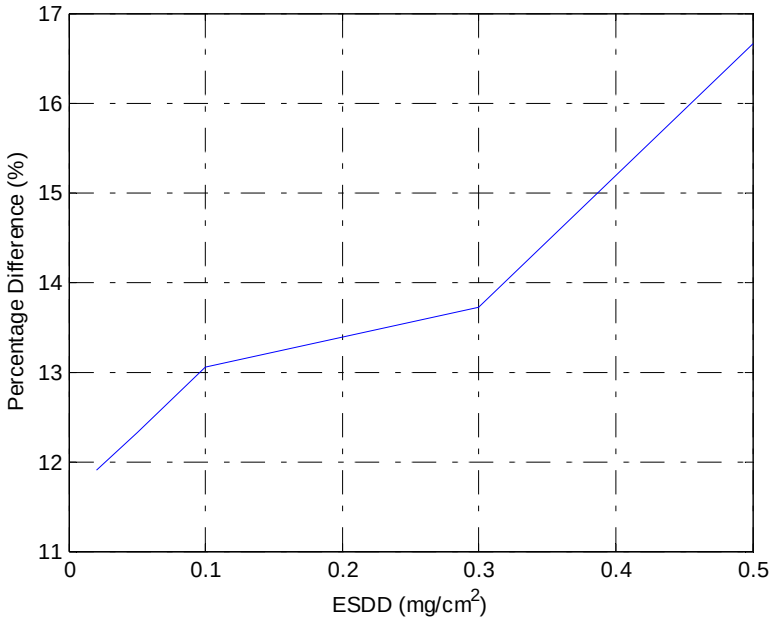

Figure 56 Percentage Difference of Polymer Insulator with Different ESDD

7.4 Source Strength Impact with Respect to Shed Diameter

For different insulator shed diameters, different flashover performances are usually observed in both field and laboratory. In this study, a suspension type insulator and post type insulator with same insulating materials were investigated.

The insulators used in this study has following geometry as shown in Figure 57 (a) and (b). Insulators have the following dimensions as shown in Table 23.

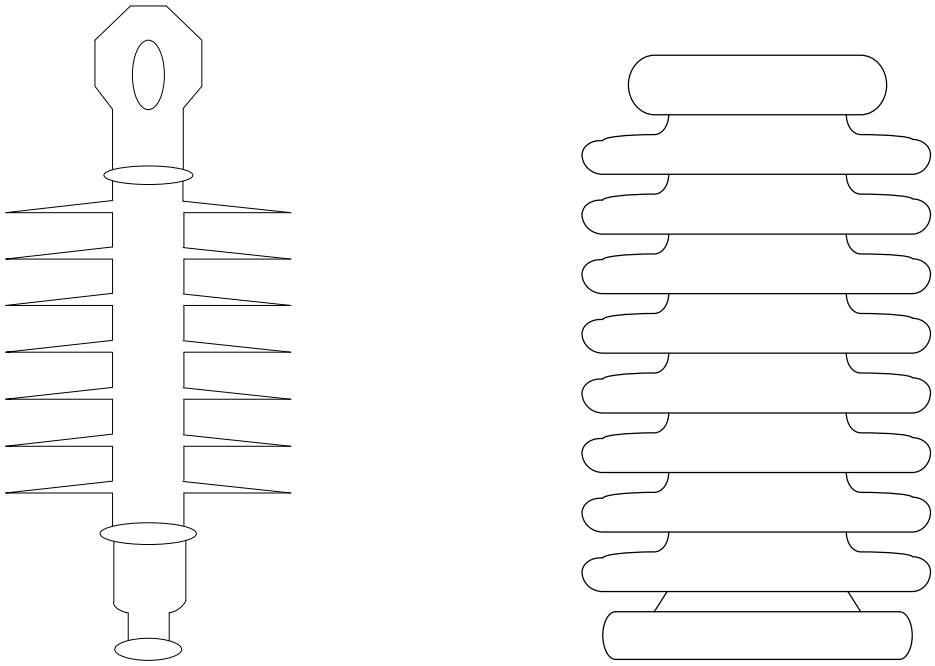

(a) (b)

Figure 57 Insulators with Different Diameters

Table 23 Insulators Dimensions

Insulator type	Suspension	Post
Number of sheds	7	8
Shed diameter	126 mm	160 mm
Trunk diameter	26 mm	90 mm
Unit spacing	623 mm	334 mm
Leakage distance	980 mm	986 mm

To begin with, the same test source was used to compare their flashover performance.

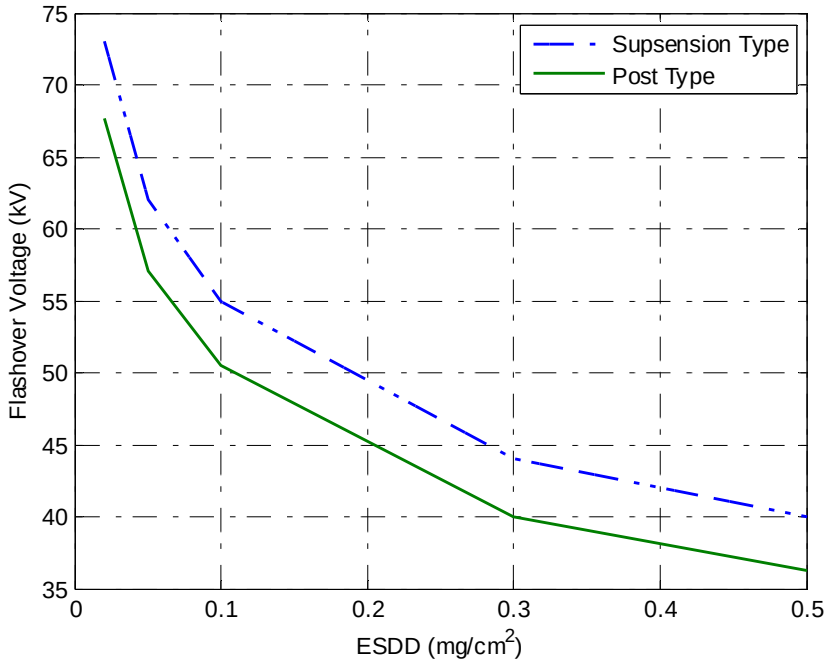

Figure 58 Flashover Voltages of Different Diameters

The percentage difference is shown in Figure 59.

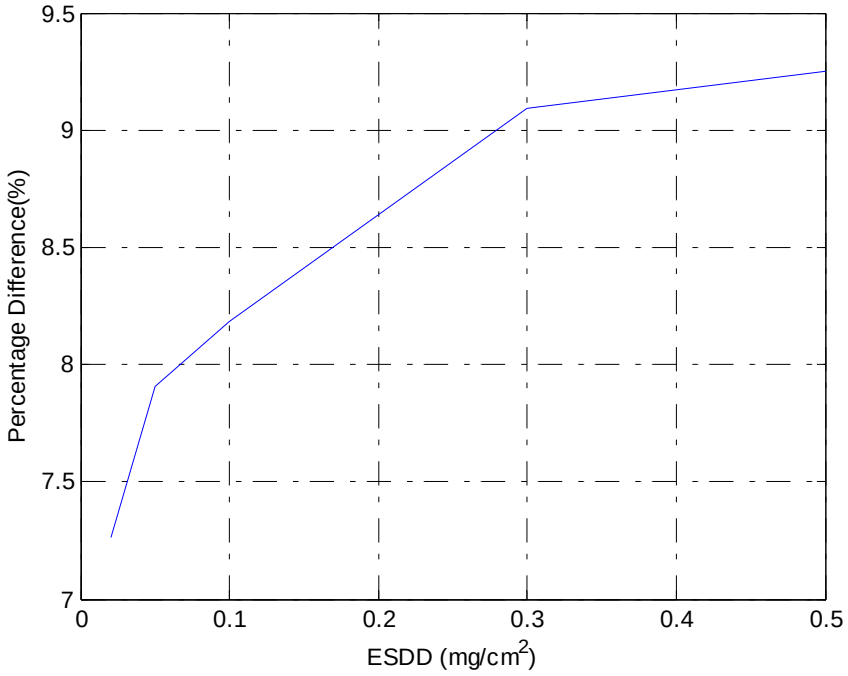

Figure 59 Percentage Difference of Flashover Voltages

Assume both insulators is fed by same powerful source and weak source. The source strength influence for different shed diameters is studied.

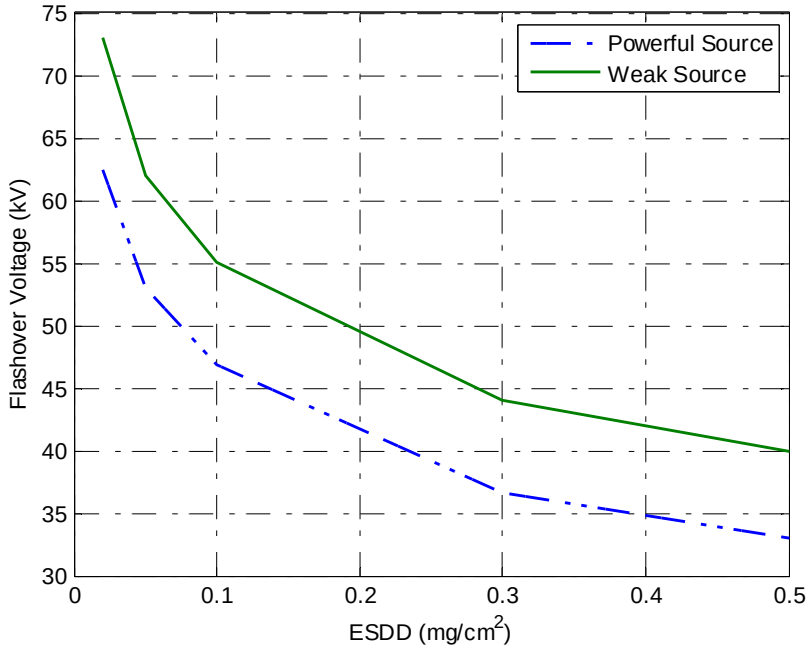

Figure 60 Source Strength Impact of Suspension Insulator

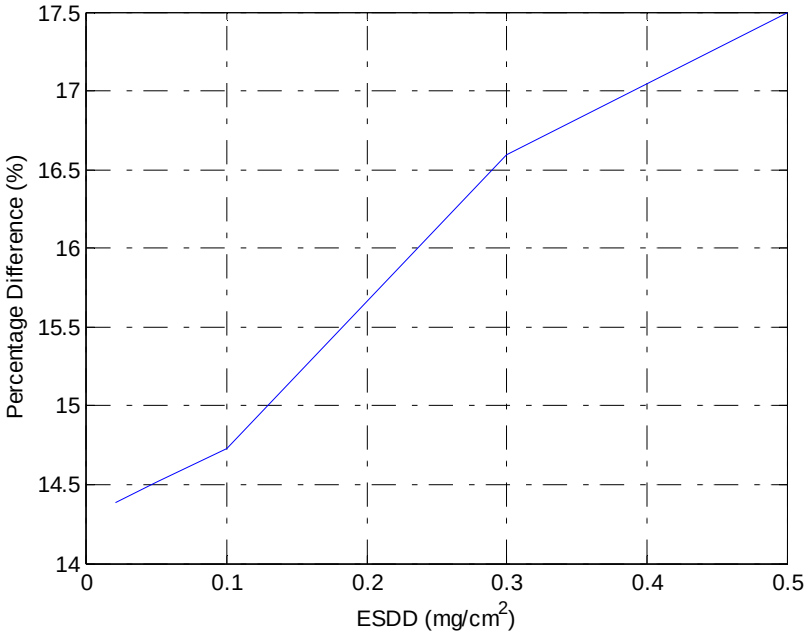

Figure 61 Percentage Difference of Flashover Voltage

The simulation of post type insulator is shown in Figure 62. The percentage difference of flashover voltage is shown in Figure 63.

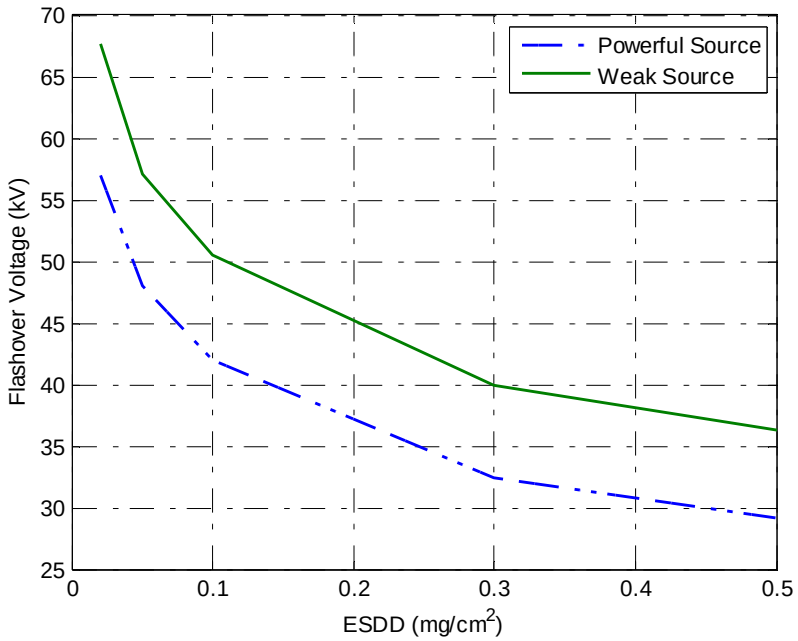

Figure 62 Source Strength Impact on Post Insulator

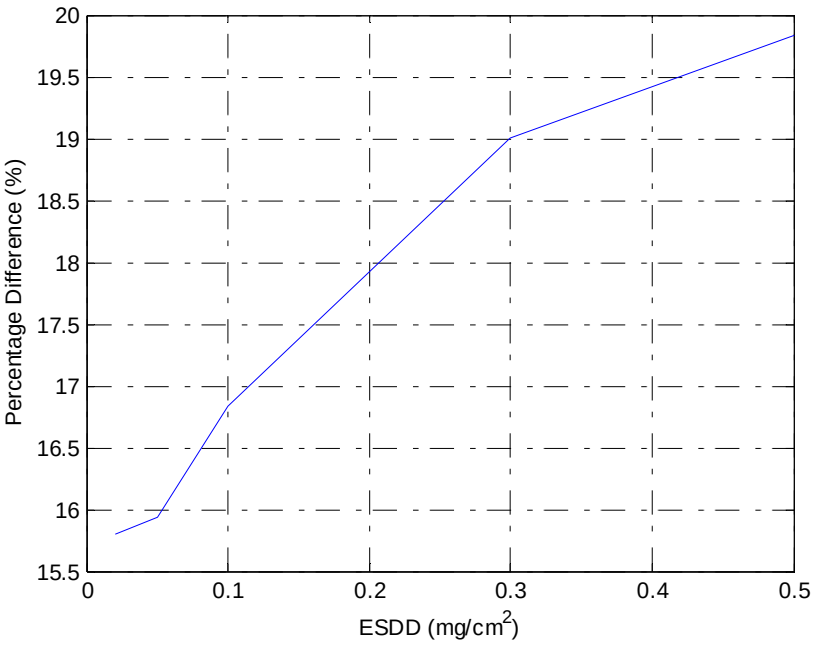

Figure 63 Percentage Difference of Flashover Voltage

7.5 Source Strength Impact with Respect to Voltage Level

It is also the interest of this research to investigate different voltage levels influence on the source strength effects on flashover voltage. In this section, 230 kV class, 345 kV class, and 500 kV class outdoor insulators are studied. For each voltage level, a porcelain suspension insulator, a polymer suspension insulator and a porcelain post insulator were compared [58-60]. The insulators used in this study are shown in Figure 64 (a), (b), (c).

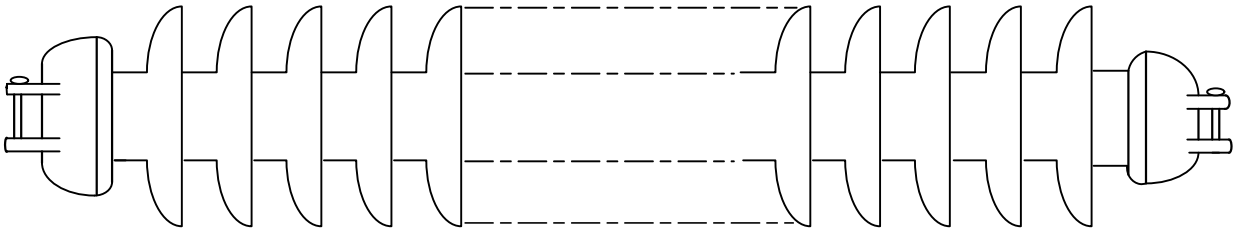

(a) Porcelain Suspension Insulator

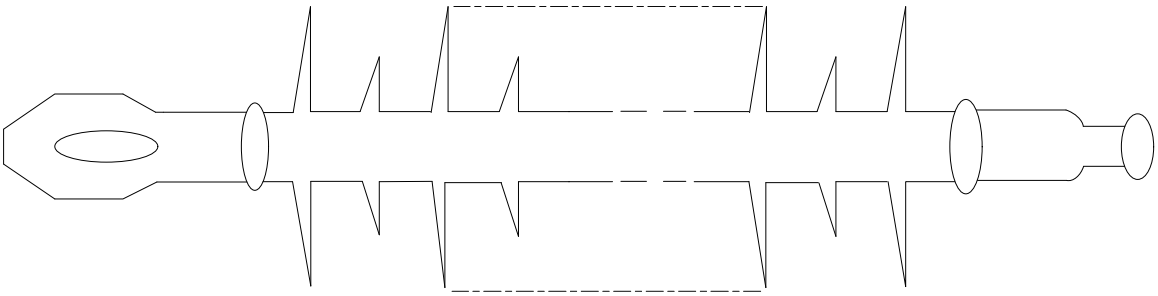

(b) Polymer Suspension Insulator

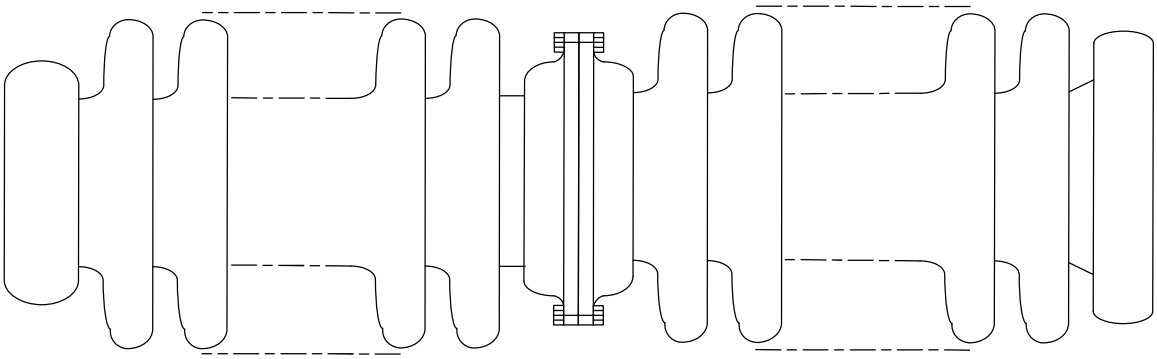

(c) Porcelain Post Insulator

Figure 64 Three Different Types of Insulators

7.5.1 Source Strength Impact on 230 kV Insulators

Insulators dimensions are shown in Table 24.

Table 24 230 kV Insulator Details

Insulator type	Porcelain Suspension	Polymer Suspension	Porcelain Post
Number of sheds	14	30/29	32
Shed diameter	25.4 cm	10.6/7.6 cm	24.4 cm
Trunk diameter	10.8 cm	4 cm	21.6 cm
Unit spacing	204.4 cm	207.5	203.2 cm
Leakage distance	427 cm	418.9 cm	419.1 cm

To begin with, flashover voltages for three different types of insulators under the same test source were studied. The simulation results are shown in Figure 65.

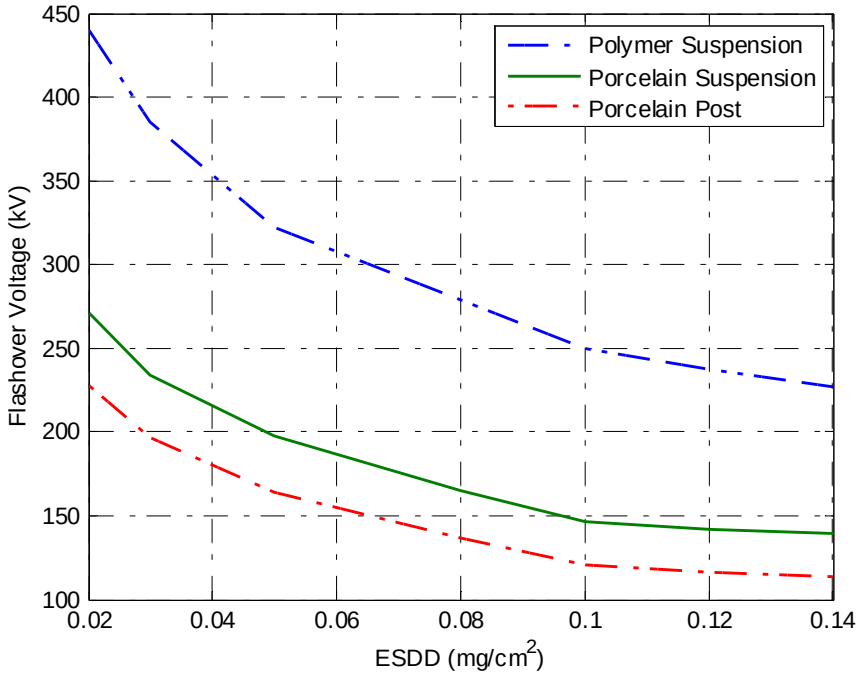

Figure 65 Flashover Voltages Comparison

The percentage difference between porcelain suspension and polymer suspension insulators is shown in Figure 66. The percentage difference between porcelain suspension and porcelain post insulators is shown in Figure 67.

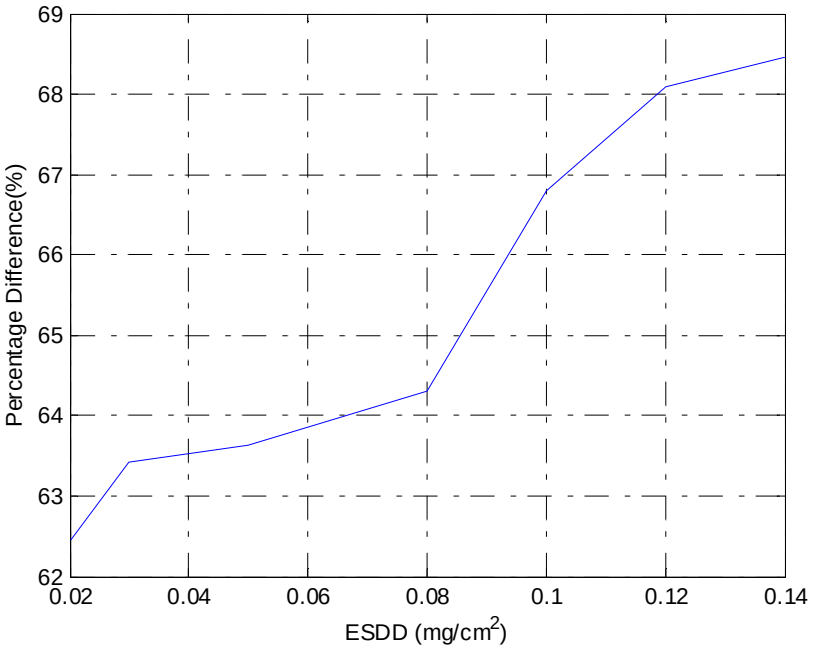

Figure 66 Porcelain and Polymer Comparison

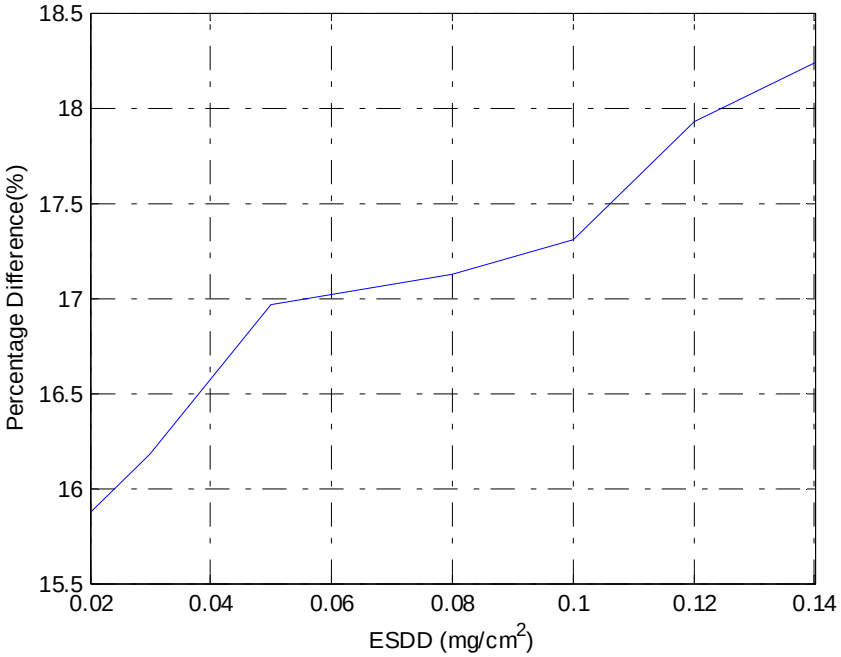

Figure 67 Porcelain Suspension and Post Comparison

For the same sources parameters, the simulation results of source strength impact on flashover voltage are shown in Figure 68-73. The simulation result of porcelain

suspension insulator is shown in Figure 68, and percentage difference is shown in Figure 69.

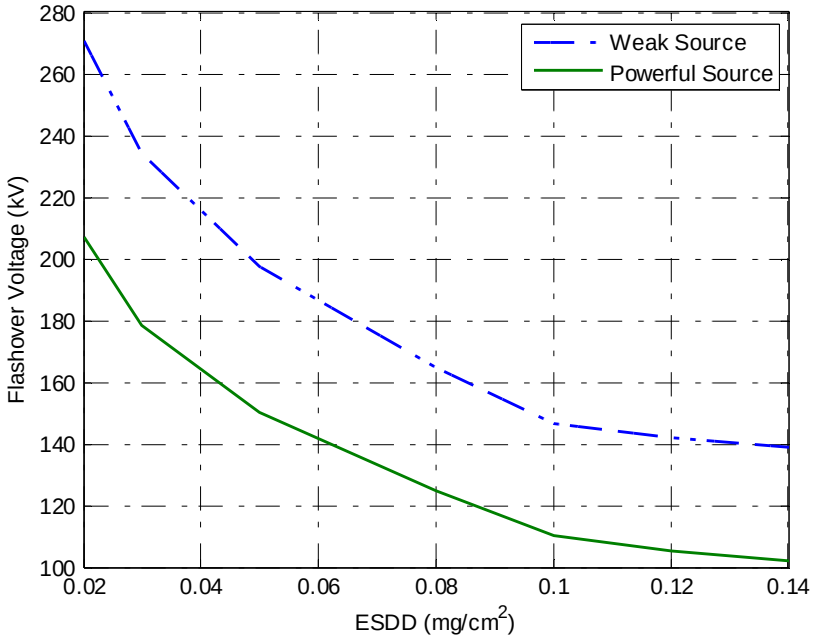

Figure 68 Source Strength Impact of Porcelain Suspension Insulator

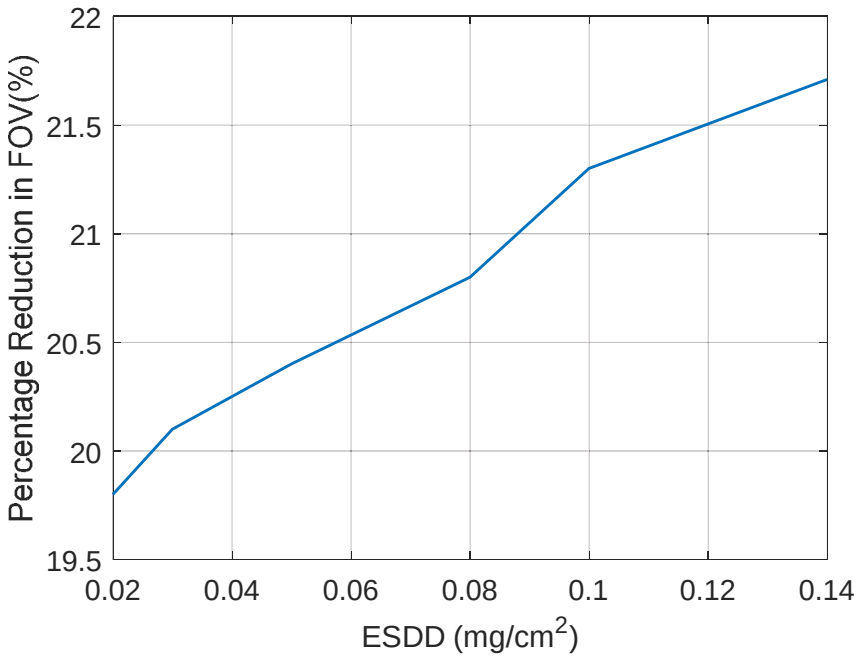

Figure 69 Percentage Difference of Porcelain Suspension Insulator

The simulation result of polymer suspension insulator is shown in Figure 70. The percentage difference of flashover voltage is shown in Figure 71.

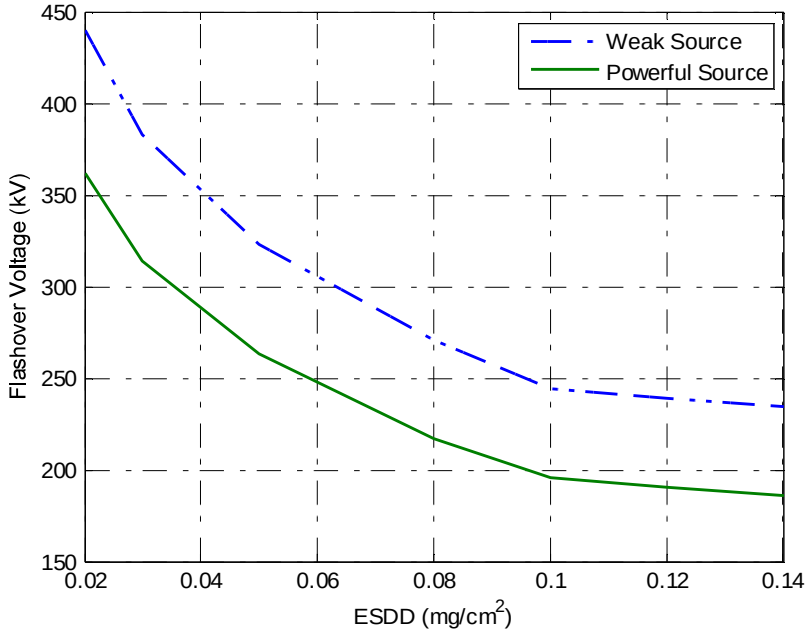

Figure 70 Source Strength Impact of Polymer Suspension Insulator

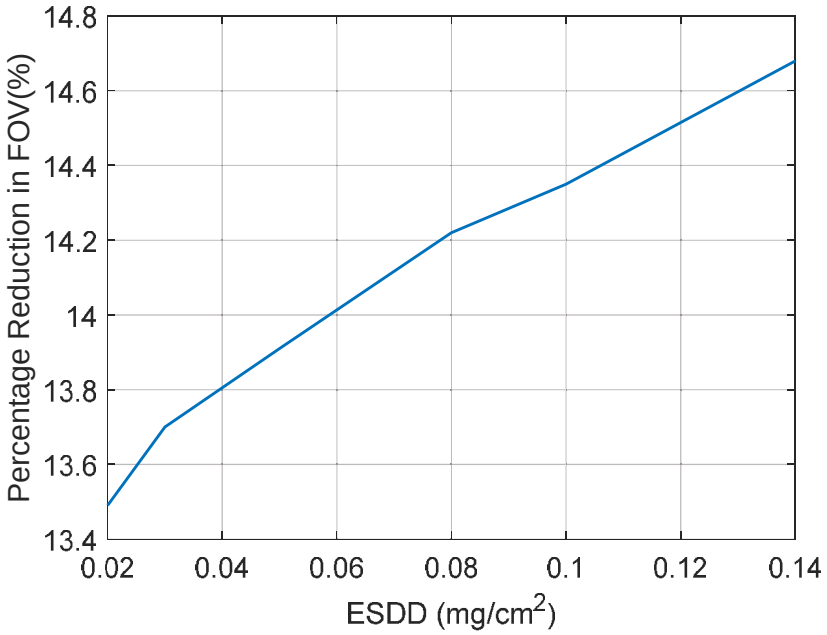

Figure 71 Percentage Difference of Polymer Suspension Insulator

The simulation result of porcelain post insulator is shown in Figure 72. The percentage difference of flashover voltage is shown in Figure 73.

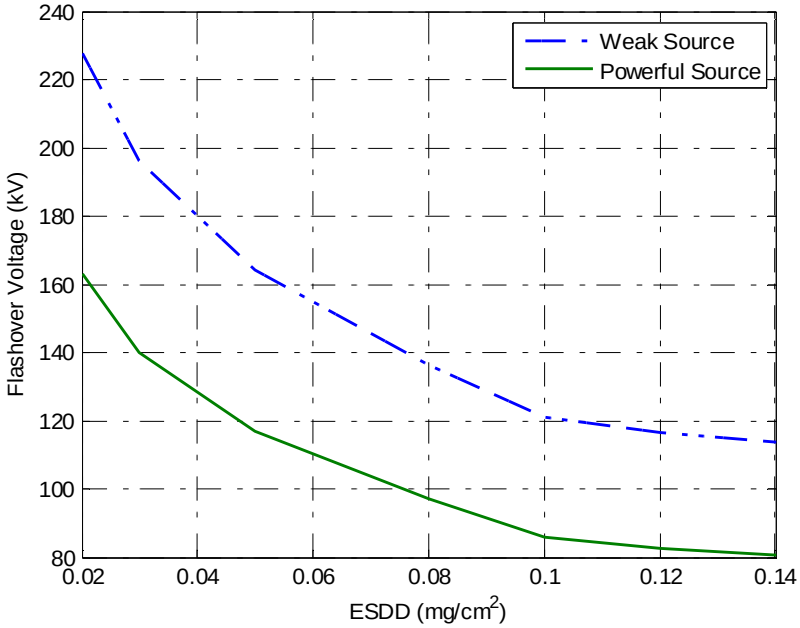

Figure 72 Source Strength Impact of Porcelain Post Insulator

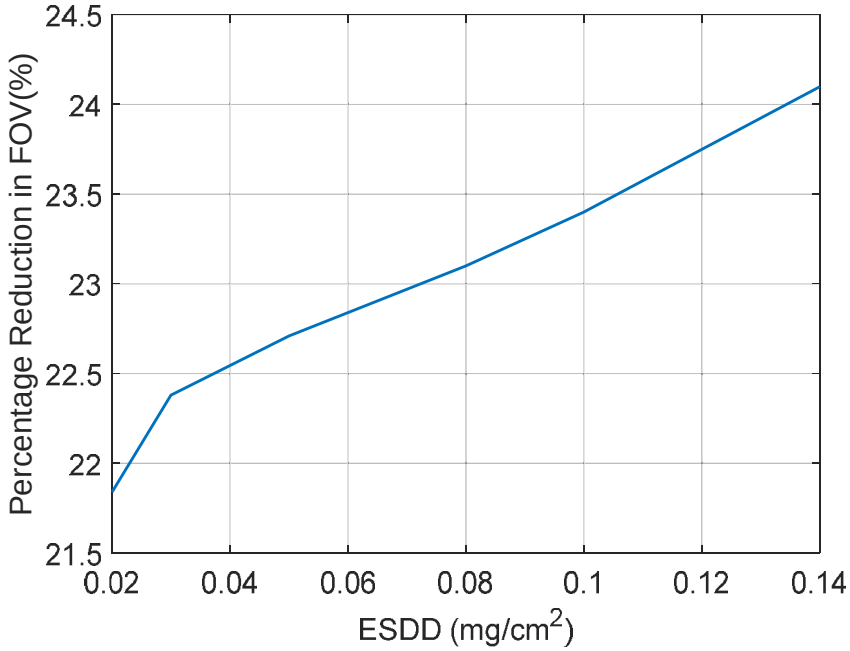

Figure 73 Percentage Difference of Porcelain Post Insulator

7.5.2 Source Strength Impact on 345 kV Insulators

Insulators dimensions are shown in Table 25.

Table 25 345 kV Insulator Details

Insulator type	Porcelain Suspension	Polymer Suspension	Porcelain Post
Number of sheds	18	37/36	44
Shed diameter	25.4 cm	10.6/7.6 cm	24.7 cm
Trunk diameter	10.8 cm	4 cm	21.6 cm
Unit spacing	262.8cm	249.5	269.2 cm
Leakage distance	549 cm	518.3 cm	586.7 cm

To begin with, the flashover voltage for three different types of insulators under the same test source was studied.

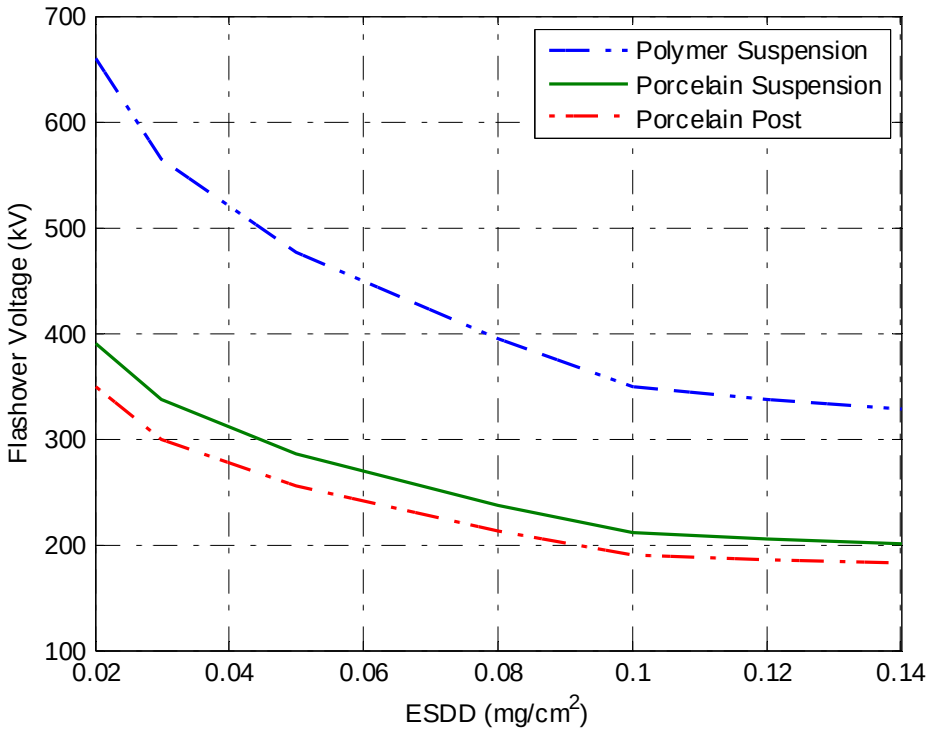

Figure 74 Flashover Voltages Comparison

For the same sources parameters shown in Table 21, the simulation results of source strength impact on flashover voltage are shown in Figure 75-80. The simulation result of

porcelain suspension insulator is shown in Figure 75. The percentage difference of flashover voltage is shown in Figure 76.

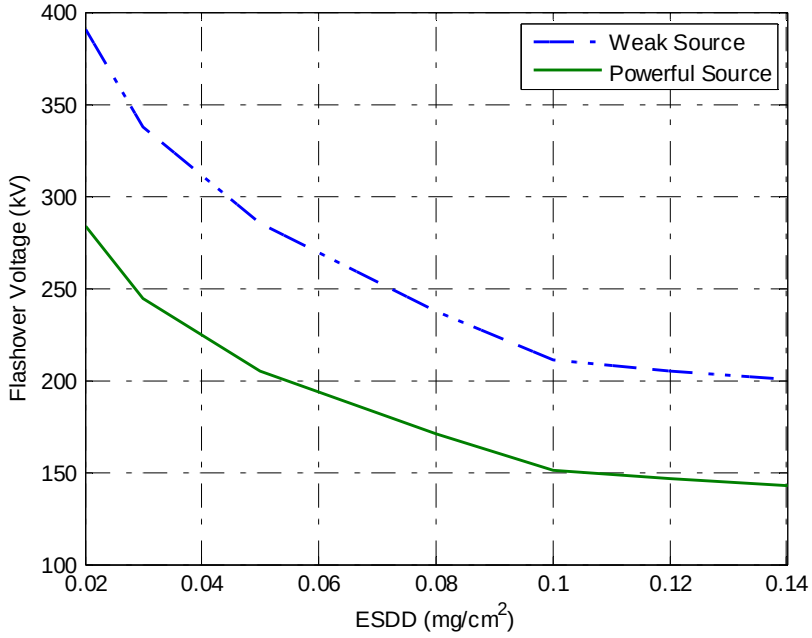

Figure 75 Source Strength Impact of Porcelain Suspension Insulator

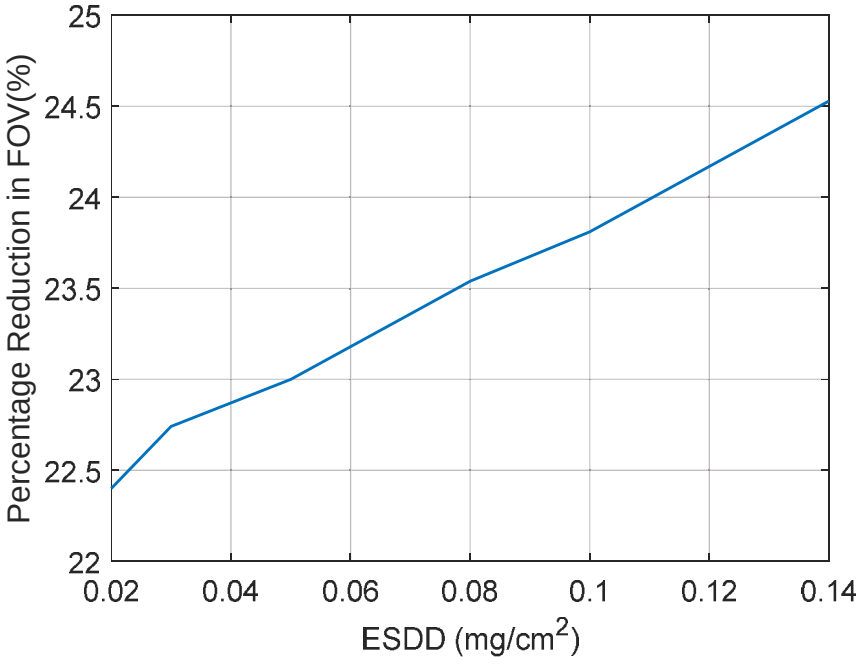

Figure 76 Percentage Difference of Porcelain Suspension Insulator

The simulation result of polymer suspension insulator is shown in Figure 77. The percentage difference of flashover voltage is shown in Figure 78.

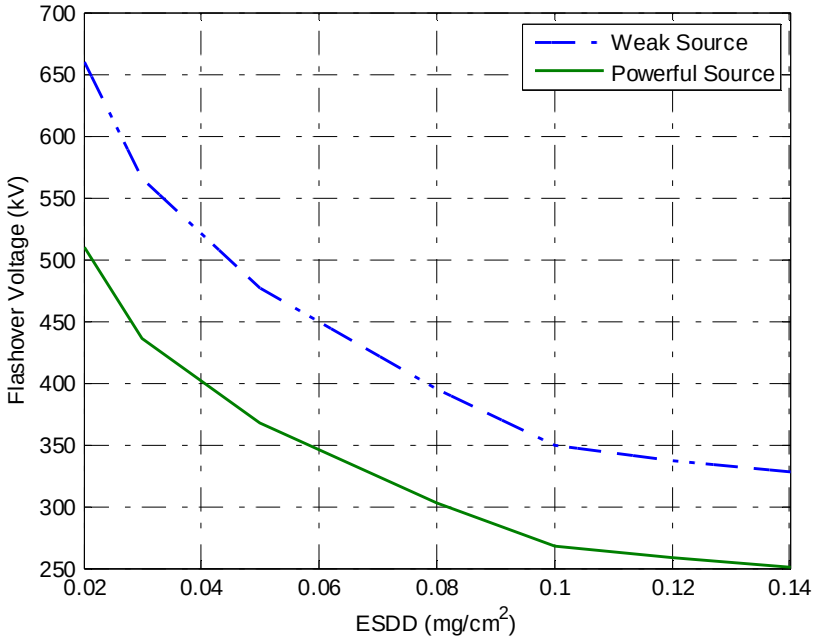

Figure 77 Source Strength Impact of Polymer Suspension Insulator

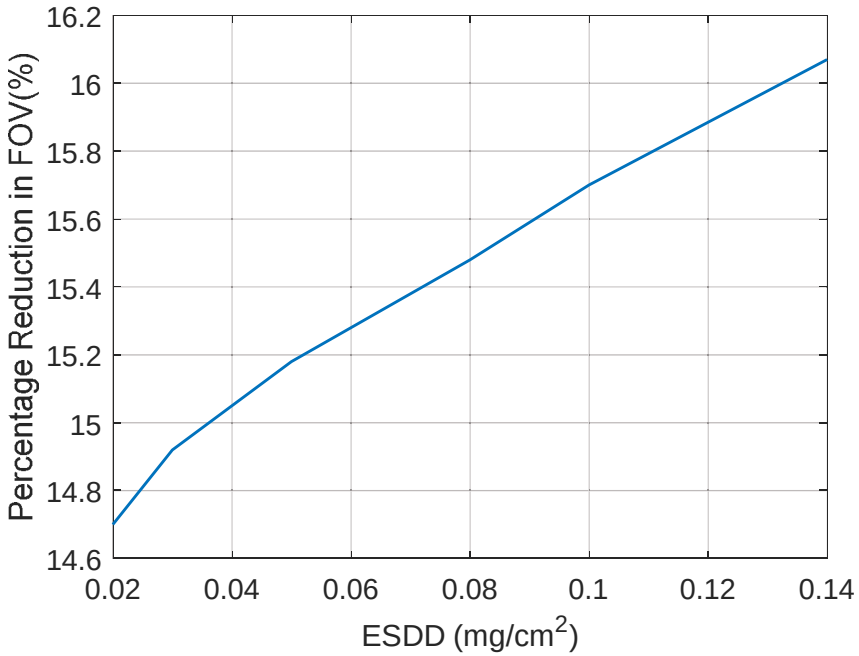

Figure 78 Percentage Difference of Polymer Suspension Insulator

The simulation result of porcelain post insulator is shown in Figure 79. The percentage difference of flashover voltage is shown in Figure 80.

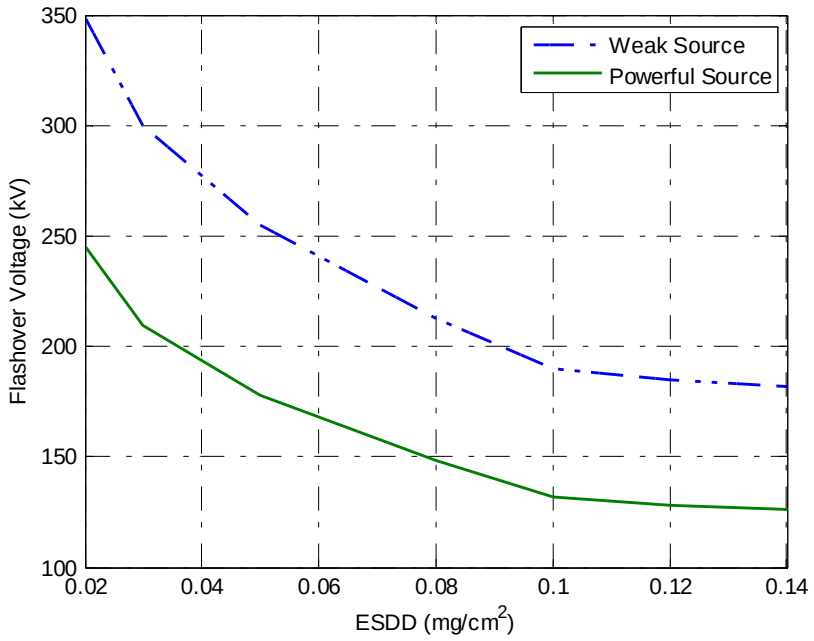

Figure 79 Source Strength Impact of Porcelain Post Insulator

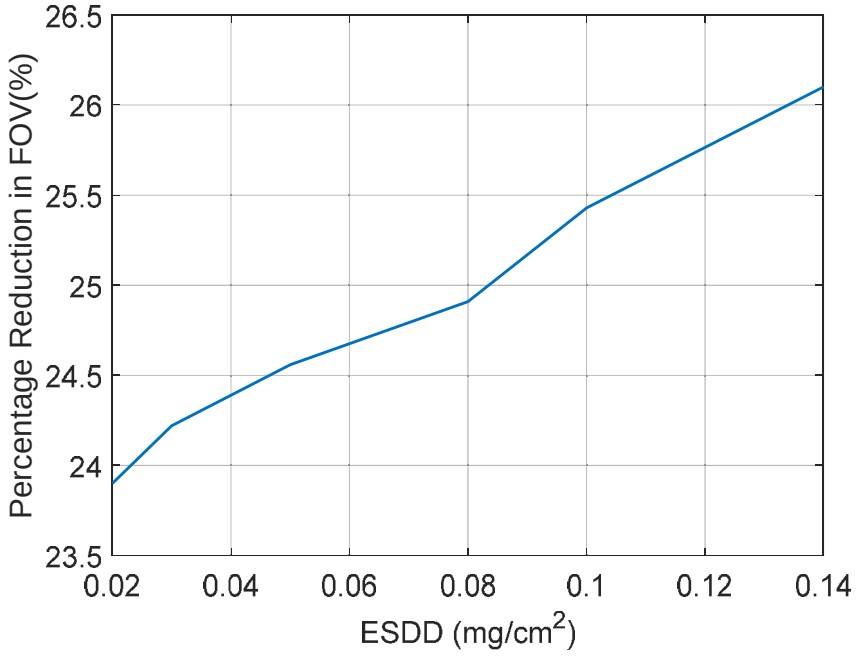

Figure 80 Percentage Difference of Porcelain Post Insulator

7.5.3 Source Strength Impact on 500 kV Insulators

Insulators dimensions are shown in Table 26.

Table 26 500 kV Insulator Details

Insulator type	Porcelain Suspension	Polymer Suspension	Porcelain Post
Number of sheds	24	55/54	54
Shed diameter	25.4 cm	10.6/7.6 cm	24.7 cm
Trunk diameter	10.8 cm	4 cm	23.8 cm
Unit spacing	350.4 cm	357.5	325.1 cm
Leakage distance	732 cm	773.9 cm	711.2 cm

To begin with, the flashover voltage for three different types of insulators under the same test source was studied.

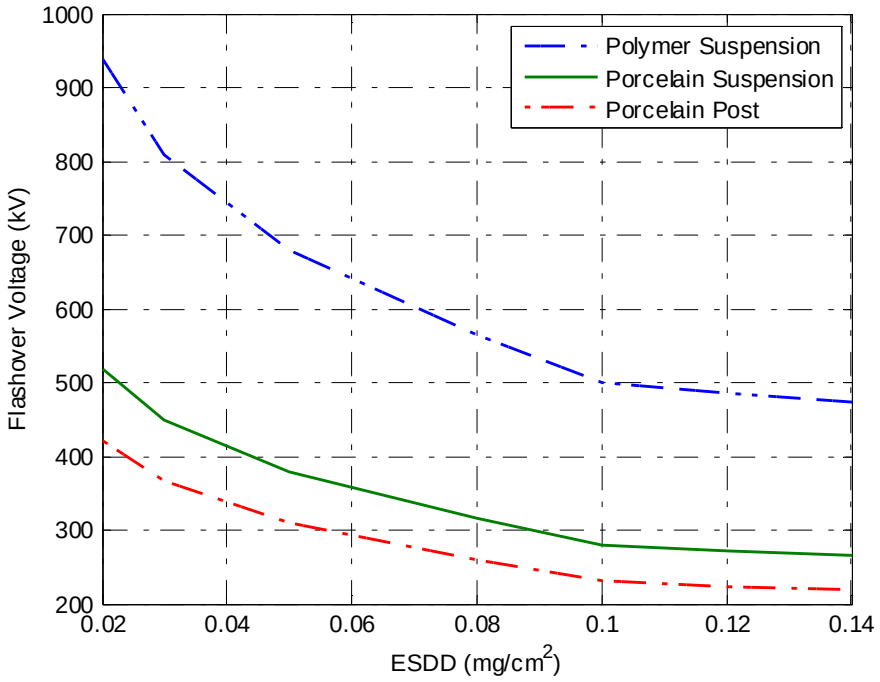

Figure 81 Flashover Voltages Comparison

For the same sources parameters, simulation results of source strength impact on flashover voltage are shown in Figure 82-87. The simulation result of porcelain suspension insulator is shown in Figure 82, and percentage difference is shown in Figure 83.

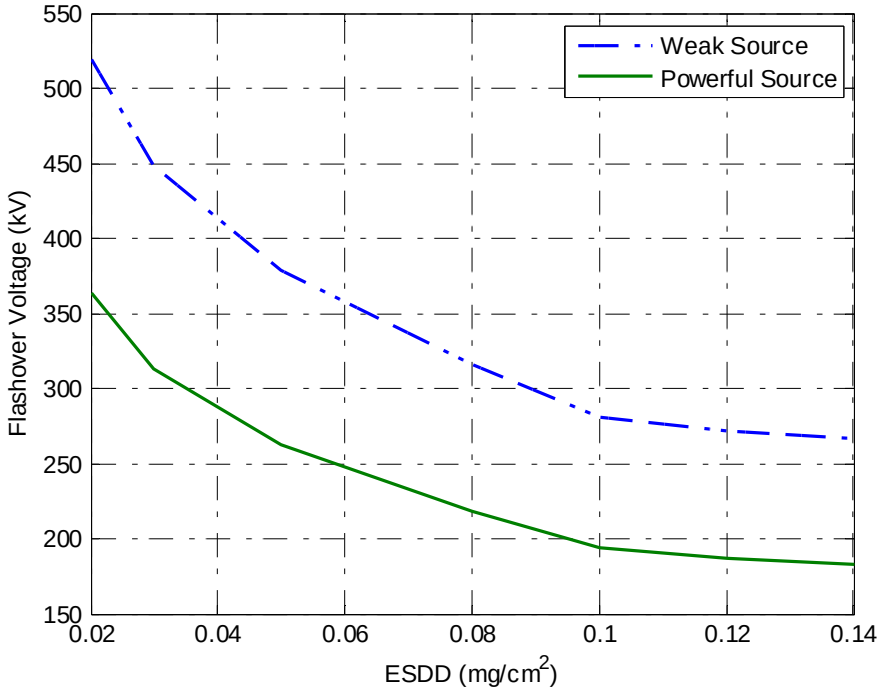

Figure 82 Source Strength Impact of Porcelain Suspension Insulator

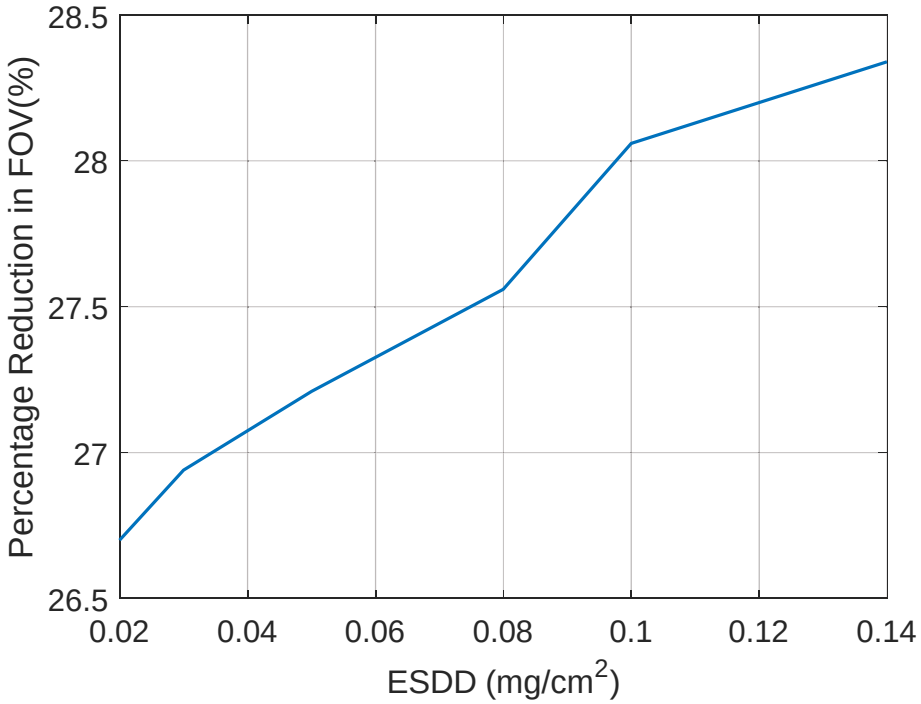

Figure 83 Percentage Difference of Porcelain Suspension Insulator

The simulation result of polymer suspension insulator is shown in Figure 84. The percentage difference of flashover voltage is shown in Figure 85.

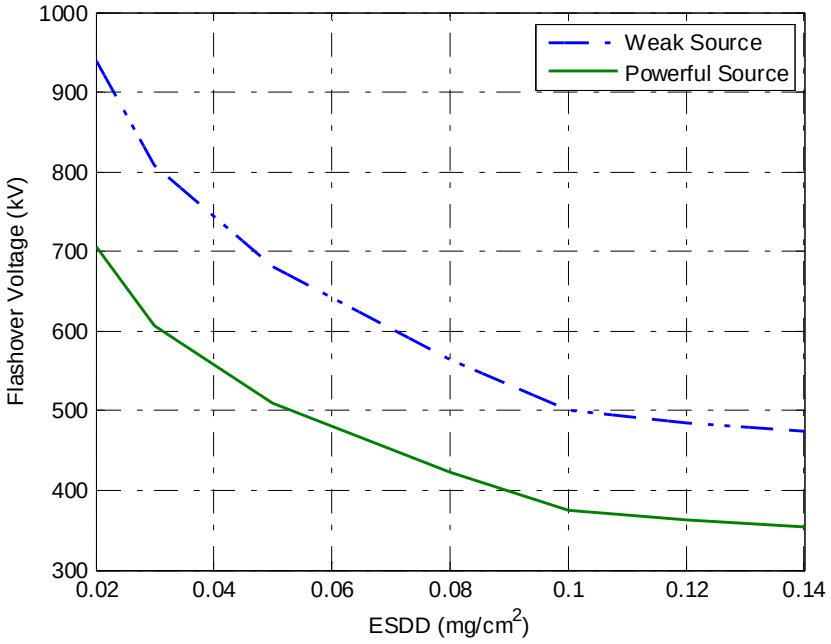

Figure 84 Source Strength Impact of Polymer Suspension Insulator

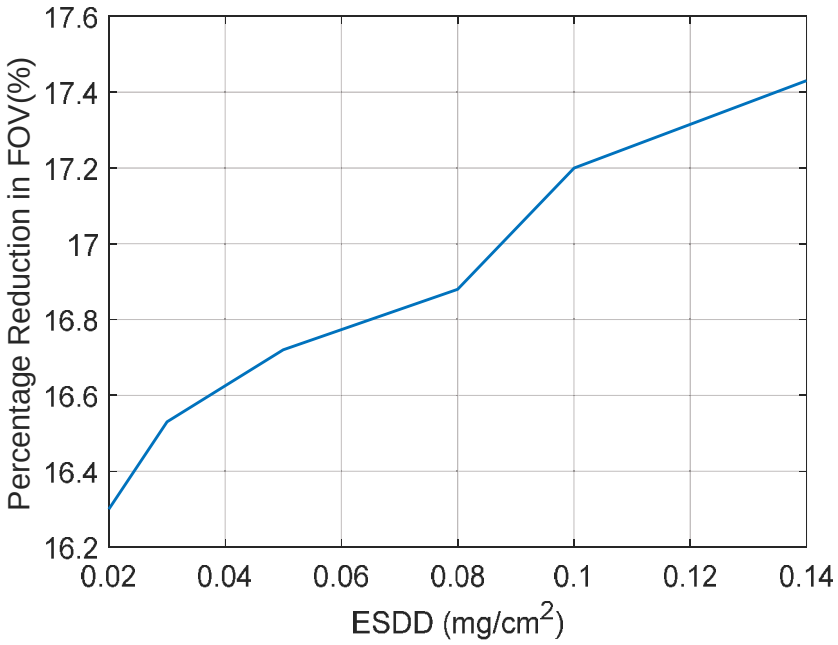

Figure 85 Percentage Difference of Polymer Suspension Insulator

The simulation result of porcelain post insulator is shown in Figure 86. The percentage difference of flashover voltage is shown in Figure 87.

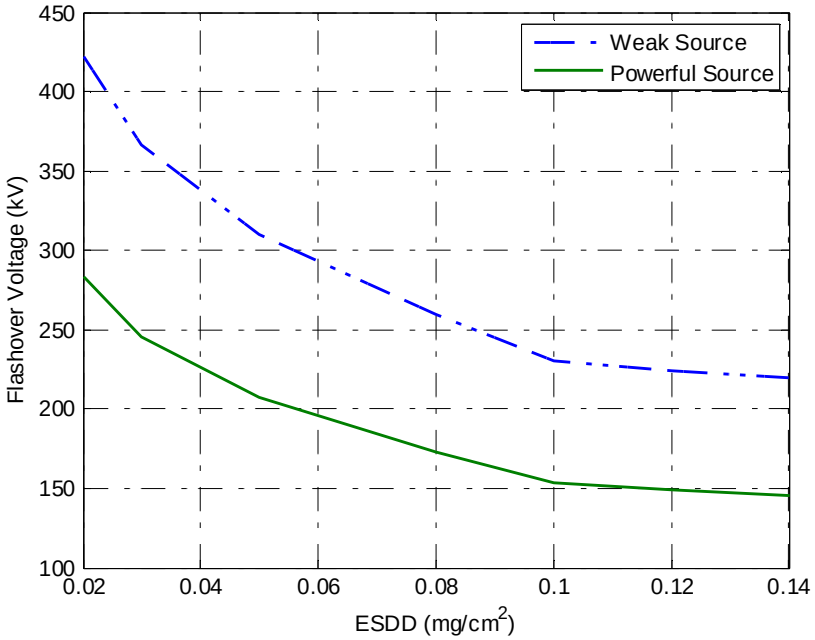

Figure 86 Source Strength Impact of Porcelain Post Insulator

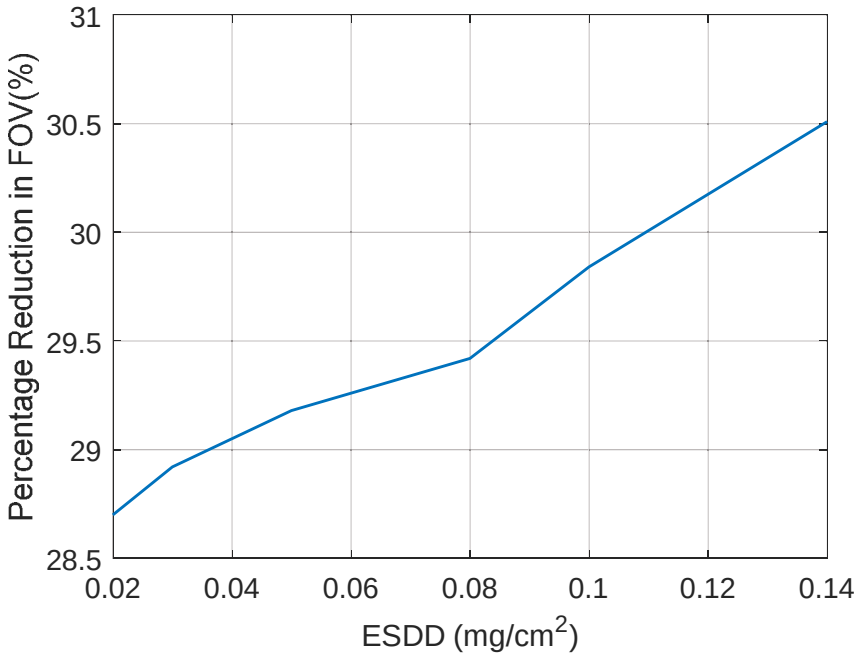

Figure 87 Percentage Difference of Porcelain Post Insulator

7.6 Conclusions

1. For all cases that were studied in this chapter, there is an obvious decrement of insulator flashover voltage when it is supplied by a powerful source when compared to a weak source.

2. Small test source capacitance value will result in a larger flashover voltage difference between weak source and powerful source.

3. Simulation results show that higher ESDD value will lead to a larger flashover voltage difference between weak source and powerful source.

4. The study of insulator with different shed profiles suggests that source strength has a larger impact on insulators with larger shed diameters.

5. From the study of source strength impact with different insulator voltage levels, source strength has the largest influence on the decrement of flashover voltage for a porcelain post type insulator. Porcelain suspension insulator has the second largest decrement, and a polymer insulator has the least decrement. For 230 kV, the difference of flashover voltage for a porcelain post insulator is 23%, a porcelain suspension insulator is 21%, and a polymer suspension insulator is 15%. For 345 kV, the difference of flashover voltage for a porcelain post insulator is 25%, a porcelain suspension insulator is 24%, and a polymer suspension insulator is 16%. For 500 kV, the difference of flashover voltage for a porcelain post insulator is 30%, a porcelain suspension insulator is 28%, and a polymer suspension insulator is 18%.

6. From the comparison with higher system voltage insulators, it can be concluded that test source strength tends to have a larger impact on flashover voltage for higher voltage level insulators.

Chapter 8

STUDY OF FLASHOVER PROBABILITY

8.1 Problem Statement

Studies that have been done so far on insulator flashover mainly focus on traditional deterministic method, in which the contamination severity is specified, and a certain level of supply voltage is applied on the insulator. Deterministic method can only predict whether an insulator would flashover or withstand. However, it has been suggested by some researchers that insulator flashover is indeed a probabilistic process given both contamination severity and the withstand voltage are probabilistic variables [61-63].

In this chapter, a probability approach to predict the likelihood of insulator flashover is proposed based on the deterministic model developed in Chapter 3.

8.2 Flashover Probability Functions

Probabilistic approaches consider parameters as variables and take into account statistical distributions of variables. The probabilities of flashover voltage and other factors are combined by assuming that all factors are independent of each other. It is proposed that the probability of insulator flashover under contamination conditions is dependent on the supply voltage and pollution severity.

Since the flashover probability function in actual test conditions is unknown, several probability functions are assumed. Three types of distribution functions that widely used in practice were studied and compared.

1. Normal Distribution

$$P(U, ESDD) = \int_0^U exp\left[-\frac{1}{2}\left(\frac{v - V_{50(ESDD)}}{\sigma}\right)^2\right] dv \quad (33)$$

where

U is the applied voltage;

$V_{50(ESDD)}$ is 50% flashover voltage at a certain ESDD which is obtained from developed computer deterministic model;

σ is the flashover voltage standard deviation;

v is the integration step.

2. Weibull Distribution

$$P = 1 - \exp\left[-\left(\frac{U-\delta}{\alpha}\right)^{\beta}\right] \quad when\ U > \delta \quad (34)$$

$$P = 0 \quad when\ U < \delta \quad (35)$$

where

U is applied voltage

β is shape parameter

α is scale parameter

$$\delta = V_{50} - \beta\sigma ln2\sqrt{\pi/2}$$

3. Logistic Distribution

$$P = \frac{1}{1 + exp[-(U - V_{50})^2/\gamma]} \quad (36)$$

where

$$\gamma = \sqrt{\frac{\pi}{8}}\sigma$$

Assuming sufficient wetting, and the same sample insulator in Figure 7 with a surface conductivity of 120 $\mu S/cm$ was studied. It has been reported that the flashover standard deviation in artificial contamination test and natural contamination conditions are 5% and 20% respectively. After obtained V_{50} from the dynamic model developed in Chapter 3, the comparison of flashover probabilities with different distribution functions is shown in Figure 88. The probability differences of any two distributions were calculated as shown in Figure 89.

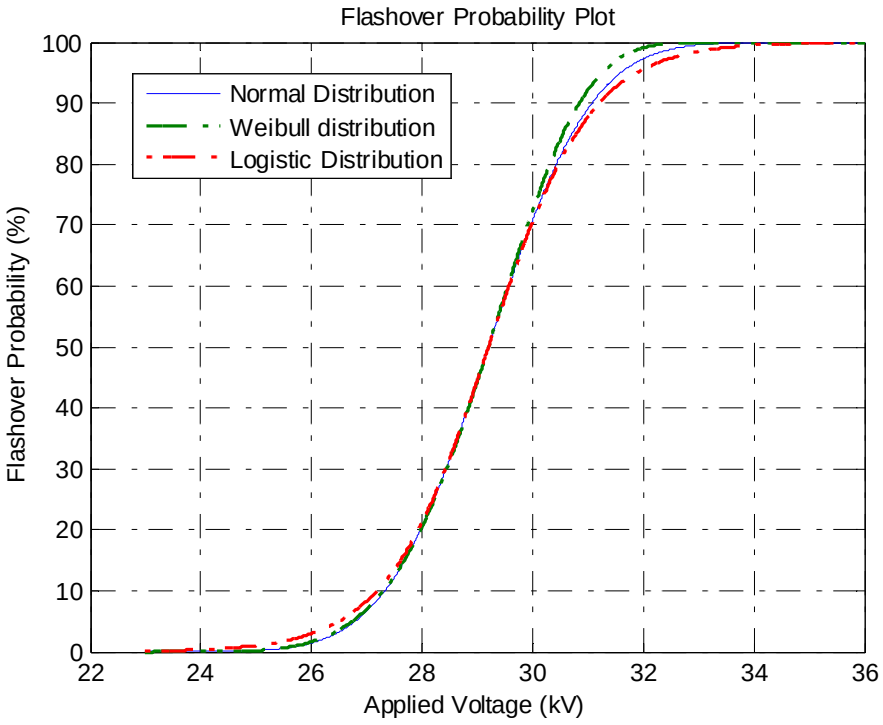

Figure 88 Flashover Probability Plots for Different Distribution Functions

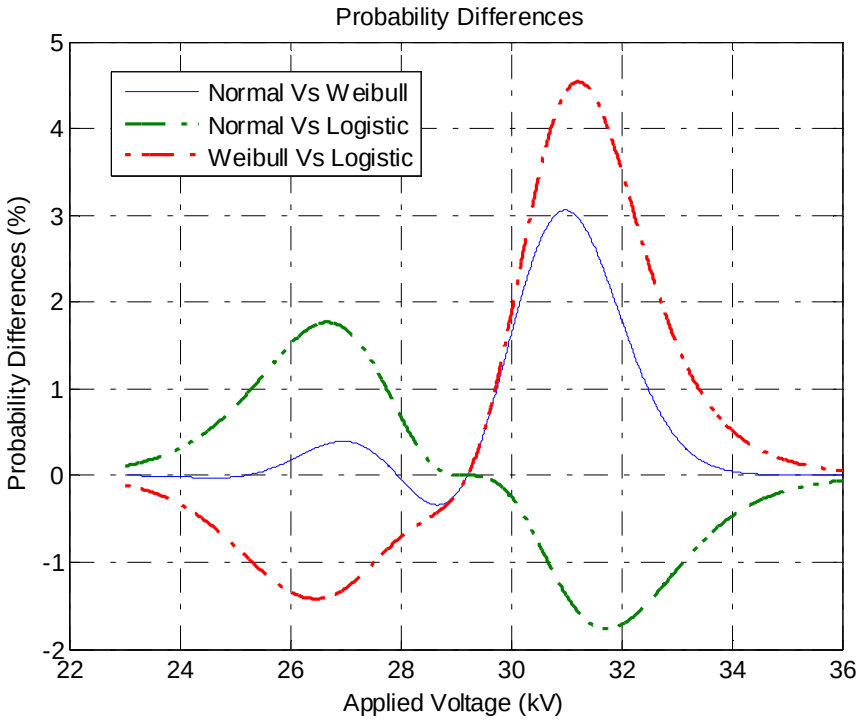

Figure 89 Probability Differences of Different Distribution Functions

From above comparisons, it can be seen that the differences among three distribution functions are relatively small, with the largest difference less than 5%. This corresponds to the conclusion from IEEE standard that for $0.15 < p < 0.85$, most theoretical distributions can be considered equivalent [7]. Since insulator flashover is normally at a low probability range, Weibull distribution was selected for further research.

8.3 Simulation of Flashover Probability

8.3.1 Effect of Source Strength

For different power sources, the flashover voltage is found to be different. It was shown in earlier study that a powerful source with high short circuit current has a lower flashover voltage than what obtained from a weak source under the same contamination

degree. In this section, it aims to study the effects of source strength on flashover probability.

It is reported that standard deviation σ is about 5% for artificially contaminated and wetted insulators. However, a higher σ around 20% is found in case of naturally contaminated insulators in natural wetting conditions [61]. Thus in this simulation $\sigma = 5\%$ is assumed for weak source and $\sigma = 20\%$ is assumed for powerful source. With the source parameters shown in Table 27, the simulation results are shown in Figure 90.

Table 27 Source Parameters

Power Source	Powerful	Weak
Short Circuit Current	1000 A	6 A
Equivalent Resistance	42.59 Ω	9358.82 Ω
Equivalent Inductance	0.24 H	68.96 H

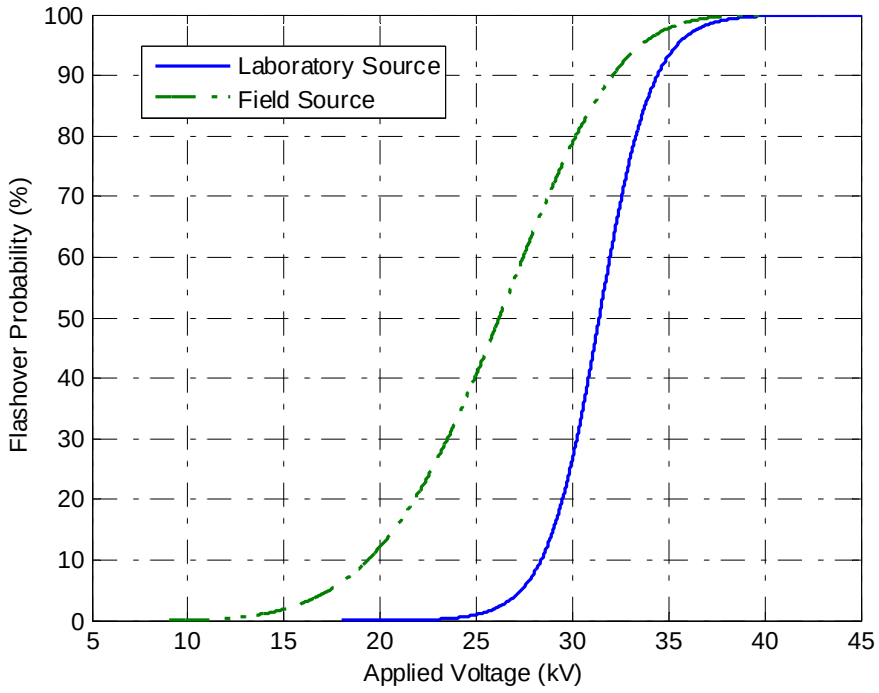

Figure 90 Source Strength Effect on Flashover Probability

By comparing the test sources in Table 27, Figure 90 shows that flashover can occur over a wider range of voltage in the field than in the laboratory (source satisfying the IEC standard). For the sample insulator in this study, flashover can happen at supply voltage as low as 13 kV for the field source, but even for a powerful laboratory source, flashover will not happen until the voltage reaches 24 kV. In the laboratory, the range of voltage that causes a change of flashover probability from 10-90% is within 13% of the critical (50%) flashover voltage value, while in the field this variation is about 48%. This suggests that insulators in service can flashover over a wider range of contamination severity than predicted by laboratory tests. The ESDD range that corresponds to 10-90% flashover probability is 0.016-0.13 mg/cm^2 for the field source. For the laboratory source, this range is 0.025-0.042 mg/cm^2.

8.3.2 Effect of Insulation Materials

High voltage insulators are usually categorized by their dielectric materials. Three main classes of dielectrics that have been used are porcelain, polymer and glass. Due to the differences of their dielectric properties, they are expected to have different flashover probabilities even under the same conditions. Both porcelain and polymer insulators rated at 230 kV were evaluated in this research. Figures 91 and 92 show the flashover probability curves as a function of applied voltage for the porcelain and polymer insulator cases, respectively.

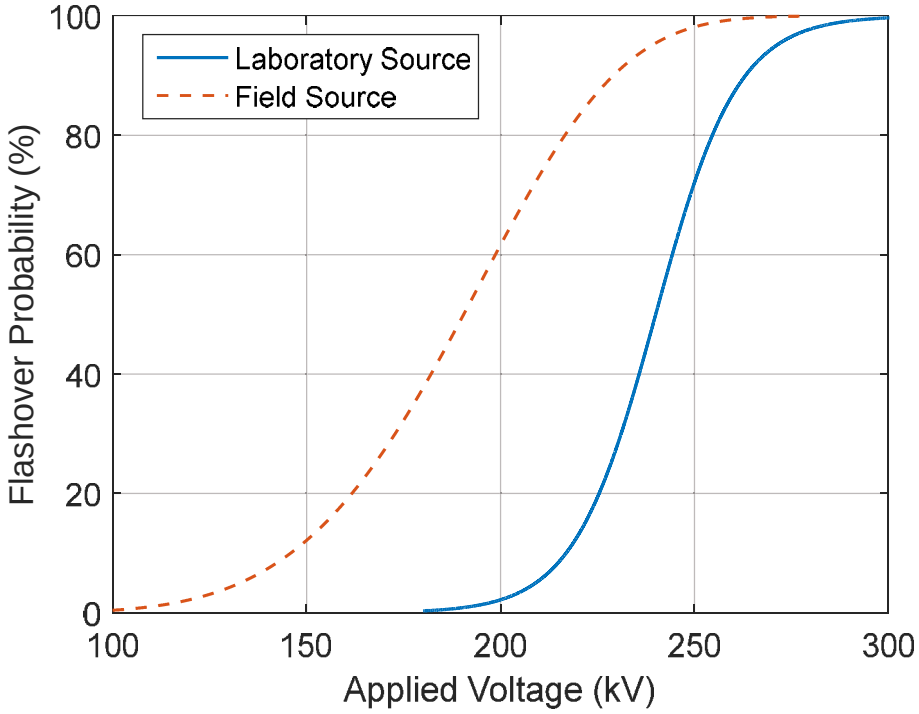

Figure 91 Flashover Probability of 230 kV Rated Porcelain Insulators

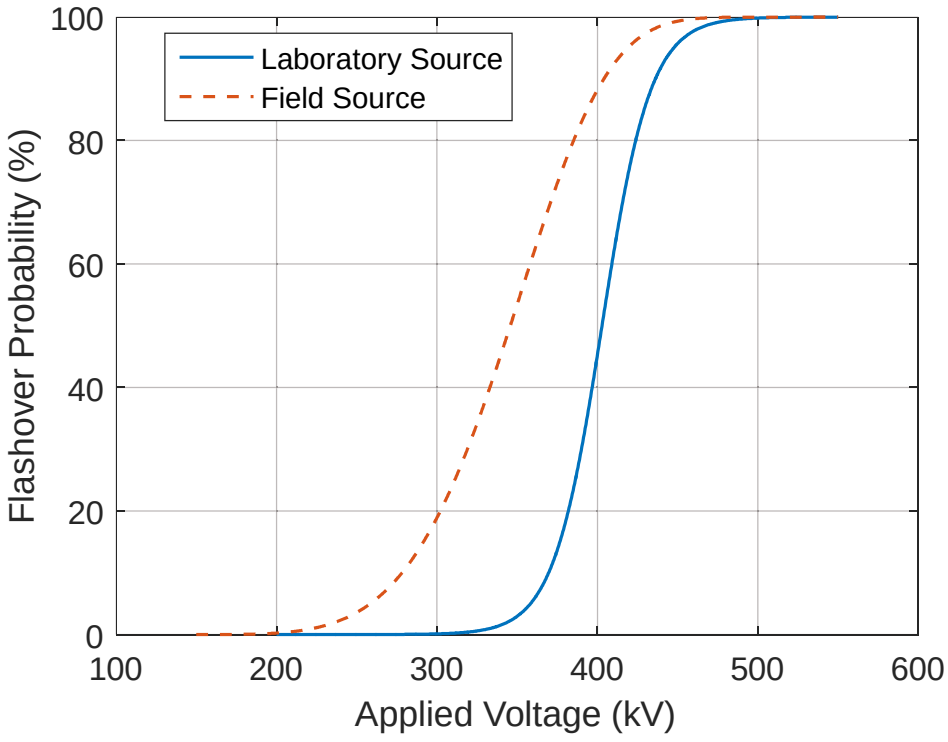

Figure 92 Flashover Probability of 230 kV Rated Polymer Insulators

For porcelain insulator in laboratory test, it has a 50% flashover probability when $V_{50\%} = 240\ kV$. It has a 10% flashover probability when applied voltage is $V_{10\%} = 217\ kV$, and a 90% flashover probability when applied voltage is $V_{90\%} = 263\ kV$. This suggests that the range of voltage that causes a change of flashover probability from 10-90% is within $\frac{V_{90\%} - V_{10\%}}{V_{50\%}} \times 100\% = 19\%$. For the same insulator in service, this range is within 44%. In comparison with polymer insulators, these ranges are 15% for the laboratory source and 34% for the field source. This result shows that flashover can happen over a wider voltage range for field source than in the laboratory. In addition, flashovers of polymer insulators most likely to happen over a tighter range of voltage compared to porcelain insulators.

8.3.3 Effect of Insulator Shapes

The flashover probability of insulator with different shapes was studied. To begin with, a long rod type insulator and a post type insulator are studied. Both insulators are porcelain material with 230 kV class. Figure 93 shows their geometry details and Table 28 shows insulator dimensions.

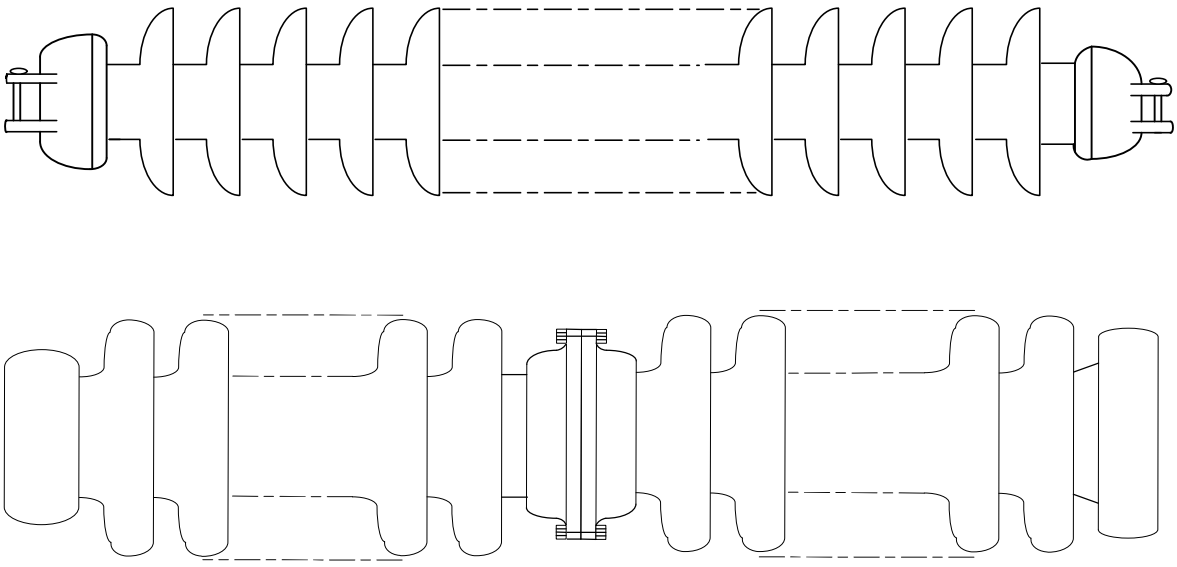

Figure 93 Insulator Geometries

Table 28 Insulator Dimensions

Insulator type	Porcelain Longrod	Porcelain Post
Number of sheds	14	32
Shed diameter	25.4 cm	24.4 cm
Trunk diameter	10.8 cm	21.6 cm
Unit spacing	204.4 cm	203.2 cm
Leakage distance	427 cm	419.1 cm

For the same pollution level at $0.1\,mg/cm^2$, the study of their flashover performance is done. Flashover probabilities of both insulators under the same supply voltage are shown in Figure 94.

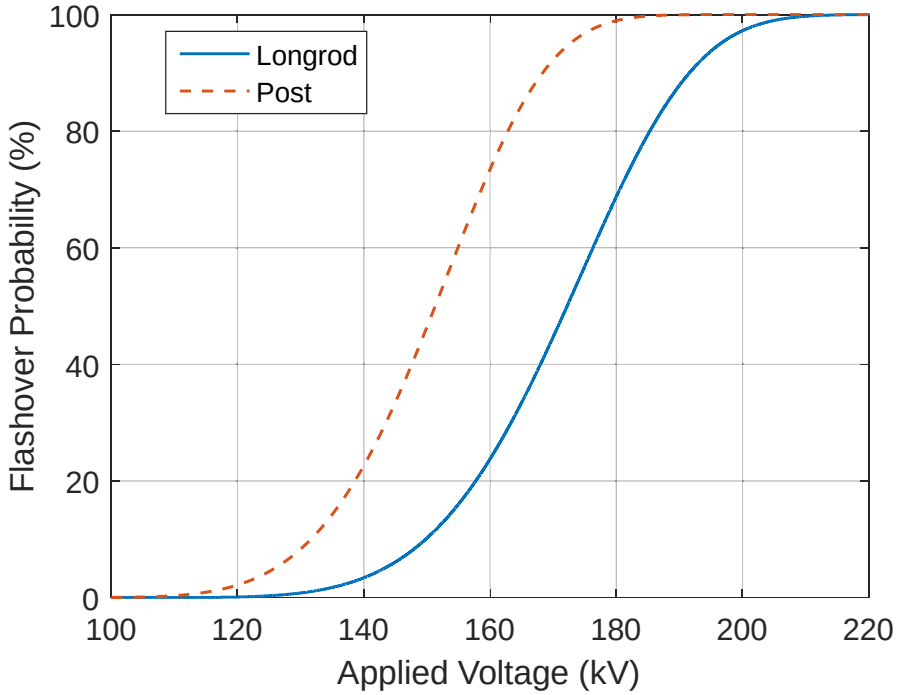

Figure 94 Flashover Probabilities Variations

It can be seen from the results that due to the lower flashover voltage, the flashover probability of post type insulator is higher than that of the longrod type insulator. For the same applied voltage at 160 kV, post type insulator has a flashover probability of 74% while longrod insulator only has a 22% probability to fail.

8.3.4 Effect of Hydrophobicity Classifications

To begin with, the simulation of insulator flashover probability was done with different hydrophobicity classifications. HC 1,3,5,7 were considered and their flashover probability curves are shown in Figure 95.

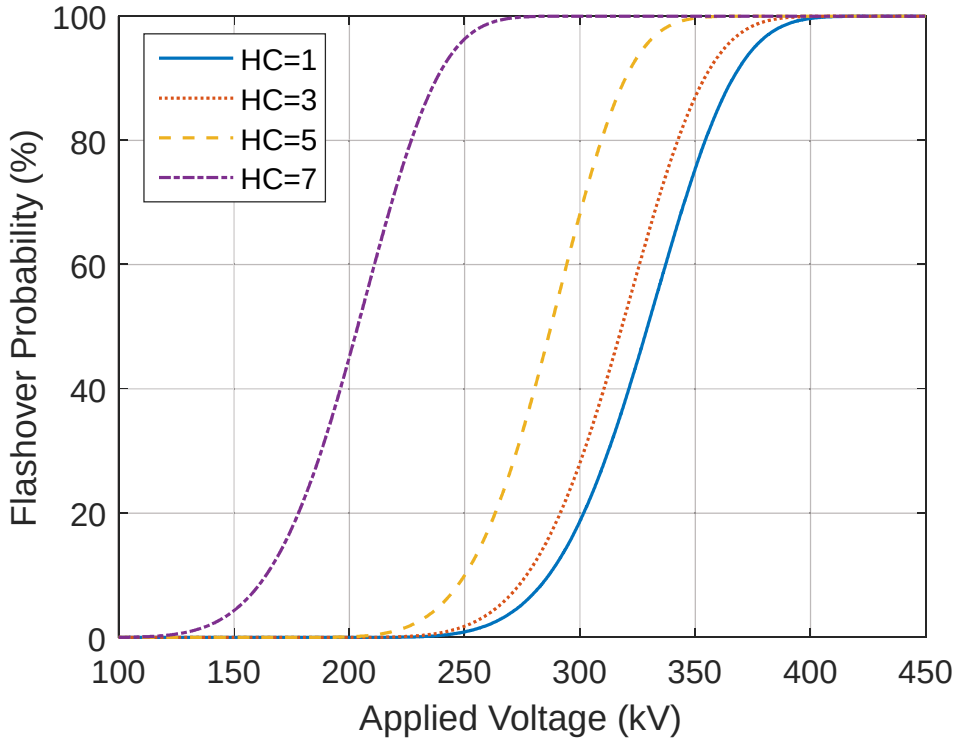

Figure 95 Flashover Probability of Different Hydrophobicity Classifications

From above figure, it can be seen that under the same supply voltage, lower HC level insulators will have lower flashover probability. For instance, HC 1 insulator has a flashover probability of 20% while the flashover probability of HC 5 insulator is 70% when the supply voltage is 300 kV.

8.3.5 Effect of Insulator Strings in Parallel

Assume there are n numbers of insulator strings connected in parallel and their flashover probabilities are independent of each other. If the flashover probability of the ith insulator string is p_i, then withstand probability of this string is

$$P = 1 - p_i \tag{37}$$

The withstand probability of all n insulator strings is

$$P = (1 - p_1) * (1 - p_2) * (1 - p_3) * \dots * (1 - p_4) = \prod_{i=1}^{n}(1 - p_i) \tag{38}$$

The probability of at least 1 insulator string flashover happens is

$$P = 1 - \prod_{i=1}^{n}(1 - p_i) \tag{39}$$

In the case that all insulator strings have the same flashover probability p, the probability of equation (39) becomes

$$P = 1 - (1 - p)^n \tag{40}$$

Equation (40) is identical to the results from EPRI red book [64].

To begin with, the simulation of insulator strings flashover probability was done to compare with the published reference [64]. Figure 96 shows the simulation results of a single string and 14 strings with respect of applied voltage per unit. A total of 8 units were selected in this study.

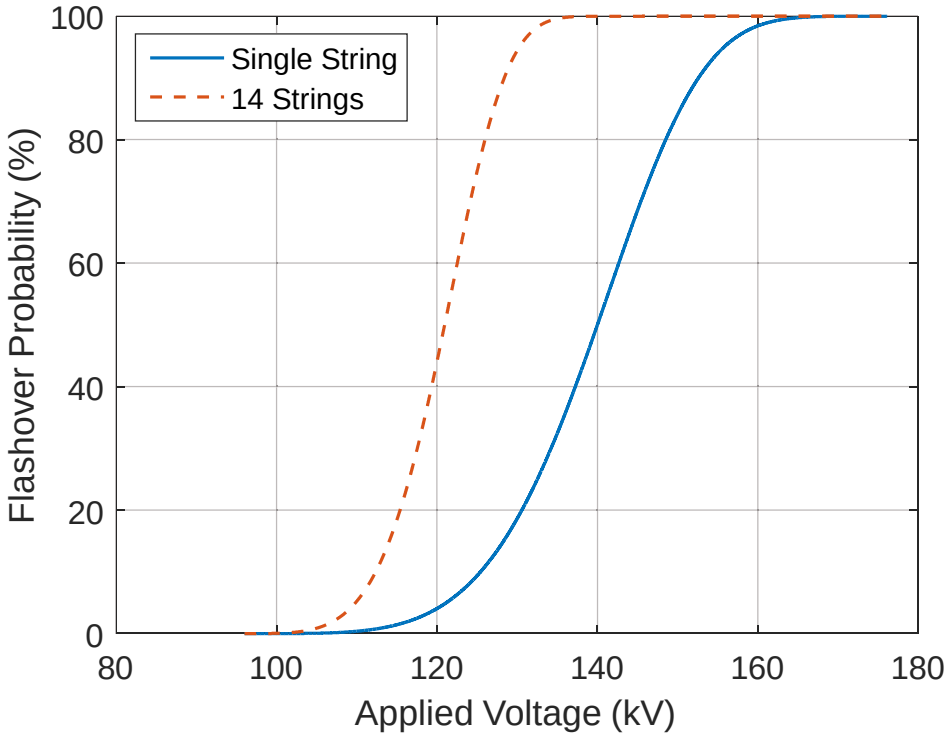

Figure 96 Simulation Results of Flashover Probability of 14 Strings

Then the influence of number of insulator strings on flashover probability was studied. A single insulator with flashover probability of 1% is assumed as the original case. It can be seen from Figure 97 that overall flashover probability will gradually increase with the increase of numbers of insulators in parallel.

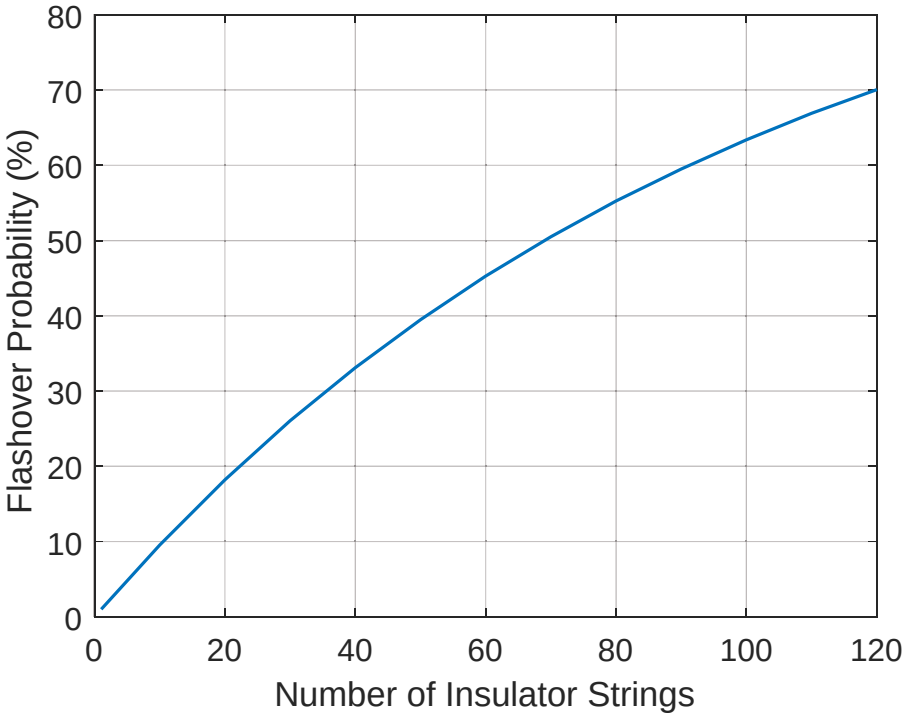

Figure 97 Numbers of Parallel Insulators Effects on Flashover Probability

The simulation also shows that with an original flashover probability of 1%, the overall probability when there are 120 units connected in parallel will increase to 70%.

In order to study the flashover probability of insulators with different HC levels. It is assumed that when HC = 1, the single insulator has a flashover probability of 0.01%. Figure 98 shows the simulation results.

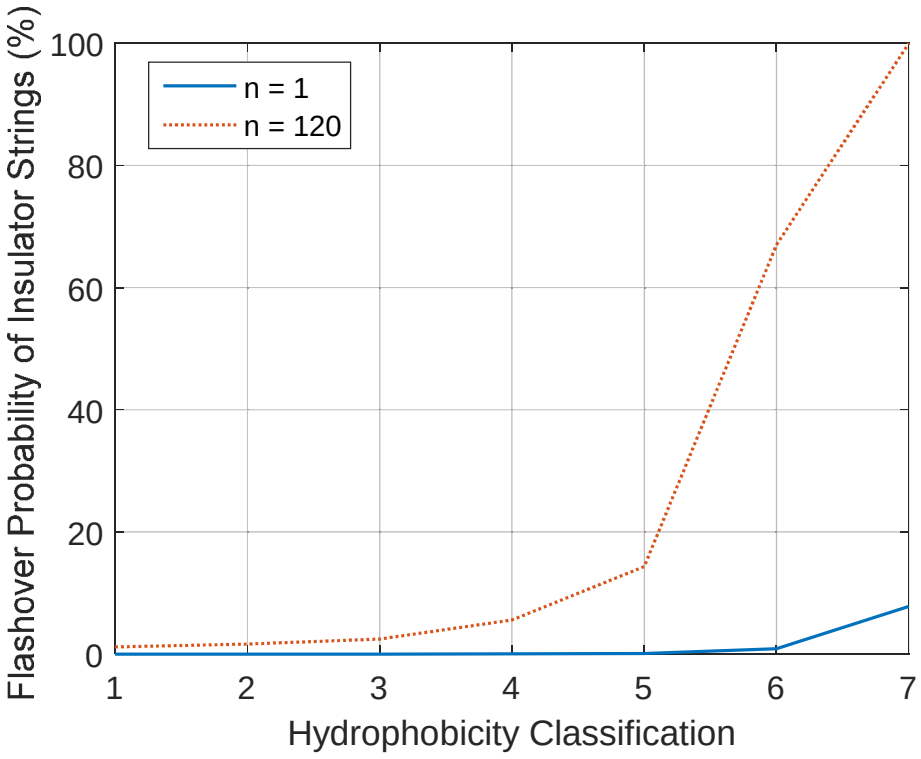

Figure 98 Flashover Probability of Multiple Strings

Table 29 shows a summary of flashover probabilities with different HC combinations of 120 insulator strings.

Table 29 Summary of Flashover Probabilities

No. of HC 1 Insulators	No. of HC 3 Insulators	No. of HC 5 Insulators	No. of HC 7 Insulators	Flashover Probability
120	0	0	0	1.2%
0	120	0	0	2.5%
0	0	120	0	14.3%
0	0	0	120	100%
30	30	30	30	91.7%

8.3.6 Effect of Leakage Distance

The flashover probability of insulator strings with different leakage distances was studied as well. The dimensions of two insulator strings are shown in Table 30. The simulation results are shown in Figure 99. Simulation results from Figure 99 was based on the assumption from [64] that the standard deviation is 10%.

Table 30 Insulator Details

Insulator String	A	B
Strings in Parallel	14	14
Units	8	10
Leakage Distance	244 cm	305 cm
50% Flashover Voltage	140.2 kV	175.6 kV

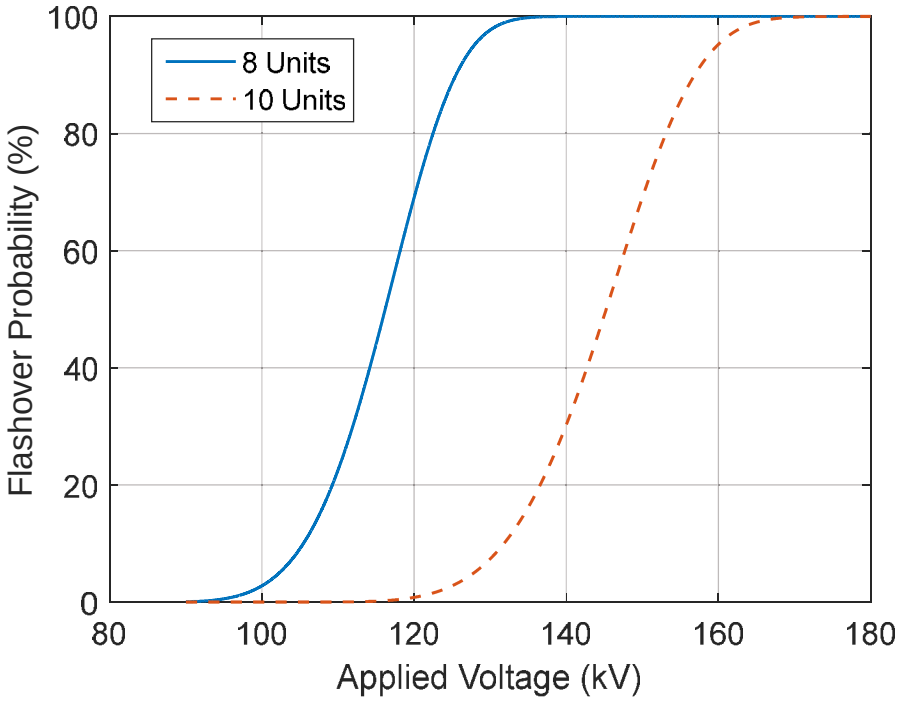

Figure 99 Flashover Probability of Different Leakage Distances

The flashover probability of polymer insulator with different leakage distances was studied as well. The dimensions of 230 kV class insulator is shown in Table 31.

Table 31 Insulator Dimensions

Insulator type	Polymer Suspension
Number of sheds	30/29
Shed diameter	10.6/7.6 cm
Trunk diameter	4 cm
Unit spacing	207.5
Leakage distance	418.9 cm

It can been seen from Table 31 that the 230 kV insulator has a leakage distance of 419 cm. In this work, the HC 1 insulator with original leakage distance is assumed to have a flashover probability of 50%. The purpose of this study is to find out what leakage distances are required for insulator with different hydrophobicity classifications to also have a flashover probability of 50%. The simulation results are shown in Figure 100. The standard deviation in this research is assumed at 10%.

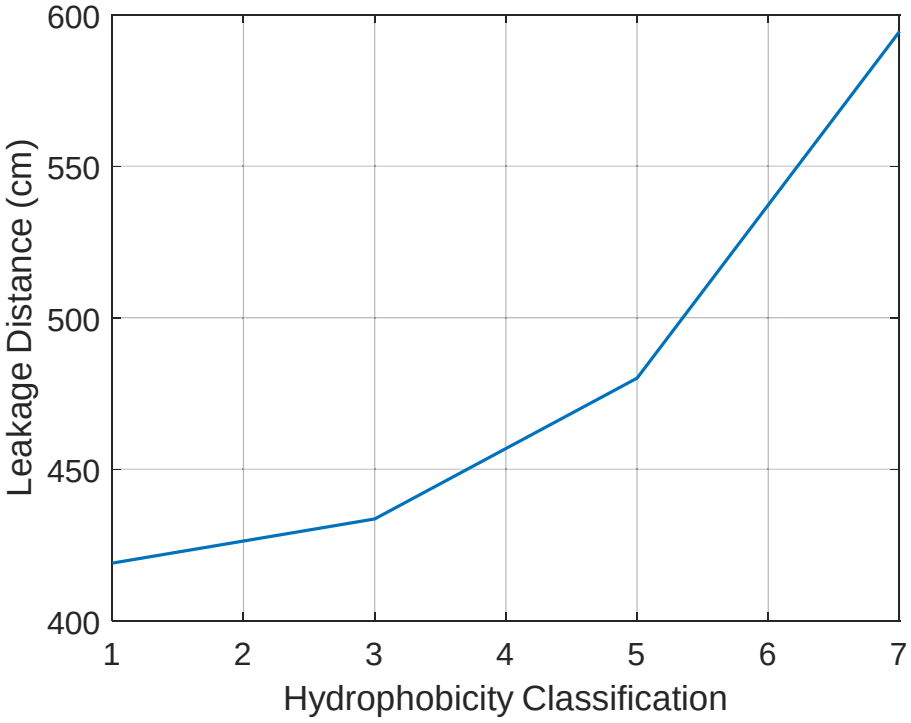

Figure 100 Leakage Distance Variations

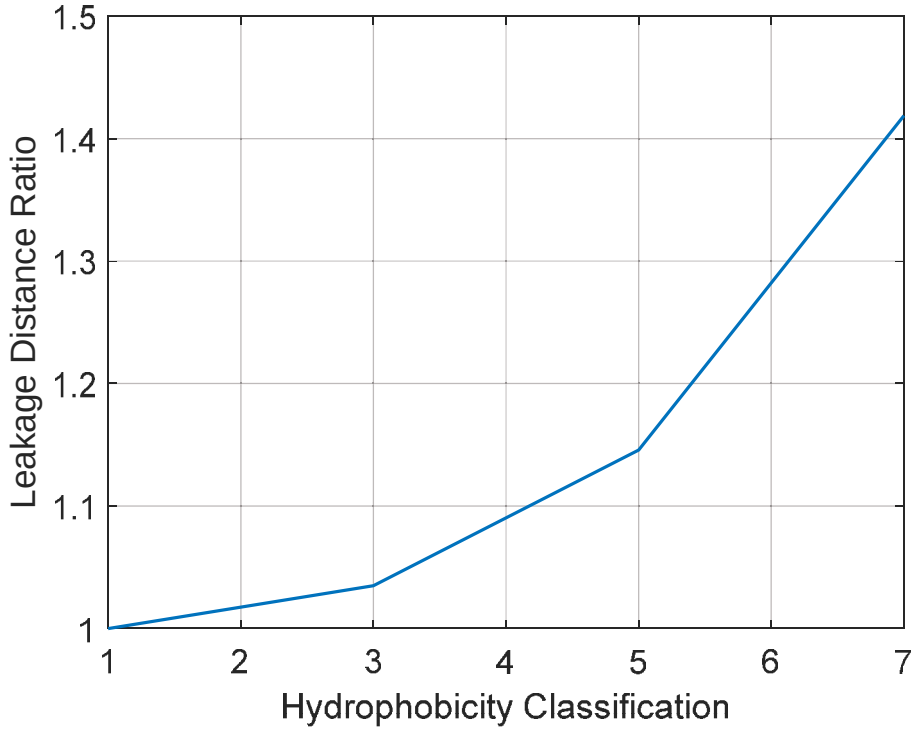

Figure 101 Leakage Distance Ratio

8.4 Conclusions

1. Three popular probability functions are studied and compared in this research. From simulation results, it can be seen that normal distribution curve lies between other two types of distribution functions. The differences between models are all less than 5% and relatively small. The largest difference occurs between Weibull distribution and logistic distribution. It is concluded that three probability models are reasonable and can well represent the insulator flashover probability. However, Weibull distribution likely to be the best choice because its advantage at low probability events.

2. The study of source strength effect on flashover probability shows that flashover probability of powerful source has a larger voltage span than that of weak source. Flashover can happens at supply voltage as low as 14 kV for powerful source, but weak source will not have flashover until the voltage reaches 26 kV. For the same applied voltage, powerful source has a higher probability to flashover than weak source.

3. The investigation on different dielectric materials show that flashover of polymer insulators likely to happen in a tighter range of voltages than that of porcelain insulators.

4. From the study of multiple insulator strings connected in parallel, it is demonstrated that multiple insulator strings will increase the risk of flashover. However, it can be mitigated by increase the insulator leakage distance.

Chapter 9

CONCLUSIONS AND FUTURE WORK

9.1 Conclusions

The conclusions drawn from this work can be summarized in five groups as follows:

1. In this dissertation mathematical dynamic models to account for insulator AC flashover under contaminated conditions were developed. The characteristics of a polluted insulator, including different phases of arcing process, namely arc dynamics, arc re-ignition and arc motion are successfully modeled. The porcelain insulator dynamic model is further developed to predict the flashover performance for polymer insulator. The aging effect of polymer insulator was also investigated in terms of hydrophobicity classifications.

2. This research constitutes a systematic investigation of the interaction between test source and insulator during flashover process. The source parameters are found to have a considerable influence on the insulator flashover outcome. The equivalent impedance of the test source can have significant influence on the source voltage drop, shape of leakage current and the transient recovery voltage. The shunt capacitance can mitigate the error generated by weak source by lowering the flashover voltage, but this effect has not been seen in flashover energized by powerful source.

3. The model is used to study the arc jumping phenomenon which is reported by some researchers. A new arc jumping mechanism is proposed by considering both the electric field and leakage current. The results of simulation show that the arc jumping can not only happens at low conductivity condition but also high conductivity if there is enough leakage current.

4. The study of source strength impact on insulator flashover performance is the main contribution of this research. Source strength influence on different types of insulators with various geometries are systematically investigated and reported. Besides that, 230 kV, 345 kV, and 500 kV insulators are studied as well to compare the effects of source strength on their flashover performance.

5. The investigation of the insulator flashover probability is also done in this dissertation. Based on the proposed insulator flashover model, different probability functions are studied to predict the probability of flashover. The impacts of source strength, insulation material, hydrophobicity classification, leakage distance, and numbers of insulators in parallel on flashover probability were studied as well.

9.2 Future Work

There are some topics that can be further pursued for future research. The following work is suggested for future study:

- Continuing work could be done to study the DC source parameters impact on the insulator flashover performance. It is interesting to study how the DC source parameters would impact the insulator flashover and its comparison to AC source.
- Non-uniform distribution of contaminant on insulator surface is another possible approach to extend present model and compare with the results under uniform contamination conditions.

- Further development of the model is required to account for the statistical nature of the phenomena including pollution distribution, wetting of the insulator surface.
- Experimental investigations of the arc jumping and the probability of flashover in AC testing could be done to compare with results from theoretical models.

REFERENCES

[1] M. Farzaneh, W. Chisholm, “Insulators for Icing and Polluted Environments”, Wiley-IEEE Press, 2009.

[2] R. Wilkins, “Flashover Voltage of High-Voltage Insulators with Uniform Surface-Pollution Films”, Proceeding of the IEE, Vol. 116, No. 3, pp. 457-465, 1969.

[3] Task Force on Testing IEEE Insulators, “The AC Clean Fog Test for Contaminated Insulators”, IEEE Transactions on Power Apparatus and Systems, Vol. 102, No. 3, pp. 604-613, 1983.

[4] F. A. M. Rizk, G. N. Trinh, High Voltage Engineering, CRC Press, 2014.

[5] R. S. Gorur, E. A. Cherney, J. T. Burnham, Outdoor Insulators, Ravi S. Gorur, Inc, 1999.

[6] J. S. T. Looms, Insulators for High Voltages, Peter Peregrinus Ltd, 1988.

[7] IEEE Standard 4, “IEEE Standard for High-Voltage Testing Techniques”, IEEE Power and Energy Society, 2013.

[8] IEC 60815, “Selection and Dimensioning of High-Voltage Insulators Intended for Use in Polluted Conditions”, International Electrotechnical Commission, 2008.

[9] B. F. Hampton, “Flashover Mechanism of Polluted Insulation”, Proceeding of the Institution of Electrical Engineers, Vol. 111, No. 5, pp. 985-990, 1964.

[10] J. O. Loberg, E. C. Salthouse, “Dry-Band Growth on Polluted Insulation”, IEEE Transactions on Electrical Insulation, Vol. 6, No. 3, pp. 136-141, 1971.

[11] F. Obenaus, “Fremdschichtueberschlag und Kriechweglaenge”, Deutsche Elektrotechnik, pp. 135-136, 1958.

[12] L. L. Alston, S. Zoledziowski, “Growth of Discharges on Polluted Insulation”, Proceedings of IEE, Vol. 110, No. 7, pp. 1260-1266, 1963.

[13] J. P. Holtzhausen, “A Critical Evaluation of AC Pollution Flashover Models for HV Insulator Having Hydrophilic Surfaces”, Ph.D. Dissertation, The University of Stellenbosch, 1997.

[14] F. A. M. Rizk, “Application of Dimensional Analysis to Flashover Characteristics of Polluted Insulators”, Proceedings of IEE, Vol. 117, No. 12, pp. 2257-2260, 1970.

[15] F. A. M. Rizk, D. H. Nguyen, “AC Source-Insulator Interaction in HV Pollution Tests”, IEEE Transactions on Power Apparatus and Systems, Vol. 103, No. 4, pp 723-732, 1984.

[16] D. C. Jolly, T. C. Cheng and D. M. Otten, “Dynamic Theory of Discharge Growth over Contaminated Insulator Surfaces”, Conference Paper No. 74-068-3, IEEE PES Winter Power Meeting, 1974.

[17] R. Sundararajan and R. S. Gorur, “Dynamic Arc Modeling of Pollution Flashover Insulators under DC Voltages”, IEEE Transactions on Electrical Insulation, Vol. 28, No. 2, pp. 209-218, 1993.

[18] F. A. M. Rizk, “Mathematical Models for Pollution Flashover”, Electra, Vol. 78, pp. 71-103, 1981.

[19] A. Al-Baghdadi, “The Mechanism of Flashover on Polluted Insulators”, Ph.D. Dissertation, University of Manchester, 1970.

[20] IEC 60507, “Artificial Pollution Tests on High-Voltage Insulators to be Used on A.C. Systems”, International Electrotechnical Commission, 1993.

[21] S. C. Chapra, Applied Numerical Methods, McGraw Hill, 2005.

[22] L. Bo, R. S. Gorur, “Modeling Flashover of AC Outdoor Insulators under Contaminated Conditions with Dry Band Formation and Arcing”, IEEE Transactions on Dielectrics and Electrical Insulation, Vol. 19, No. 3, pp. 1037-1043, 2012.

[23] T. Seta, “Studies on Performance of Contaminated Insulators Energized with DC Voltage”.

[24] T. C. Cheng, “EPRI-HVDC insulator studies part II: laboratory simulation studies”.

[25] I. Kimoto, K. Naito, “Performance of insulators for direct current transmission line under polluted condition”.

[26] T. M. Parnell, “The Influence of Circuit Parameters on Power Frequency Flashover Tests”, Electrical and Mechanical Engineering Transactions, Vol. 3, No. 2, pp 105-118, 1961.

[27] S. D. Merkhalov, E. A. Solomonik, “The Effect of Short-Circuit Capacity of Test Circuit on the AC Flashover Characteristics of Polluted Insulators”, Elektrichestvo, Vol. 9, No. 9, pp 43-46, 1966.

[28] M. P. Verma, W. Petrusch, “Results of Pollution Tests on Insulators in the ≥1100 kV Range and Necessity of Testing in the Future”, IEEE Transactions on Electrical Insulation, Vol. 16, No. 3, 1981.

[29] F. A. M. Rizk, M. Bourdages, “Influence of AC Source Parameters on Flashover Characteristics of Polluted Insulator”, IEEE Transactions on Power Apparatus and Systems, Vol. 104, No. 4, 1985.

[30] H. Mohseni, “A Method of Increment Short-Circuit Current in Test of Ceramic and Composite Polluted Insulators”, IEEE Transactions on Power Delivery, Vol. 22, No. 2, 2007.

[31] R. W. S. Garcia, “A Mathematical Model to Study the Influence of Source Parameters in Polluted Insulators Tests”, Proceedings of the 3rd International Conference on Properties and Applications of Dielectric Materials, 1991.

[32] Q. Huang, G. G. Karady, “Numerical Simulation of Dry-Band Arcing on the Surface of ADSS Fiber-Optic Cable”, IEEE Transactions on Dielectrics and Electrical Insulation, Vol. 12, No. 3, pp. 496-503, 2005.

[33] R. Matsuoka, K. Naito, “Evaluation Methods of Polymer Insulators under Contaminated Conditions”, PES Transmission and Distribution Conference, 2002.

[34] P. J. Lambeth, “Effect of Pollution on High Voltage Simulation”, Proceedings of IEE, Vol. 118, No. 9, pp. 1107-1130, 1971.

[35] J. P. Holtzhausen, D. A. Swift, “The Pollution Flashover of AC and DC Energised Cap and Pin Insulators: The Role of Shortening of the Arc”, Eleventh International Symposium on High Voltage Engineering, Vol. 4, pp 333-336, 1999.

[36] K. Shenoi, R. S. Gorur, “Evaluating Station Post Insulator Performance From Electric Field Calculations”, IEEE Transactions on Dielectrics and Electrical Insulation, Vol. 15, No. 6, pp. 1731-1738, 2008.

[37] N. L. Allen, “Dielectric Breakdown in Nonunifrom Field Air Gaps”, IEEE Transactions on Electrical Insulation, Vol. 2, No. 2, pp. 183-191, 1993.

[38] COULOMB 9.1 Users and Technical Manual, Integrated Engineering Software, Canada.

[39] G. G. Karady, M. Shah, R. L. Brown, “Flashover Mechanism of Silicone Rubber Insulators Used for Outdoor Insulation - I”, IEEE Transactions on Power Delivery, Vol. 10, No. 4, pp. 1965-1971, 1995.

[40] A. de la O, R. S. Gorur, “Flashover of Contaminated Nonceramic Outdoor Insulators in a Wet Atmosphere”, IEEE Transactions on Dielectric and Electrical Insulation, Vol. 5, No. 6, pp. 814-823, 1998.

[41] Y. Chen, Z. Guan, X. Liang, “Analysis of Flashover on the Contaminated Silicone Rubber Composite Insulator”, Proceedings of the 5th International Conference on Properties and Applications of Dielectric Materials, pp. 914-917, 1997.

[42] S. Venkataraman, R. S. Gorur, “Prediction of Flashover Voltage of Non-ceramic Insulators under Contaminated Conditions”, IEEE Transactions on Dielectric and Electrical Insulation, Vol. 13, No. 4, pp. 862-869, 2006.

[43] R. Matsuoka, H. Shinokubo, K. Kondo, “Assessment of Basic Contamination Withstand Voltage Characteristics of Polymer Insulator”, IEEE Transactions on Power Delievery, Vol. 11, No. 4, pp. 1895-1900, 1996.

[44] R. Hackam, “Outdoor HC Composite Polymeric Insulators”, IEEE Transactions on Dielectrics and Electrical Insulation, Vol. 6, No. 5, pp. 557-585, 1999.

[45] X. Jiang, J. Yuan, L. Shu, Z. Zhang, J. Hu and F. Mao, “Comparison of DC pollution flashover performance of various types of porcelain, glass, and composite insulators”, IEEE Transactions on Power Delivery, Vol. 23, No. 2, pp. 1183-1190, 2009.

[46] G. N. Ramos, M. T. R. Campillo and K. Naito, “A study on the characteristics of various conductive contaminants accumulated on high voltage insulators”, IEEE Transactions on Power Delivery, Vol. 8, No. 4, pp. 1842-1850, 1993.

[47] G. G. Karady, “Flashover mechanism of non-ceramic insulators”, IEEE Transactions on Dielectrics and Electrical Insulation., Vol. 6, No. 5, pp. 718-723, 1999.

[48] M. Shah, G. G. Karady, R. L. Brown, “Flashover Mechanism of Silicone Rubber Insulators Used for Outdoor Insulation - II”, IEEE Transactions on Power Delivery, Vol. 10, No. 4, pp. 1972-1978, 1995.

[49] Hydrophobicity classification guide, STRI Guide 92/1, Swedish Transmission Research Institute, 1992.

[50] IEC 62073, “Guidance on the measurement of wettability of insulator surfaces”, International Electrotechnical Commission, 2003.

[51] D. A. Swift, C. Spellman and A. Haddad, “Hydrophobicity transfer from silicone rubber to pollutants and its effect on insulator performance”, IEEE Trans. Dielectr. Electr. Insul., Vol. 13, No. 4, pp. 820-829, 2006.

[52] S. L. Rice, “Absorption of silicone oil by a dimethylsiloxane elastomer”, J. Testing and Evaluation, Vol. 61, No. 2, pp. 194-204, 1988.

[53] A. Eriksson and D. Wikstrom, “Influence of the hydrophobicity of outdoor insulators on the flashover voltage”, Nord-Is, paper 1.1, 1994.

[54] A. De La O, R. S. Gorur and J. Chang, “AC clean fog tests on non-ceramic insulation materials and a comparison with porcelain”, IEEE Trans. Power Delivery, Vol. 9, No. 4, pp. 2000-2008, 1994.

[55] S. Zhao, X. Jiang, Z. Zhang, J. Hu, L. Shu, “Flashover voltage prediction of composite insulators based on the characteristics of leakage current”, IEEE Trans. Power Delivery, Vol. 28, No. 3, pp. 1699-1708, 2013.

[56] R. Christie, Power system test archive, Aug. 1999. [Online]. Available: http://www.ee.washington.edu/research/pstca.

[57] P. M. Anderson, Analysis of Faulted Power Systems, The Iowa State University Press, 1973.

[58] A. C. Baker, M. Farzaneh, R. S. Gorur, "Insulator Selection for AC Overhead Lines with Respect to Contamination", IEEE Transactions on Power Delivery, Vol. 24, No. 3, pp. 1633-1641, 2009.

[59] NGK Locke, Inc., Polymer Suspension Insulators 69 kV to 765 kV, [Online], Available: http://www.ngk-locke.com/pdf/NGK-Locke-Poly-Suspension.pdf

[60] NGK Locke, Inc., Locke Solid-Core Station Post Insulators, Part 2, [Online], Available: http://www.ngk-locke.com/pdf/station2.pdf

[61] Y. Suzuki, K. Naito, "Probabilistic Assessment of Flashover Performance of Transmission Lines in Contaminated Areas", IEEE Transactions on Dielectrics and Electrical Insulation, Vol. 6, No. 3, pp. 337-341, 1999.

[62] J. Montesinos, R. S. Gorur, "Estimation of Flashover Probability of Aged Nonceramic Insulators in Service", IEEE Transactions on Power Delivery, Vol. 15, No. 2, pp. 820-826, 2000.

[63] N. Hylten-Cavallius, F. A. Chagas, "Possible Precission of Statistical Insulation Test Methods", IEEE Transactions on Power Apparatus and Systems, Vol. 102, No. 8, pp. 2372-2378, 1983.

[64] EPRI, Transmission Line Reference Book: 345 kV and Above, Electric Power Research Institute, 1987.